MARMARA UNIVERSITY
INSTITUTE FOR GRADUATE STUDIES
IN PURE AND APPLIED SCIENCES

MODELLING OF START-UP PHASE OF THE DEAMMONIFICATION SYSTEMS

NESLİCAN UZKURT KALJUNEN

MASTER THESIS

Department of Environmental Engineering

Thesis Supervisor
Assoc.Prof. Bilge ALPASLAN KOCAMEMİ

ISTANBUL, 2019

MARMARA UNIVERSITY
INSTITUTE FOR GRADUATE STUDIES
IN PURE AND APPLIED SCIENCES

MODELLING OF START-UP PHASE OF THE DEAMMONIFICATION SYSTEMS

NESLİCAN UZKURT KALJUNEN

524315001

MASTER THESIS

Department of Environmental Engineering

Thesis Supervisor

Assoc.Prof. Bilge ALPASLAN KOCAMEMİ

ISTANBUL, 2019

MARMARA UNIVERSITY
INSTITUTE FOR GRADUATE STUDIES IN PURE AND APPLIED SCIENCES

Neslican UZKURT KALJUNEN, a Master of Science student of Marmara University Institute for Graduate Studies in Pure and Applied Sciences, defended her thesis entitled "**Modelling of Start-up Phase of the Deammonification Systems**", on September 3, 2019 and has been found to be satisfactory by the jury members.

Jury Members

Assoc.Prof. Bilge ALPASLAN KOCAMEMİ (Advisor)
Marmara University .....

Prof. Dr. Barış ÇALLI (Jury Member)
Marmara University .....

Prof.Dr. Erkan ŞAHİNKAYA (Jury Member)
Istanbul Medeniyet University .....

APPROVAL

Marmara University Institute for Graduate Studies in Pure and Applied Sciences Executive Committee approves that Neslican UZKURT KALJUNEN be granted the degree of Master of Science in Department of Environmental Engineering on 04.09.2019 (Resolution no: 2019/18)-02

Director of the Institute
Prof.Dr. Bülent EKİCİ

Acknowledgment

I would first like to thank my supervisor Assoc. Prof. Bilge Alpaslan Kocamemi of the Environmental Engineering Department at Marmara University for her efforts, guidence and immense knowledge.

I also would like to acknowledge Scientific Research Projects Unit of Marmara (BAPKO) for the financial support of thesis through project number FEN-C-YLP 130219-0036.

I gratefully ackowledge Bursa Metropolitan Municipality Water and Sewage Administration (BUSKI), Dr. Mehmet Emre Bastopcu – Deputy General Manager of Kuzu Toplu Konut Insaat, Mr.Eren Alp - Plant Manager of Bursa Dogu STP, Mr.Idris Vardar - Chief of Operation of Bursa Dogu STP and all operation/laboratory team of Bursa Dogu STP. My very special thanks goes to Ms. Sumeyye Celik, - Process Engineer of Kuzu Toplu Konut Insaat who helped me and provided me information regarding pilot plant whenever I need. Without her patient participation and input, the data from the pilot plant could not have been successfully conducted.

I would like to express my sincere gratitude to Dr. Christopher Bye -Vice-President of Software with EnviroSim Associates Ltd. and Dr. Daniela Conidi – Senior Process Engineer of Envirosim Associates Ltd. for their valuable input and support during my study.

I would also like to thank Mrs. Ozden Gun Yazici, my previous department head in Va Tech Wabag Gmbh for her warm support during my entire MSc. study.

Finally, I must express my very profound gratitude to my parents and to my spouse Juho, for providing me with unfailing support and continuous encouragement throughout my study and through the process of researching and writing this thesis. This accomplishment would not have been possible without them.

Thank you.

Neslican Uzkurt Kaljunen

Ağustos 2019

Table of Contents

ÖZET v

ABSTRACT vi

SYMBOLS vii

ABBREVIATIONS viii

LIST OF FIGURES ix

LIST OF TABLES xiii

1. INTRODUCTION 1

1.3. Conventional Biological Nitrogen Removal Technologies 2

1.3.1. Nitrification 2

1.3.1.1. Stoichiometry of nitrification 2

1.3.1.2. Kinetics of nitrification 3

1.3.2. Denitrification 4

1.3.2.1. Stoichiometry of denitrification 5

1.4. Deammonification 5

1.4.1. Partial nitritation 6

1.4.2. Anaerobic ammonium oxidation (Anammox) 6

1.4.2.1. Stoichiometry of Anammox 7

1.4.2.2. Kinetics of Anammox 8

1.4.3. Deammonification Configurations 8

1.5. MBBR Type Deammonification Systems 9

1.5.1. Description of MBBR 9

1.6. Modelling of MBBR Type Deammonification Systems 11

1.6.1. Biofilm Kinetics 11

1.6.2. General information regarding modelling 13
1.6.3. Simulation Softwares 17
1.7. BioWin® 6.0 Software 19
2. MATERIALS AND METHODS 21
2.1 Description of The Bursa Deammonification Pilot Plant 21
2.2 General Description of Modelling Studies for the Start-up Phase of MBBR Type Deammonification Pilot Plant in Bursa 22
2.3 Consolidation of Mainstream Deammonification Set-up For Pilot Plant in BioWin® 6.0 Software 23
2.3.1 Editing influent 25
2.3.2 Editing influent state variable 25
2.3.3 Editing bioreactor 26
2.3.4 Editing clarifier 28
2.3.5 Sludge 29
2.3.6 Effluent 29
2.3.7 Project 30
2.3.8 Simulate 34
2.4 Steady State Simulations 36
2.4.1 Description of Set-up 1 36
2.4.2 Description of Set-up 2 37
2.5 Dynamic Simulations 38
2.5.1 Set-up 2 dynamic simulation 38
2.6 Sensitivity Analysis 39
2.7 Data Evaluation 40
2.7.1 Methodology of naming the simulations 40

2.7.2 Steady-state simulations 41
2.7.3 Dynamic simulations 43
2.7.4 Sensitivity analysis 44
3. RESULTS AND DISCUSSIONS 45
3.1. Set-up 1 45
3.2. Set-up-2 72
3.3. Sensitivity Analysis 77
3.4. Dynamic simulation 81
4. CONCLUSION 83
REFERENCES 86
CIRRICULUM VITAE 93
Annex 1 - Table 1. Kinetic, stoichiometric and general bioflm parameters used for Set-up 1 and Set-up 2 in BioWin® 6.0 95
Annex 2 - Table 1. Sensitivity Analysis results for kinetic, stoichiometric and general bioflm parameters used in BioWin® 6.0. 105

ÖZET

DEAMONİFİKASYON SİSTEMLERİNİN DEVREYE ALMA AŞAMASININ MODELLENMESİ

Kısmi nitritasyon ve Anammox prosesini içeren deamonifikasyon prosesi, daha az enerji tüketimi ve daha az çamur üretimi nedeniyle, geleneksel azot giderimi teknolojisi olan nitrifikasyon ve denitrifikasyon prosesleri ile değiştirilmesinde iyi bir adaydır. Bununla birlikte, tüm prosesler aynı tankta aynı biyofilm içinde gerçekleştiğinden bu prosesin MBBR sisteminde başlatılması ve işletilmesi oldukça zordur.

Bu çalışma, tek kademeli deammonifikasyon MBBR sistemlerinde devam etmekte olan prosesleri anlamak için atıksu arıtma simülatörlerinin olası kullanımını değerlendirmek ve farklı işletme koşulları altında Anammox bakterilerinin çoğalmasina sebebiyet veren en optimum çalışma şemasını belirlemek amacıyla yapılmıştır. Bu çalışma, Türkiye'de Bursa Doğu Atıksu Arıtma Tesisi' ndeki MBBR deamonifıkasyon pilot tesisinden elde edilen gerçek veriler kullanılarak yapılmıştır. Simülatör olarak BioWin® 6.0 yazılımı kullanılmıştır.

Havalandırma düzeninde set DO ve oksik-anoksik sürelerin TN çıkış ve mikrobiyal popülasyon dağılımı üzerindeki etkisi düşük (10˚C), ortalama (20˚C) ve maksimum (25˚C) sıcaklık koşulları altında tespit edilmiştir. Dinamik simülasyon sınırlamaları belirlenmiştir. Kalibrasyonun ön basamağı olan duyarlılık analizi, kalibrasyon üzerinde etkili olacak kinetik/stokiyometrik/biyofilm genel parametrelerini belirlemek için detaylı bir şekilde yapılmıştır.

ABSTRACT

MODELLING OF START-UP PHASE OF THE DEAMMONIFICATION SYSTEMS

Deammonification process which includes partial nitritation and Anammox process is a good candidate to replace with conventional nitrogen removal technologies of nitrification and denitrification processes due to less energy consumption and less sludge production. However, start-up and operation of this process in a single-stage moving bed biofilm reactor (MBBR) system is quite difficult since all processes are occuring in the same tank trough the biofilm depth simultaneously.

This study aims to evaluate possible use of wastewater treatment simulators to understand the ongoing processes in single-stage deammonification MBBR systems and to identify the most optimum operation scheme favoring Anammox growth under different operational conditions.The study was performed using the data from a real pilot MBBR deammonification plant in Bursa Dogu STP in Turkey. BioWin® 6.0 software was used as simulator.

The effect of set DO and oxic-anoxic durations in aeration pattern on the TN effluent and microbial population distribution were identified under low (10˚C), average (20˚C) and maximum (25˚C) temperature conditions. Dynamic simulation limitations were identified. The sensitivity analysis which is the preliminary step of calibration was done deeply to identify kinetic/stoichiometric/biofilm general parameters that will be influential on calibration.

SYMBOLS

®	Trademark
S_{ij}	Coefficient for sensitivity analysis

ABBREVIATIONS

AAO	Anaerobic ammonia oxidizing bacteria
AOB	Ammonia oxidizing bacteria
ASM1/2/2d/3	Activated sludge model 1/2/2d/3
BAT	Best available technology
BOD	Biological oxygen demand
COD	Chemical oxygen demand
CSTR	Continuous flow stirred-tank reactor
DO	Dissolved oxygen
HRT	Hydraulic retention time
IWA	International water association
MBBR	Moving bed biofilm reactor
N	Nitrogen
N_2	Nitrogen gas
NH_4^+	Ammonium ion
NO_2^-	Nitrite ion
NO_3^-	Nitrate ion
NOB	Nitrite oxidizing bacteria
OHO	Ordinary heterotrophic organisms
PAO	Phosphorus accumulating organisms
SBR	Sequencing Batch Reactor
SS	Suspended solids
STP	Sewage treatment plant
T	Temperature
TKN	Total Kjelldal nitrogen
TN	Total nitrogen
TP	Total phosphorus
TS	Total sulphur
Q	Flow rate

LIST OF FIGURES

Figure 1.1. Nitrogen pathways on Earth (Francis et al., 2007) 1
Figure 1.2. Deammonification process. (Wett et al., 2007) 6
Figure 1.3 A 16s ribosomal rNA-gene-based phylogenetic tree of anammox bacteria (Kuenen, 2008) 7
Figure 1.4 Two-stage and single-stage deammonification systems (Growth and Metabolism of Anammox Bacteria, 2008) 9
Figure 1.5. Schematic view of MBBR system (1) inlet, (2) pump, (3) biofilm carrier, (4) air bubble in case of aerobic conditions,(5) mixer, runs only during the anoxic/anaerobic conditions, (6) outlet (Chamorro et al., 2010) 10
Figure 1.6 Different types of MBBR carriers 10
Figure 1.7. Biofilm layers in media carrier for deammonification process (Ødegaard, 2016) 11
Figure 1.8 Conceptual profile of substrate concentration in a biofilm environment (Zhu and Chen, 2001). 11
Figure 1.9. Model Building Process (Peterson et al., 2002) 14
Figure 1.10 Stoichiometry of the deammonification model (Trojanowicz et al. 2017) 16
Figure 1.11 Kinetic equations of the deammonification model (Trojanowicz et al. 2017). 16
Figure 1.12 Example screenshot of drawing board in BioWin® 6.0. 17
Figure 1.13 Summary of key process aspects for side-stream process (BioWin Help Manual, 2019). 20
Figure 2.1 Deammonification MBBR pilot plant in Bursa Doğu STP/Turkey. 21
Figure 2.2 General description of MBBR deammonification configuration set-up consolidation in BioWin® 6.0. 24
Figure 2.3 Editing influent in BioWin® 6.0. 25
Figure 2.4 Editing influent state variable element in BioWin® 6.0 26
Figure 2.5 Editing side-stream (media) bioreactor element in BioWin® 6.0 27
Figure 2.6 Editing model page of side-stream bioreactor element in BioWin® 6.0 27
Figure 2.7 Editing model clarifier element in BioWin® 6.0. 28

Figure 2.8 Screenshot of sludge element in BioWin® 6.0 29
Figure 2.9 Screenshott od effluent element in BioWin® 6.0..... 29
Figure 2.10 Aeratiom/mass transfer parameter editor 30
Figure 2.11 Kinetic parameters and Stoichiometric parameter editors in BioWin® 6.0..... 31
Figure 2.12 Settling parameter and Biofilm properties editors in BioWin® 6.0. 31
Figure 2.13 Physical/chemical parameter and other parameters editors in BioWin® 6.0... 32
Figure 2.14 Temperature editing in BioWin® 6.0 32
Figure 2.15 Project options page in BioWin® 6.0 33
Figure 2.16 Numerical parameters page in BioWin® 6.0 34
Figure 2.17 Steady-state simulation box in BioWin® 6.0 35
Figure 2.18 Dynamic simulation box in BioWin® 6.0 35
Figure 2.19. Set-up 1 flow diagram in BioWin® 6.0. 36
Figure 2.20. Set-up 2 flow diagram in BioWin® software. 38
Figure 2.21 Methodology of naming BioWin® simulations 41
Figure 2.22 Sample screen shot of BioWin® 6.0 album menu details..... 42
Figure 2.23. Sample screenshot of BioWin® 6.0 album showing effluent chart for a steady state simulation. 42
Figure 2.24. Sample screenshot of BioWin® 6.0 album showing the microbial population distribution as mg COD/l in bulk liquid of deammonification MBBR reactor. 43
Figure 2.25. Sample screenshot of effluent chart for dynamic simulation in the album of BioWin® 6.0. 44
Figure 3.1. Influent and effluent charts of simulation R-S1T1-SS-20-DO0.5-1. 47
Figure 3.2. Microbial population distribution through biofilm layers of the simulation R-S1T1-SS-20-DO0.5-1. 47
Figure 3.3 Influent and effluent charts of simulation R-S1T1-SS-20-DO0.5-10 48
Figure 3.4 Microbial population distribution in biofilm layers of simulation R-S1T1-SS-20-DO0.5-10 48
Figure 3.5 DO concentration profile through biofilm layers of simulations at DO set 0.5 mg/l and 20˚C wastewater temperature 50
Figure 3.6 Influent and effluent charts of simulation R-S1T1-SS-20-DO1.0-1 52

Figure 3.7 Microbial population distribution in biofilm layers of simulation R-S1T1-SS-20-DO1.0-1 52
Figure 3.8 Influent and effluent charts of simulation R-S1T1-SS-20-DO1.0-7 53
Figure 3.9 Microbial population distribution in biofilm layers of simulation R-S1T1-SS-20-DO1.0-7 53
Figure 3.10 DO concentration profile through biofilm layers of simulations at DO set 1.0 mg/l and 20˚C wastewater temperature 54
Figure 3.11 DO concentrations through biofilm layers of simulations at DO set 1.5 mg/l, 20˚C 57
Figure 3.12. Influent and effluent charts of simulation R-S1T1-SS-20-DO1.5-1. 58
Figure 3.13. Microbial population distribution in biofilm layers of simulation R-S1T1-SS-20-DO1.5-1. 58
Figure 3.14. Influent and effluent charts of simulation R-S1T1-SS-20-DO1.5-6. 59
Figure 3.15. Microbial population distribution in biofilm layers of simulation R-S1T1-SS-20-DO1.5-6. 59
Figure 3.16 Influent and effluent charts of simulation R-S1T1-SS-20-DO1.5-7 60
Figure 3.17 Microbial population distribution in biofilm layers of simulation R-S1T1-SS-20-DO1.5-7 60
Figure 3.18 Influent and effluent charts of simulation R-S1T1-SS-20-DO2-4 63
Figure 3.19 Microbial population distribution in biofilm layers of simulation R-S1T1-SS-20-DO2-4 63
Figure 3.20 Influent and effluent charts of simulation R-S1T1-SS-20-DO2-1 64
Figure 3.21 Microbial population distribution in biofilm layers of simulation R-S1T1-SS-20-DO2-1 64
Figure 3.22. Influent and effluent charts of simulation R-S1T1-SS-20-DO2-5. 65
Figure 3.23. Microbial population distribution in biofilm layers of simulation R-S1T1-SS-20-DO2-5 65
Figure 3.24 Influent and effluent charts of simulation R-S1T1-SS-20-DO2-3 66
Figure 3.25 Microbial population distribution in biofilm layers of simulation R-S1T1-SS-20-DO2-3 66

Figure 3.26 DO concentrations trough biofilm layers of simulations at DO set 2.0 mg/l, 20˚C. 67
Figure 3.27 TN effluent values in optimum simulations for DO set values of 0.5, 1.0, 1.5 and 2.0 mg/l at 10˚C, 20˚C and 25˚C wastewater temperatures. 69
Figure 3.28 Microbial population distribution in the deeper layer (L1) of biofilm of optimum simulations for DO set values of 0.5, 1.0, 1.5 and 2.0 mg/l at 10˚C, 20˚C and 25˚C. 69
Figure 3.29 AAO populations trough biofilm layers in Set-up 1 and Set-up 2 simulations at 20˚C with DO set 0.5, 1.0, 1.5 and 2.0 mg/l. 74
Figure 3.30 Influent and effluent charts of simulation R-S2T1-SS-20-DO1.5-1. 75
Figure 3.31. Microbial population distribution in biofilm layers of simulation R-S2T1-SS-20-DO1.5-1. 75
Figure 3.33. Influent and effluent charts of simulation R-S2T1-SS-10-DO2-4. 76
Figure 3.32 Microbial population distribution in biofilm layers of simulation R-S2T1-SS 10-DO2-4 76
Figure 3.34 Dynamic simulation effluent results of deammonification MBBR model for 21 days. 82
Figure 3.35 Actual effluent data of Bursa deammoification MBBR pilot plant for 21 days. 82

LIST OF TABLES

Table 1.1. A group of available simulators that includes biofilm reactor models. 18
Table 2.1 Carrier characteristics - Aquaflex® 22
Table 2.2 Design avarage influent values of Bursa Doğu STP..... 23
Table 2.3. Influent data for dynamic simulation of Set-up 2. 39
Table 2.4. European Legislation discharge limits for sensitive areas (without P removal) (91/271/EEC). 41
Table 3.1 Set-up 1 effluent values at T=20 ˚C, DO=0.5 mg/l 46
Table 3.2 Set-up 1 population distribution of microbial species at T=20 ˚C, DO=0.5 mg/l46
Table 3.3 Set-up 1 effluent values at T=20 ˚C, DO=1.0 mg/l 51
Table 3.4 Set-up 1 Population distribution of microbial species at T=20 ˚C, DO=1.0 mg/l51
Table 3.5 Set-up 1 effluent values at T=20 ˚C, DO=1.5 mg/l 55
Table 3.6 Set-up 1 microbial distribution(as mgCOD/l) values at T=20 ˚C, DO=1.5 mg/l 55
Table 3.7 Set-up 1 effluent values at T=20 ˚C, DO=2.0 mg/l 62
Table 3.8 Set-up 1 microbial distribution(as mgCOD/l) values at T=20 ˚C, DO=2.0 mg/l 62
Table 3.9 Effluent values of optimum simulations for DO set values 0.5, 1.0, 1.5 and 2.0 mg/l at 10˚C, 20˚C and 25˚C wastewater temperature. 68
Table 3.10 Microbial population distribution of optimum simulations for DO set values 0.5, 1.0, 1.5 and 2.0 mg/l at 10˚C, 20˚C and 25˚C wastewater temperature. 68
Table 3.11 Effluent results of simulations performed under 10˚C wastewater temperature. 71
Table 3.12 Microbial population distribution of simulations performed under 10˚C wastewater temperature. 71
Table 3.13 Comparison table of Set-up 1 and Set-up 2 simulations under 20 ˚C wastewater temperature with 0.5, 1.0, 1.5 and 2.0 mg/l set DO..... 73
Table 3.14 Microbial population distribution of simulations performed under 20˚C wastewater temperature. 73
Table 3.15 Influential Parameters - $0{,}25 \leq S_{ij} < 1$ 78

Table 3.16 Very Influential Parameters - $1 \leq S_{ij} < 2$ 79
T**able 3.17** Extremely Influential Parameters - $S_{ij} \geq 2$ 79

1. INTRODUCTION

1.1. Nitrogen Cycle on Earth

The nitrogen element (N) is a vital nutrient for all organisms. Nitrogen is fundamental to the structures and biochemical processes that define life. This element N is cycled on Earth as shown in Figure 1.1. (Francis et al., 2007). The dinitrogen gas (N_2) in the atmosphere is transformed to ammonium ($NH_4^+ - N$) during nitrogen fixation. $NH_4^+ - N$ is oxidized by the Ammonia oxidizing bacteria (AAO) in the initial part of the nitrification process where $NH_4^+ - N$ is transformed to nitrite ($NO_2^- - N$) aerobically. The 2nd subprocess of nitrification is nitritation/nitrite oxidation and the product nitrate ($NO_3^- - N$) is obtained aerobically by nitrite oxidizing bacteria (NOB). Denitrification is the process that occurs in the absence of dissolved oxygen via heterotrophic bacteria. $NO_3^- - N$ is converted to N_2 gas during this process (Stein and Klotz, 2016). Anammox process is the short cut of nitrogen removal where the $NO_2^- - N$ used as electron acceptor by AAO and the product is directly N_2 gas (Francis et al., 2007).

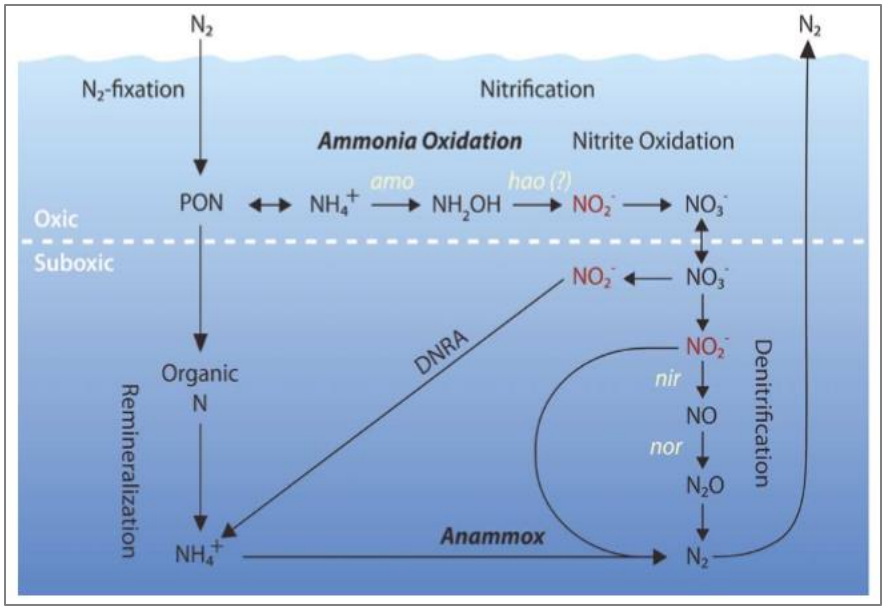

Figure 1.1. Nitrogen pathways on Earth (Francis et al., 2007)

1.2. Nitrogen Removal From Wastewater

Nitrogen can be found in wastewater as following forms : $NH_4^+ - N$, $NO_3^- - N$, $NO_2^- - N$ and organic-N. The dominant nitrogen form in raw wastewater is ammonia/ammonium (NH_3 / NH_4^+). It is necessary to remove nitrogen from wastewater in order to decrease the environmental impact of ammonia/ammonium, such as eutrophication, development of algae and aquatic plants and toxicity to aquatic life on the receiving water bodies.

The removal of nitrogen from wastewater can be done biologically, chemically or physically. However, it is commonly achieved through a nitrification-denitrification process due to being economically feasible. In this process, ammonia is biologically transformed to dinitrogen gas and returned to atmosphere. Nitrification-denitrification processes are conventional and well known but energy intensive. Over the past decade, the discoveries of new biological nitrogen pathways have made it possible to develop novel nitrogen removal processes. Anaerobic ammonium oxidation (Anammox) is the main alternative process (Mulder et al., 1995).

1.3. Conventional Biological Nitrogen Removal Technologies

1.3.1. Nitrification

Conventionally, the removal of nitrogen, typically in the form of ammonium ($NH_4^+ - N$), is accomplished by the combination of nitrification and denitrification processes. Two processes are involved in nitrification process. Firstly, $NH_4^+ - N$ is oxidized aerobically to nitrite (nitritation) by ammonia-oxidizing bacteria (AOB), secondly nitrite is oxidized to nitrate (nitratation) by nitrite oxidizing bacteria (NOB) (Sedlak, 1991). Both bacteria groups AOB and NOB are aerobic chemoautotrophs. The common species of AOB are Nitrosomonas, Nitrosococcus, Nitrosolobus and the common species for NOB are Nitrobacter, Nitrospira, Nitrospina (Metcalf & Eddy, 2014).

1.3.1.1. Stoichiometry of nitrification

NH_3/NH_4^+ are electron donor as shown in Equation 1.1.1 for AOB and NO_2^- is electron donor as shown in Equation 1.1.2 for NOB. NO_2^- is the product of nitritation process and NO_3^- is

the product of nitratation process. Mostly, the electron acceptor in this process is oxygen as shown in the Equation 1.1.3.

$$2NH_4^+ + 3O_2 \rightarrow 2NO_2^- + 4H^+ + 2H_2O \quad (1.3.1)$$

$$2NO_2^- + O2 \rightarrow 2NO_3^- \quad (1.3.2)$$

$$NH_4^+ + 2O_2 \rightarrow NO_3^- + 2H^+ + H_2O \quad (1.3.3)$$

The oxygen required for the above process is comprised of 4.57 mg O_2/ $NH_4^+ - N$ oxidized (Metcalf & Eddy, 2014).

During nitrification, alkalinity is consumed as following Equations 1.3.4-1.3.5;

$$3\ NH_4^+ + 4CO_2 + HCO_3^- + H_2O \rightarrow C_5H_7NO_2 + 5O_2 \quad (1.3.4)$$

The complete oxidation and assimilation reaction is;

$$22NH_4^+ + 37O_2 + 4CO_2 + HCO_3^- \rightarrow C_5H_7NO_2 + 21NO_3^- + 20H_2O + 42H^+ \quad (1.3.5)$$

The alkalinity is consumed during the nitrification process is 7.09 g as CaCO3/g NH_4^+-N with assuming the synthesis yield coefficient as 0.04 g VSS/g NO_2^--N (Metcalf & Eddy, 2014).

1.3.1.2. Kinetics of nitrification

The generally used nitrification kinetic is the Monod growth kinetics as given in Equation 1.3.6 and 1.3.7 for nitrification process (Metcalf & Eddy, 2014).

$$\mu_{AOB} = \mu_{max,AOB}\left(\frac{SNH}{SNH+KNH}\right)\left(\frac{SO}{SO+KO,AOB}\right) - b_{AOB} \quad (1.3.6)$$

$$\mu_{NOB} = \mu_{max,NOB}\left(\frac{SNO}{SNO+KNO}\right)\left(\frac{SO}{SO+KO,NOB}\right) - b_{NOB} \quad (1.3.7)$$

μ_{AOB} = specific growth rate of the AOB, g VSS/g VSS.d

μ_{NOB} = specific growth rate of the NOB, g VSS/g VSS.d

$\mu_{max,AOB}$ = maximum specific growth rate of the AOB, g new cells/g cells.d

$\mu_{max,NOB}$ = maximum specific growth rate of the NOB, g new cells/g cells.d

b_{AOB} = specific endogeneous decay rate of AOB g VSS lost/ g VSS.d

b_{NOB} = specific endogeneous decay rate of NOB g VSS lost/ g VSS.d

S_{NH} = NH_4-N concentration, mg/l

K_{NH} = half- velocity constant for NH_4-N, mg/l

So = DO concentration, mg/l

$K_{O,AOB}$ = half- velocity constant for DO for AOB, mg/l

S_{NO} = NO_2-N concentration, mg/l

K_{NO} = half- velocity constant for NO_2-N, mg/l

$K_{O,NOB}$ = half- velocity constant for DO for NOB, mg/l

The range of maximum specific growth rate varies between 0.25 - 0.77 g VSS/g VSS at 20 °C (Metcalf & Eddy, 2014). The following factors; pH, DO, temperature, free ammonia concentration, toxic compounds are influential for nitrification process.

1.3.2. Denitrification

The conversion of $NO_3^- - N$ to N_2 gas by consuming the organic matter is called heterotrophic denitrification (Laureni et al., 2015). Nitrification-denitrification system is energy consuming and associated with high operating costs. This process together with the carbon removal via air supply has an additional economical and environmental impact due to high biomass production and greenhouse gas emission, which promote global warming (Hu et al., 2015).

The denitrifying bacteria need an energy source for denitrification process and it utilize complex organic substances thus 3-6 grams of COD is consumed for one gram of N removed.

Therefore COD/N ratio is an important factor in wastewater treatment. As the wastewater characteristics are fluctuating in time, COD/N ratio might also be fluctuating or can be always low for a specific raw wastewater. In this case, if this ratio goes down additional carbon source (such as methanol) needed to be added for the denitrification process (Metcalf and Eddy, 2003).

1.3.2.1. Stoichiometry of denitrification

The stoichiometry of denitrification process is described as follows:

$$0.25O_2 + H^+ + e^- \rightarrow 0.5H_2O \quad (1.3.8)$$

$$0.2NO_3^- + 1.2H+ + e^- \rightarrow 1.2N_2 + 0.6H_2O \quad (1.3.9)$$

$$0.34NO_2^- + 1.36H+ + e^- \rightarrow 0.17N_2 + 0.68H_2O \quad (1.3.9)$$

The oxidation-reduction half reactions shhowed that 0.25 mole of O2 is equivalent to 0.2 mole NO_3^- for electron transfer. The O_2 equivalent of NO_3^- is (0.25 x 32 g O_2) divided by the NO_3^- equivalent (0.20 x 14 g N) equals to 2.86 g O_2/ g NO_3^--N (Metcalf and Eddy, 2003). Dissimilation and synthesis processes are presented as Equations 1.3.10-1.3.11.

$$NO_3^- + 1.08CH_3OH + 0.24H_2CO3 \rightarrow 0.056C_5H_7O_2N + 0.47N_2 + 1.68H_2O + HCO_3^- \quad (1.3.10)$$

$$NO_2^- + 0.53CH_3OH + 0.67H_2CO_3 \rightarrow 0.04C_5H_7O_2N + 0.48N_2 + 1.23H_2O + HCO_3^- \quad (1.3.11)$$

1.4. Deammonification

Deammonification is a novel nitrogen removal technology and it is a cost-efficient alternative to conventional nitrification-denitrification processes (Rothstein, 2015). Deammonification (Figure 1.2) involves two process steps: the partial nitritation of ammonia by AOB and the

subsequent anaerobic oxidation of the residual ammonia by nitrite to nitrogen gas (Rothstein, 2015).

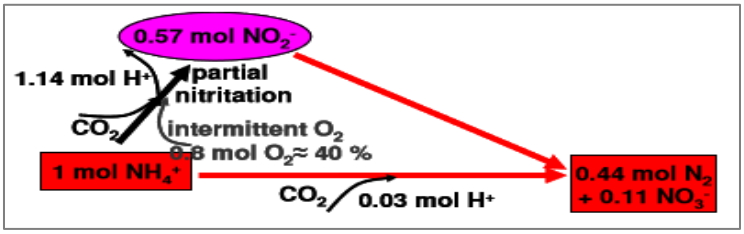

Figure 1.2. Deammonification process. (Wett et al., 2007)

Deammonification systems were initially developed for warm side stream treatment. Over the last decade there have been many full-scale side stream deammonification plants implemented with several different configurations, such as ANITA®Mox, DeAmmon, DEMON® and SHARON-ANAMMOX® (Dongen et al.,2001). Applying deammonification systems as a mainstream treatment option has been more challenging. Currently there are just few full-scale plants in the world (Wett et al. 2013).

1.4.1. Partial nitritation

Partial nitritation is preliminary step for nitrification and deammonification process. It requires a stoichiometric oxygen demand of only 40% compared to complete nitrification (Wett et al., 2007). The partial nitritation stoichiometry is presented in Equation 1.4.1. The equation includes bicarbonate to neutralize the acidity produced by the reaction.

$$2.34NH_4^+ + 1.87O_2 + 2.66HCO_3^- \rightarrow 0.02C_5H_7NO_2 + NH_4^+ + 1.32NO_2^- + 2.55CO_2 + 3.94H_2O \quad (1.4.1)$$

1.4.2. Anaerobic ammonium oxidation (Anammox)

In the mid of 1990s, the Anammox bacteria (AAO) and their pathway in the nitrogen cycle has been investigated (Mulder et al., 1995). The process is performed by anaerobic species within the phylum Planctomycete. The following species are the defined Anommox species until now and divided into five genera: (i) Candidatus Kuenenia, (ii) Candidatus Brocadia

(iii) Anammoxoglobus, (iv) Candidatus Jettenia 1 and (v) Candidatus Scalindua (Kartal et al., 2013) (Figure 1.3). The optimum temperature condition range for AAO is reported as between 30 - 40 °C (WEF, 2015).

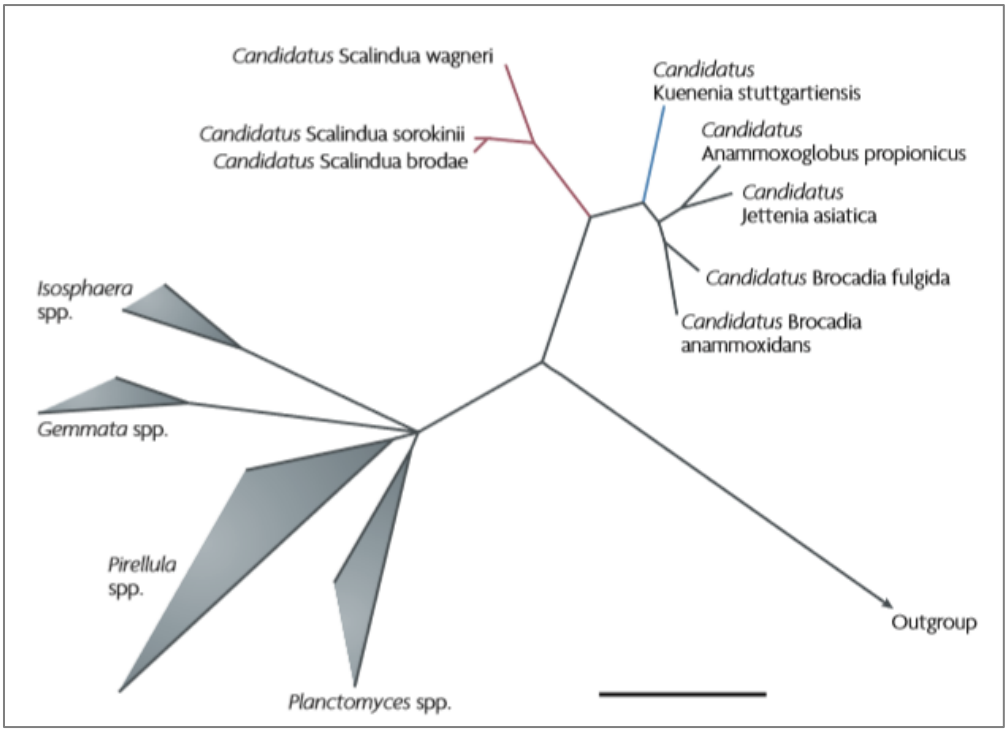

Figure 1.3 A 16s ribosomal rNA-gene-based phylogenetic tree of anammox bacteria (Kuenen, 2008)

1.4.2.1. Stoichiometry of Anammox

Anommox Process is an anaerobic/anoxic process where the NO_2^- is electron acceptor, NH_4^+ is electron donor for AAO. The products of this process are N_2 gas and NO_3^- shown in Equations 1.4.1 (Klaus et al., 2017.; Strous et al., 1998).

$$NH_4^+ + 1.32\ NO_2^- + 0.066\ HCO_3^- + 0.13\ H^+ \rightarrow 0.26\ NO_3^- + 1.02\ N_2 + 0.066 CH_2\ O_{0.5}\ N_{0.15} + 2.03 H_2O \quad (1.4.3)$$

The ratio of NH_4^+ to NO_2^- is 1:1.32 and a ratio of NH_4^+ to NO_3^- is 1:0.26 (Equation 1.4.3). Anammox bacteria are autotrophs. In overall reaction of Anammox, 1 mole HCO_3^- is consumed to oxidize 15 mole NH_4^+ and produce 0.23 mg of alkalinity as $CaCO_3$. 0.26 mol of NO_3^- is produced. Maximum specific growth rate of the Anammox bacteria around 0.054-

0.2 d^{-1} (Strous et al., 1999). Based on the study of Van Hulle et al., 2010, hydroxylamine or hydrazine dosing to the system was increased the Anammox activity.

1.4.2.2. Kinetics of Anammox

The specific growth rate of Anammox (μ_{AN}) is expressed by the Monod model (Yao et al., 2015).

$$\mu_{AN} = \mu_{MAX,AN}\left(\frac{S_{NH_4}}{K_{AN,SNH_4^+}+S_{NH_4^+}}\right)\left(\frac{S_{NO_2}}{S_{NO_2}+K_{AN,SNO_2}}\right) \quad (1.4.4)$$

In this kinetic;

μ_{AN} = specific growth rate of anammox, g VSS/g VSS

$\mu_{MAX,AN}$ = maximum specific growth rate, g VSS/g VSS

S_{NH4} and S_{NO2} = NH_4^+-N and NO_2^--N concentrations in the bulk, mg/l

$K_{AN,SNH4}$ = NH_4^+-N half saturation constants for anammox, mg/l

$K_{SNO2,AN}$ = NO2--N half saturation constants for anammox, mg/l

1.4.3. Deammonification Configurations

There are two main process configurations for the deammonification process; (Rothstein, 2015) (Figure 1.4)

- Two Stage Deammonification Process: It runs in two separate reactors. First reactor is used for partial nitritation and second one is used for Anammox process to denitrify the products to N_2 gas (Dongen et al., 2001).
- Single Stage Deammonification Process: Partial nitritation and Anammox processes are applied in a single process unit (Klaus et al., 2017).

In the deammonification systems, the bacteria growth type can be suspended growth, granular sludge, biofilm or hybrid (both suspended and attached growth). SBR systems (Tikilili, 2016), Upflow anaerobic sludge blanket (UASB) systems (Abma et al., 2007),

moving bed biofilm reactors (MBBR) (Christensson et al., 2013) and IFAS (Trela, 2015) are the most common configurations for suspended growth, granular, attached growth and hybrid applications, respectively.

The AOB grows very slowly and they are very sensitive to temperature fluctuations (Rothstein, 2015; Suarez et al., 2015). The biofilm carriers are useful and safe for slow-growing and temperature-sensitive bacteria (Boltz et al., 2009). Moreover, they provide separated zones (anaerobic, anoxic and oxic) as biofilm layers on the surface of the media. Today, in the deammonification applications the most used biofilm reactors are either the IFAS reactor with activated sludge or MBBR reactor without activated sludge.

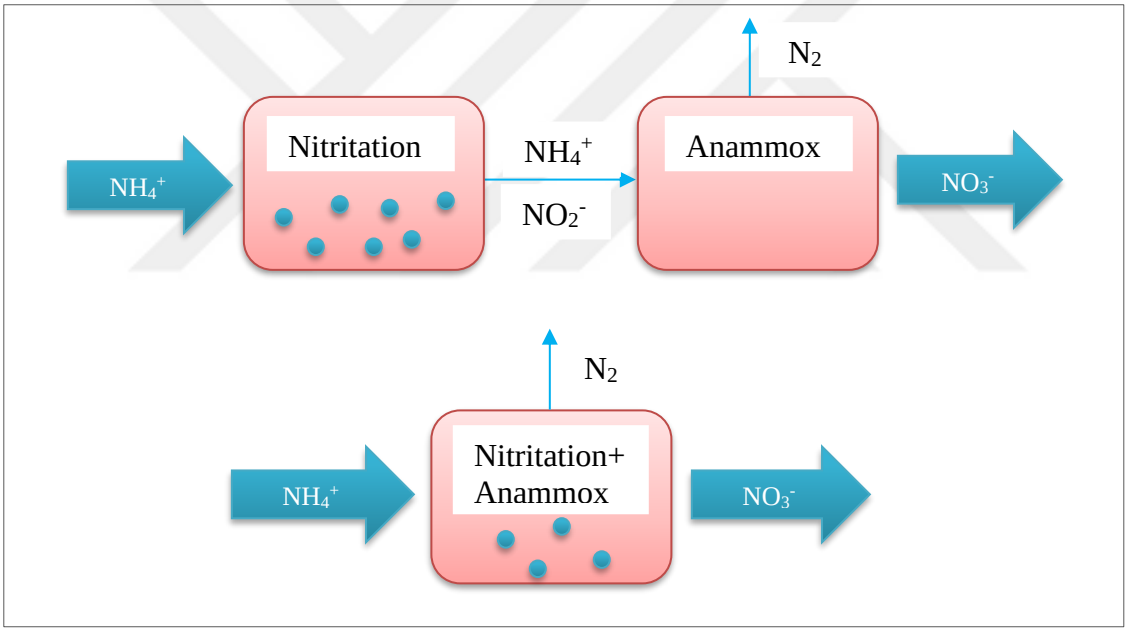

Figure 1.4 Two-stage and single-stage deammonification systems (Growth and Metabolism of Anammox Bacteria, 2008)

1.5. MBBR Type Deammonification Systems

1.5.1. Description of MBBR

MBBR systems (Figure 1.5) was discovered in 1980s (Odegard, 1980). The main component of the MBBR systems is plastic biofilm carrier media, which is lighter than water (Boltz et al., 2011). This media is circulated/mixed by aeration equipment in aerated reactors ensuring

excellent oxygen and substrate transfer to the biomass. In anoxic or anaerobic conditions the mixer in the reactor does the mixing of the received wastewater. The considerable advantages of the MBBR systems are smaller footprint area, lower sludge production and higher resistance to the flow and load fluctuations (Metcalf & Eddy, 2003). In addition, the MBBR is a continuous-flow process that does not require a special operational cycle for biofilm thickness control (Boltz et al., 2011).

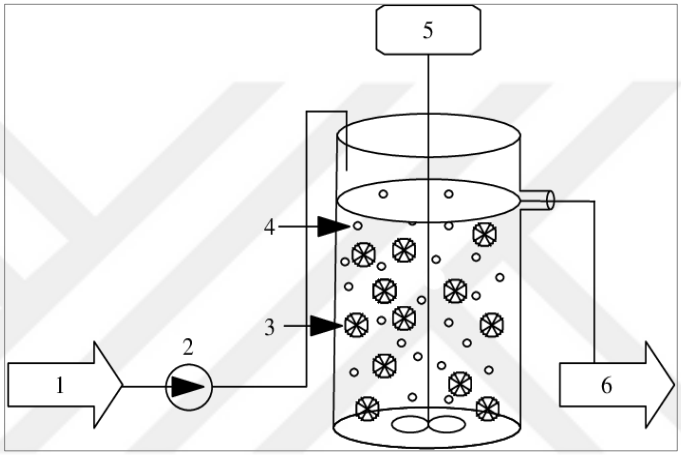

Figure 1.5. Schematic view of MBBR system (1) inlet, (2) pump, (3) biofilm carrier, (4) air bubble in case of aerobic conditions,(5) mixer, runs only during the anoxic/anaerobic conditions, (6) outlet (Chamorro et al., 2010)

Source of figures : Va Tech Wabag ®, AnoxKaldnes®, Multi Umwelttechnologie AG®

Figure 1.6 Different types of MBBR carriers

In a deammonification MBBR (Figure 1.3), the conversion of $NH_4^+ - N$ takes place in the biofilm attached to the plastic media in which AerAOB exist on the exterior of the biofilm, while AnAOB exist deeper within the biofilm in an anoxic environment (Figure 1.4) (Lackner et al., 2014).

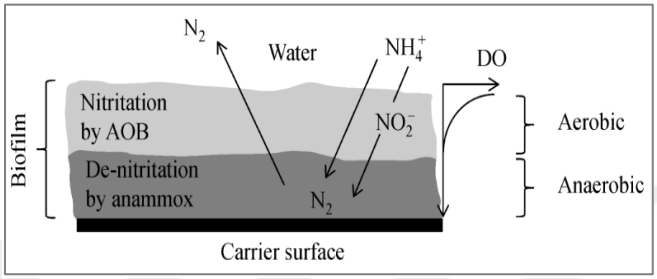

Figure 1.7. Biofilm layers in media carrier for deammonification process (Ødegaard, 2016)

1.6. Modelling of MBBR Type Deammonification Systems

1.6.1. Biofilm Kinetics

Biofilms are essential part of an MBBR model. The mass balance and substrate fluxes in MBBR systems are fundamentally different compared to conventional kinetics in activated sludge models. The biofilm thickness and density may vary, and on between the biofilm and the bulk liquid there is a stagnant liquid film (diffusion boundary layer) which limits the substrate diffusion to and from the biomass (Zhu and Chen, 2001). The substrate concentrations vary depending on the thickness of the biofilm, as shown in Figure 1.8. The following equations describe the substrate flux and utilization rate as well as the mass balance in a biofilm process.

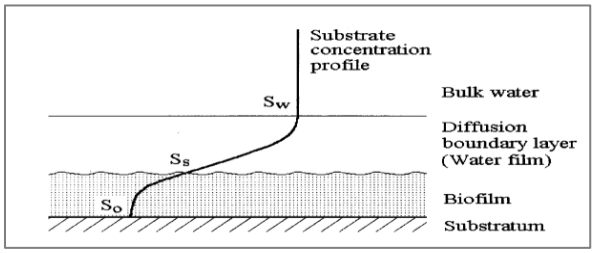

Figure 1.8 Conceptual profile of substrate concentration in a biofilm environment (Zhu and Chen, 2001).

Substrate flux from bulk liquid to biofilm over the stagnant layer:

$$r_{sf} = -D_w \frac{dS}{dx} - D_w \frac{(S_b - S_s)}{L} \quad (1.6.1)$$

where r_{sf} = rate of substrate surface flux, g/m^2·d

D_w = diffusion coefficient of substrate in water, m^2/d

dS/dx = substrate concentration gradient, g/m^3·m

S_b = bulk liquid substrate concentration, g/m^3

S_x = substrate concentration at outer layer of biofilm, g/m^3

L = effective thickness of stagnant film, m

Thickness of the stagnant layer depends on process design and fluid properties. Choosing higher bulk liquid velocities produces thinner films and greater flux rates.

Mass transfer of substrate in biofilm is governed by Fick's law with a modified diffusion constant for the effect of the biofilm structure on diffusion (Metcalf and Eddy,2014):

$$r_{bf} = -D_e \frac{dS_f}{dx} \quad (1.6.2)$$

where r_{bf} = rate of substrate flux in biofilm due to mass transfer, g/m^2·d

D_e = effective diffusivity coefficient in biofilm, m^2/d

dS_f/dx = substrate concentration gradient, g/m^3·m

Substrate utilization rate at any given point (Metcalf and Eddy,2014):

$$r_{su} = \frac{kS_f X}{K_s + S_f} \quad (1.6.3)$$

where r_{su} = rate of substrate utilization in biofilm, g/m^2·d

k = maximum specific substrate utilization rat, g substrate/g microorganisms·d

S_f = substrate concentration at a point in the biofilm, g/m^3

X = biomass (microorganism) concentration, g/m^3

K_s = half-velocity constant, sustrate concentration at one-half the maximum specific substrate utilization rate, g/m^3

The general mass balance for the biofilm can be expressed as (Metcalf and Eddy,2014):

$$D\frac{d^2S_f}{dx^2} - X\left(\frac{kS_f}{K_s+S_f}\right) = 0 \qquad (1.6.4)$$

assuming that the substrate flux through the stagnant layer equals the flux at the biofilm surface and that the flux through the carrier media does not exist. (Metcalf & Eddy, 2014).

In addition to biofilm kinetics, attachment and detachment of biofilm have significant impact on the process. Biase et al. (2019) described biofilm attachment and detachment in well-structured manner. Biofilm attaches to the surface through various steps. In successive order: adsoprtion to the surface, cell transportation, adhesion and permanent attachement occure before mature biofilm is formed. Throughout the steps microcolonies and extra-cellular polymeric substances are produced. The last stage is an equilibrium between growth and detachment. Parts of the biofilm are detached due to mechanical phenomena: carrier collision, erosion by liquid shear forces, sloughing or grazing by protozoa or metazoa. (Rittmann et al., 2018).

1.6.2. General information regarding modelling

Both physical and mathematical modeling are required to research the potential of the deammonification systems and estimating its prospects for biotechnology (Nikolaeva et al.,2017). A model is as a purposeful representation or description of a system of interest. Models simplify the reality, describing a system that is important to understand and deal with. Time and scale are the most impactful aspects of a model. In general, the model state from the perspective of time are frozen, dynamic or steady state and equilibrium. Models usually describe the dynamic state, the state where variations occur as a function of time. Frozen

state means that the process will change in time but not in the period of interest. Steady state or equilibrium conditions are states where the process occurs so rapidly that the rate of change exceeds the dynamics that one is interested in (Henze et al., 2008).

Modelling includes using or developing mathematical tools for the integration of knowledge concerning specific phenomena. It is a useful tool in experimental designing, the evaluation of experimental results and testing hypotheses. It also helps to reveal correlations between different variables, to predict the evolution of a system, and in the design of optimized processes and management strategies (Magri et al., 2007).

There are several types of models, which can be categorized as follows; physical, verbal or conceptual and mathematical model. A physical one is a spatial scale representation of a system. A verbal or conceptual model is a qualitative description, usually developed from detailed observations; these models can be shown as schematic diagrams (e.g. flow diagrams). A mathematical model is a quantitative description: with a mathematical model, it is possible to formulate the rates of the processes or reactions affecting the system. The mathematical formulations need to be incorporated in a solving procedure that takes care of the physical constraints and characteristics within the system boundaries (e.g. temperature and mixing conditions) (Wentzel and Ekama, 1997). Model building process methodology is presented in Figure 1.9.

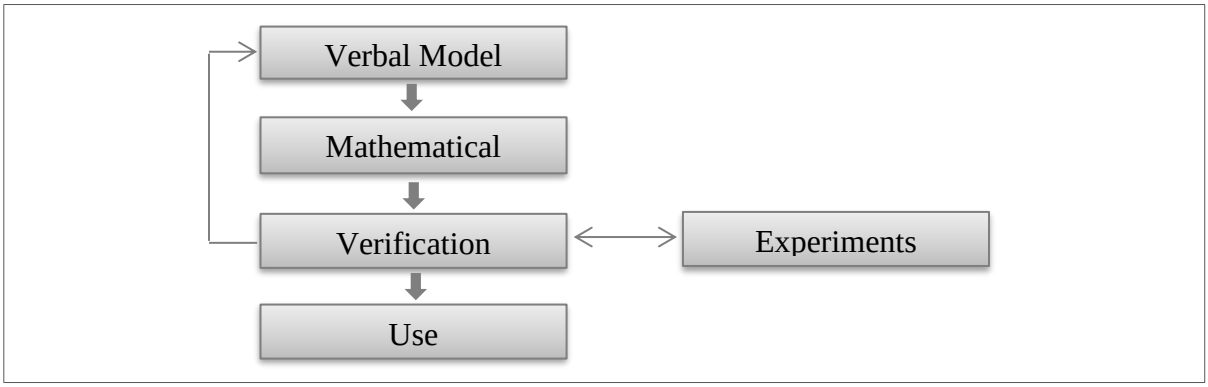

Figure 1.9. Model Building Process (Peterson et al., 2002)

Building up a wastewater treatment model requires the following steps:

- Definition of the model purpose or the objectives of the simulation study
- Model selection
- Determination of the hydraulic models
- Wastewater and biomass characterization
- Calibration of the activated sludge model parameters
- Model falsification
- Scenario evaluation.

Biofilm systems are complex and heterogeneous aggregates (Figure 1.5). Building such a model is advantageous and includes the steps mentioned above with additional details.

The most renowned and utilized mathematical models for activated sludge processes are the Activated Sludge Models (ASM) by the International Water Association (IWA). The Activated Sludge Model No.1 (ASM1) (Henze et al. 1987) which is first version of ASMs was published in 1987. This version was able to simulate dynamically the organic matter and the nitrification/denitrification processes. In ASM2 (Henze et al. 1995), phosphorus removal module was included. ASM2d includes denitrifying phosphorus-accumulating organisms (Henze et al. 1999). The latest model, ASM3 (Gujer et al. 1999) is a last development of ASM1 and ASM2.

The ASMs can be considered best available technology (BAT) and are used across platforms modelling wastewater treatment plants. They consist of a set of differential equations describing the dynamics of the state variables. As an activated sludge model is independent of the type and the size of the reactor because it describes a conversion process. An ASM can work together with models for other processes used in STPs as well.
The kinetic equations and the stoichiometry of the deammonification model are presented as Figures 1.10 and 1.11, respectively.

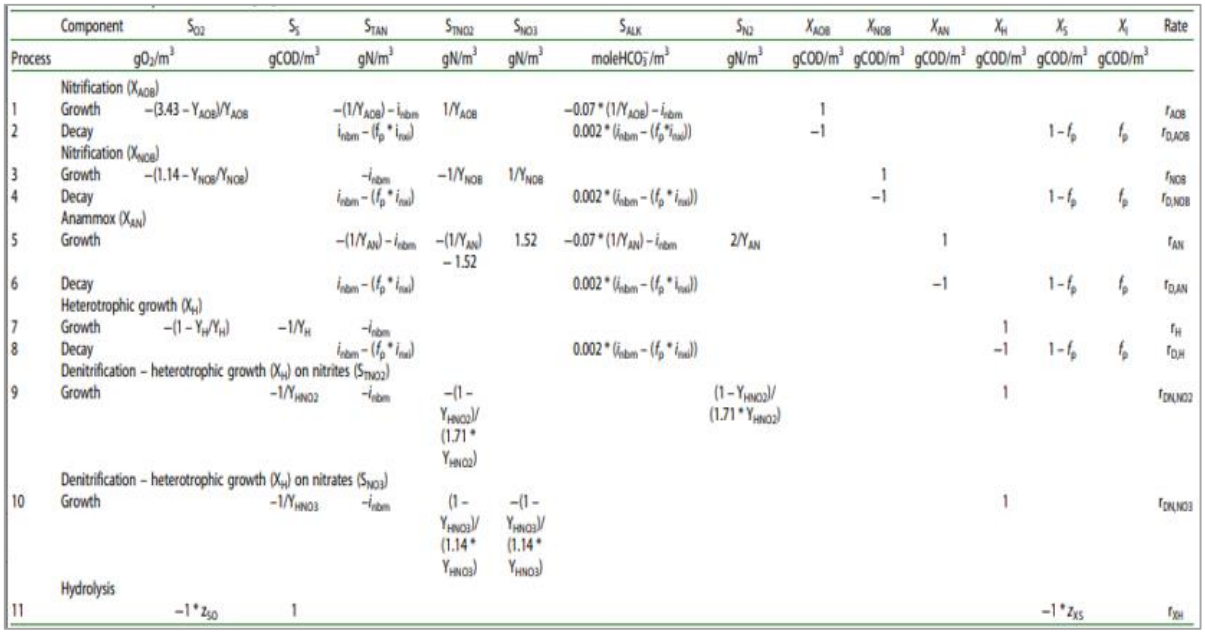

Process	Component	S_{O2} gO_2/m^3	S_S $gCOD/m^3$	S_{TAN} gN/m^3	S_{NO2} gN/m^3	S_{NO3} gN/m^3	S_{ALK} $moleHCO_3^-/m^3$	S_{N2} gN/m^3	X_{AOB} $gCOD/m^3$	X_{NOB} $gCOD/m^3$	X_{AN} $gCOD/m^3$	X_H $gCOD/m^3$	X_S $gCOD/m^3$	X_I $gCOD/m^3$	Rate
	Nitrification (X_{AOB})														
1	Growth	$-(3.43-Y_{AOB})/Y_{AOB}$		$-(1/Y_{AOB})-i_{nbm}$	$1/Y_{AOB}$		$-0.07*(1/Y_{AOB})-i_{nbm}$		1						r_{AOB}
2	Decay			$i_{nbm}-(f_p*i_{ns})$			$0.002*(i_{nbm}-(f_p*i_{ns}))$		−1				$1-f_p$	f_p	$r_{D,AOB}$
	Nitrification (X_{NOB})														
3	Growth	$-(1.14-Y_{NOB}/Y_{NOB})$		$-i_{nbm}$	$-1/Y_{NOB}$	$1/Y_{NOB}$				1					r_{NOB}
4	Decay			$i_{nbm}-(f_p*i_{ns})$			$0.002*(i_{nbm}-(f_p*i_{ns}))$			−1			$1-f_p$	f_p	$r_{D,NOB}$
	Anammox (X_{AN})														
5	Growth			$-(1/Y_{AN})-i_{nbm}$	$-(1/Y_{AN})-1.52$	1.52	$-0.07*(1/Y_{AN})-i_{nbm}$	$2/Y_{AN}$			1				r_{AN}
6	Decay			$i_{nbm}-(f_p*i_{ns})$			$0.002*(i_{nbm}-(f_p*i_{ns}))$				−1		$1-f_p$	f_p	$r_{D,AN}$
	Heterotrophic growth (X_H)														
7	Growth	$-(1-Y_H/Y_H)$	$-1/Y_H$	$-i_{nbm}$								1			r_H
8	Decay			$i_{nbm}-(f_p*i_{ns})$			$0.002*(i_{nbm}-(f_p*i_{ns}))$					−1	$1-f_p$	f_p	$r_{D,H}$
	Denitrification – heterotrophic growth (X_H) on nitrites (S_{NO2})														
9	Growth		$-1/Y_{HNO2}$	$-i_{nbm}$	$-(1-Y_{HNO2})/(1.71*Y_{HNO2})$			$(1-Y_{HNO2})/(1.71*Y_{HNO2})$				1			$r_{DN,NO2}$
	Denitrification – heterotrophic growth (X_H) on nitrates (S_{NO3})														
10	Growth		$-1/Y_{HNO3}$	$-i_{nbm}$	$(1-Y_{HNO3})/(1.14*Y_{HNO3})$	$-(1-Y_{HNO3})/(1.14*Y_{HNO3})$						1			$r_{DN,NO3}$
	Hydrolysis														
11		$-1*z_{SO}$	1										$-1*z_{XS}$		r_{XH}

Figure 1.10 Stoichiometry of the deammonification model (Trojanowicz et al. 2017)

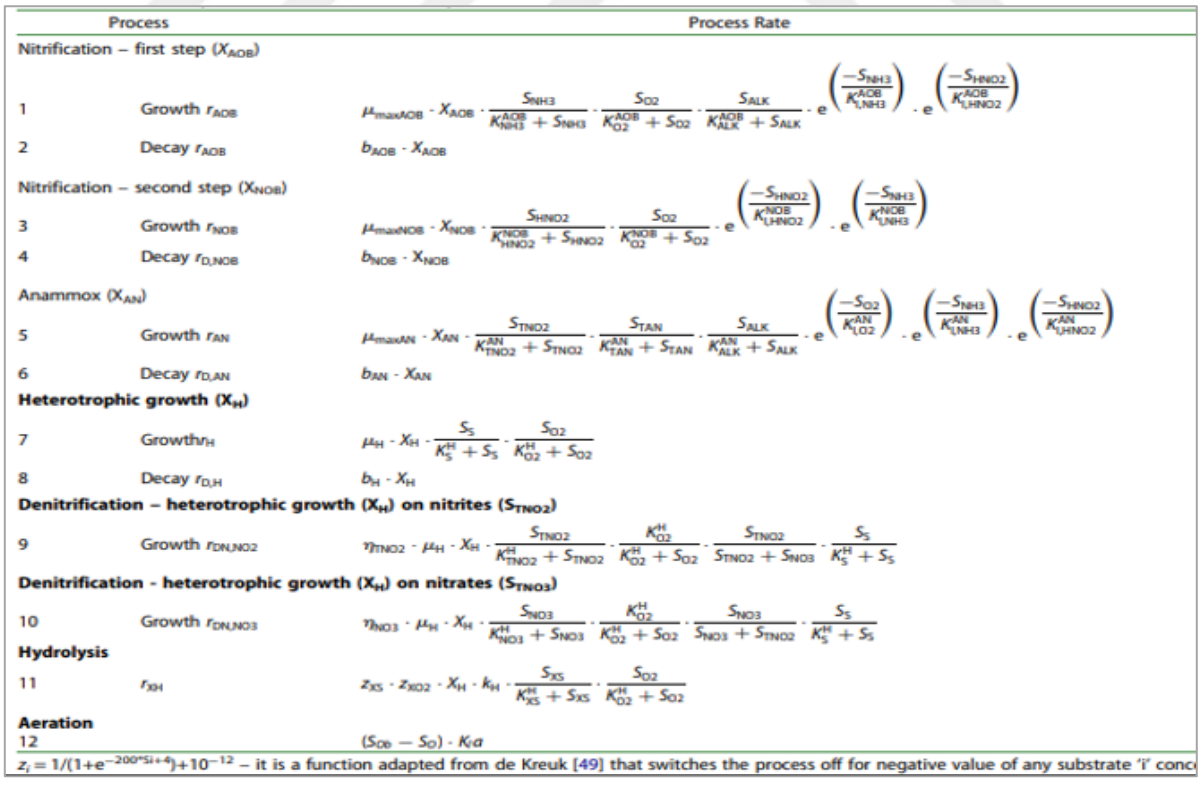

Process		Process Rate
Nitrification – first step (X_{AOB})		
1	Growth r_{AOB}	$\mu_{maxAOB}\cdot X_{AOB}\cdot\frac{S_{NH3}}{K^{AOB}_{NH3}+S_{NH3}}\cdot\frac{S_{O2}}{K^{AOB}_{O2}+S_{O2}}\cdot\frac{S_{ALK}}{K^{AOB}_{ALK}+S_{ALK}}\cdot e^{\left(\frac{-S_{NH3}}{K^{AOB}_{I,NH3}}\right)}\cdot e^{\left(\frac{-S_{HNO2}}{K^{AOB}_{I,HNO2}}\right)}$
2	Decay r_{AOB}	$b_{AOB}\cdot X_{AOB}$
Nitrification – second step (X_{NOB})		
3	Growth r_{NOB}	$\mu_{maxNOB}\cdot X_{NOB}\cdot\frac{S_{HNO2}}{K^{NOB}_{HNO2}+S_{HNO2}}\cdot\frac{S_{O2}}{K^{NOB}_{O2}+S_{O2}}\cdot e^{\left(\frac{-S_{HNO2}}{K^{NOB}_{I,HNO2}}\right)}\cdot e^{\left(\frac{-S_{NH3}}{K^{NOB}_{I,NH3}}\right)}$
4	Decay $r_{D,NOB}$	$b_{NOB}\cdot X_{NOB}$
Anammox (X_{AN})		
5	Growth r_{AN}	$\mu_{maxAN}\cdot X_{AN}\cdot\frac{S_{TNO2}}{K^{AN}_{TNO2}+S_{TNO2}}\cdot\frac{S_{TAN}}{K^{AN}_{TAN}+S_{TAN}}\cdot\frac{S_{ALK}}{K^{AN}_{ALK}+S_{ALK}}\cdot e^{\left(\frac{-S_{O2}}{K^{AN}_{I,O2}}\right)}\cdot e^{\left(\frac{-S_{NH3}}{K^{AN}_{I,NH3}}\right)}\cdot e^{\left(\frac{-S_{HNO2}}{K^{AN}_{I,HNO2}}\right)}$
6	Decay $r_{D,AN}$	$b_{AN}\cdot X_{AN}$
Heterotrophic growth (X_H)		
7	Growthr_H	$\mu_H\cdot X_H\cdot\frac{S_S}{K^H_S+S_S}\cdot\frac{S_{O2}}{K^H_{O2}+S_{O2}}$
8	Decay $r_{D,H}$	$b_H\cdot X_H$
Denitrification – heterotrophic growth (X_H) on nitrites (S_{TNO2})		
9	Growth $r_{DN,NO2}$	$\eta_{TNO2}\cdot\mu_H\cdot X_H\cdot\frac{S_{TNO2}}{K^H_{TNO2}+S_{TNO2}}\cdot\frac{K^H_{O2}}{K^H_{O2}+S_{O2}}\cdot\frac{S_{TNO2}}{S_{TNO2}+S_{NO3}}\cdot\frac{S_S}{K^H_S+S_S}$
Denitrification - heterotrophic growth (X_H) on nitrates (S_{TNO3})		
10	Growth $r_{DN,NO3}$	$\eta_{NO3}\cdot\mu_H\cdot X_H\cdot\frac{S_{NO3}}{K^H_{NO3}+S_{NO3}}\cdot\frac{K^H_{O2}}{K^H_{O2}+S_{O2}}\cdot\frac{S_{NO3}}{S_{NO3}+S_{TNO2}}\cdot\frac{S_S}{K^H_S+S_S}$
Hydrolysis		
11	r_{XH}	$z_{XS}\cdot z_{XI02}\cdot X_H\cdot k_H\cdot\frac{S_{XS}}{K^H_{XS}+S_{XS}}\cdot\frac{S_{O2}}{K^H_{O2}+S_{O2}}$
Aeration		
12		$(S_{Ob}-S_O)\cdot K_La$

$z_i = 1/(1+e^{-200*Si+4})+10^{-12}$ – it is a function adapted from de Kreuk [49] that switches the process off for negative value of any substrate 'i' conc

Figure 1.11 Kinetic equations of the deammonification model (Trojanowicz et al. 2017)

1.6.3. Simulation Softwares

In a mathematical model, there are a great number of calculations, interpolations and extrapolations running simultaneously. Complex models are avaliable and they are able to describe and predict the multidimensional spatial heterogeneous structure of biofilms. However, solving the equations takes a long time. To accelerate the progress of models, some computer-based simulation programs are used. A group of the commercial biofilm modelling software are shown in Table 1.1.

It is possible to model a deammonification MBBR system via BioWin® 6.0, Simba®, WEST ® etc. Among these simulators, BioWin® 6.0 software (Figure 1.12) was selected for this study due to the available knowledge of this software and the available features observed to be adventageous specifically for this work such as user-friendly, having MBBR deammonification model since August 2014.

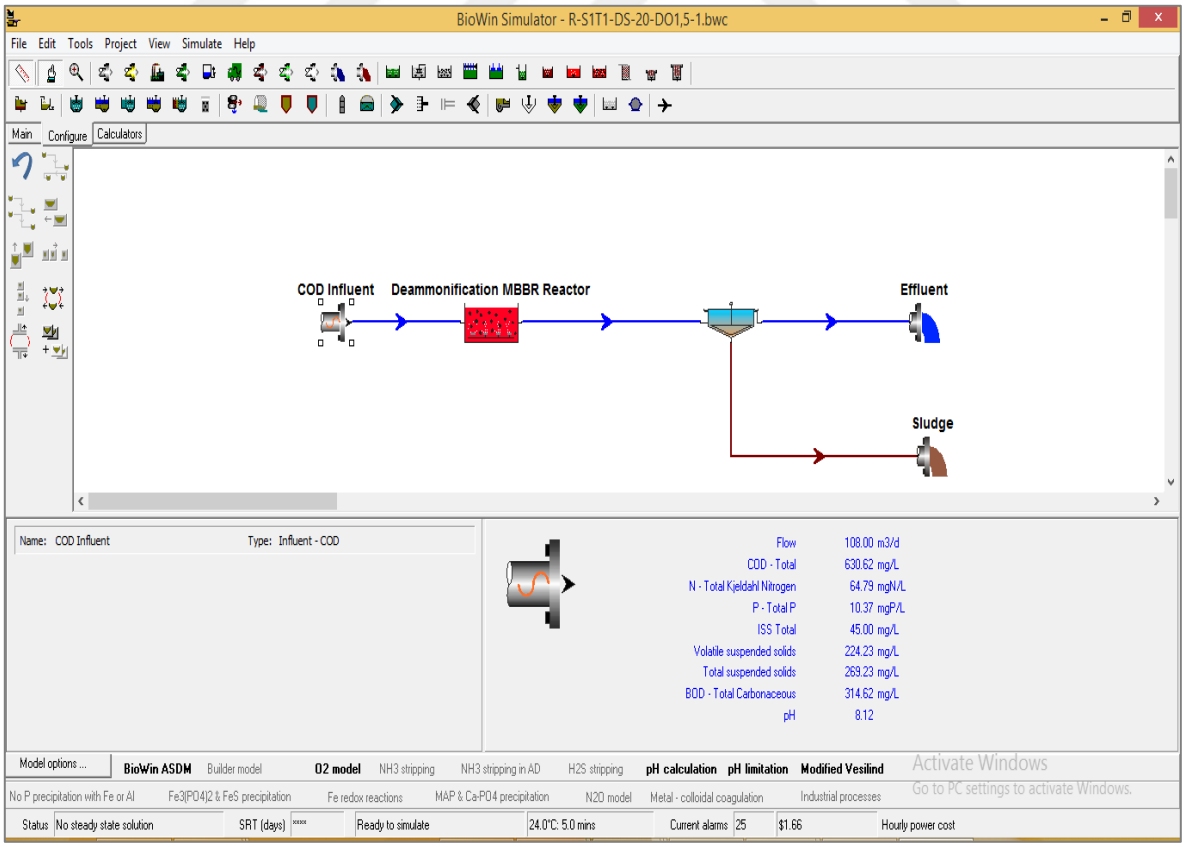

Figure 1.12 Example screenshot of drawing board in BioWin® 6.0.

Table 1.1. A group of available simulators that includes biofilm reactor models.

Name	Source	Biofilm Model	
		Model type and biomass distribution	**Reference**
AQUASIM	EAWAG, Swiss Federal Institute of Aquatic Science and Technology. Dübendorf/Switzerland	1-D, DY, N; Heterogeneous	Wanner and Gujer (1985) Wanner and Reichert (1996)
AQUIFAS	Aquaregen, Mountain View, California	1-D, SE, N; Heterogeneous	Sen and Randal (2008a, 2008b, 2008c)
BioWin	EnviroSim Assoc. Ltd. Flamborough/ Canada	1-D, DY, N; Heterogeneous	Esa (2007)
GPS-X	Hydromantis, Inc. Hamilton/Canada	1-D, DY, N; Heterogeneous	Hydromantis inc (2002)
Pro2d	CH2M HILL Inc. Englewood/ Colorado	1-D, SS, N(A); Heterogeneous	Boltz, Johnson, Daigger, Sandino, Elenter (2009)
Simba	ifak Gmbh, Magdeburg/Germany	1-D, DY, N; Heterogeneous	Wanner and Gujer (1985)
STOAT	WRc. Withshire / England	1-D, DY, N; Heterogeneous	Wanner and Gujer (1985)
WEST	MOST for WATER, Kortrjik/Belgium	1-D, DY, N(A)a, Nb; Heterogeneous	Rauch et al (1999)

SS: Steady State, DY: Dynamic, SE: Semi empirical, N: Numerical, N(A): Numerical using analytical solutions

1.7. BioWin® 6.0 Software

BioWin® 6.0 is a wastewater treatment process simulator (https://envirosim.com). BioWin® 6.0 utilizes an activated sludge/anaerobic digestion (ASDM) model. There are three solver options in BioWin®; Newton-Raphson, Hybrid and Decoupled Linear search. The default solver used in BioWin® 6.0 is hybrid solver and includes both first and third options in it (BioWin Help Manual, 2019).

BioWin includes many treatment options such as:

- Primary settling tanks
- Activated sludge (all possible configuration)
- Trickling Filter
- SBR, variable volume reactors
- MBBR, IFAS, MBR
- Anaerobic and aerobic Digestion
- Thickening and dewatering
- Other elements such as metal addition, equalization tanks, splitter etc.

Always active processes for activated sludge systems in BioWin® 6.0 are as follows:

- Growth and decay of Ordinary Heterotrophic Organisms
- Growth and decay of Methylotrophs
- Hydrolysis, adsorption, ammonification and assimilative denitrification
- Growth and decay of Ammonia Oxidizing Biomass
- Growth and decay of Nitrite Oxidizing Biomass
- Growth and decay of Anaerobic Ammonia Oxidizers (AAO)
- Growth and decay of Phosphorus Accumulating Organisms (BioWin Help Manual, 2019).

Side stream reactor was first released within BioWin® 4.1 which is the base of the model in this study. BioWin® 6.0 which released on June 2019 was used in this study since it is the last updated version currently. It includes newly added sulphur model, colloidal COD / metal interactions model, iron oxidation / reduction reactions model and many other new features

for users.

Side stream processes include one or more/combination of below listed processes in BioWin® 6.0:

- Nitritation mediated by ammonia oxidizing autotrophic bacteria (AOB) or partial nitritation.
- Nitratation mediated by nitrite oxidizing autotrophic bacteria (NOB).
- Denitritation mediated by ordinary heterotrophic organisms (OHOs) where nitrite serves as an electron acceptor on the addition of organic substrate with production of nitrogen gas.
- Denitratation mediated by heterotrophic bacteria where nitrate serves as an electron acceptor on the addition of organic substrate with production of nitrite.
- Nitrogen removal by autotrophic anaerobic ammonia oxidizing bacteria (AAO) (BioWin Help Manual, 2019).

The key process aspects for side-stream process is presented in Figure 1.13.

Process Aspect	Model Process	Important Considerations
Nitrification	• AOB growth and decay • NOB growth and decay	Different growth rates, temperature dependencies and inhibition effects.
Heterotrophic Denitrification	• Growth on substrate through denitritation (using nitrite as an electron acceptor) • Growth on substrate through denitratation (using nitrate as an electron acceptor)	Differences in yield must be accounted for.
Deammonification (ANAMMOX™)	Growth and decay of AAO	Appropriate inhibitions (*i.e.* nitrite toxicity) and limitations must be included.
pH	All significant equilibrium relationships (*i.e.* nitric and nitrous acid, ammonia and carbonate system)	pH modeling is essential because, for example, some inhibition effects are caused by unionized species concentrations.
Gas-liquid interactions	Stripping of certain model components such as ammonia and carbon dioxide	Gas-liquid interactions are essential to represent pH and in some cases, to properly represent growth-limiting conditions.

Figure 1.13 Summary of key process aspects for side-stream process (BioWin Help Manual, 2019).

2. MATERIALS AND METHODS

2.1 Description of The Bursa Deammonification Pilot Plant

The study has been done based on the data acquired from the MBBR deammonification pilot plant which has been started up in 2018 in Bursa Dogu STP/Turkey (Figure 2.1).

The pilot plant is a single-stage mainstream deammonification MBBR system. This pilot plant was started up with mixed activated sludge seed from Bursa Doğu STP, no Anammox seed was used.The pilot reactor was operated as Sequencing Batch Reactor (SBR) for initial attachment of activated sludge on carriers. After that it was operated as continuous flow stirred-tank reactor (CSTR).

Figure 2.1 Deammonification MBBR pilot plant in Bursa Doğu STP/Turkey.

Pilot reactor is designed to be provide both continous and batch running options. Pilot reactor fed with a submersible pump with the capacity of 4.5 m^3/h located at the outlet of grit chamber of Bursa Doğu STP. Active volume of the pilot reactor is 50 m^3 and 35 % of the reactor is filled with biofilm media which has 550 m^2/m^3 specific surface area (Table 2.1). Aeration required for partial nitritation was supplied through medium buble disc diffusers connected to roots type blower. Aeration pattern was controlled due to constant set DO controlled by PID in SCADA system. The pH was kept around 7.3-8.0 by dosing acid/base through SCADA system. There are 3 vertical shaft submersible mixers which are running during both aerated and unaerated periods in the system.

$NH_4^+ - N$, $NO_3^- - N$, $NO_2^- - N$ analyses were done continuously. Temperature, pH, DO and

ORP were also continously monitored and recorded through probes located in the middle of the tank.

Table 2.1 Carrier characteristics - Aquaflex®

Parameter	Specification	Unit
Diameter of carrier	26	mm
Width of carrier	10	mm
Surface area	550	m^2/m^3
Material	PP	-
Hole numbers	19	pcs.

2.2 General Description of Modelling Studies for the Start-up Phase of MBBR Type Deammonification Pilot Plant in Bursa

This study aimed to model the start-up phase of Bursa mainstream deammonification pilot plant in different perspectives.

The study mainly consists of three main parts: (i) steady-state simulations, (ii) sensitivity analysis, (iii) dynamic simulations.

In steady-state simulations, it was aimed to study the effect of changing the operational conditions mainly DO and temperature on reactor performance together with microbial population distribution. For this purpose two different set-ups were consolidated. In Set-up 1, all simulations were performed avarage design values of Bursa mainstream influent (Table 2.2). In Set-up 2 simulations, main aim was to observe the effect of nitrite spike into the reactor in order to accelerate the enrichment of Anammox species. Hence, Set-up 2 simulations were done using Bursa mainstream average design values in addition of nitrite spike (0.55 m^3/d, 2000-8000 mg/l) to reactor regularly in unaerated periods.

Sensitivity analysis were performed as a preliminary study for dynamic simulations in order to decide the stoichiometric and kinetic coefficients having significant influence on the results and hence valuable to change during calibration of dynamic simulation results due to the plant results.

Lastly, dynamic simulation of the pilot plant were done using real influent data of the plant for a specific time period. Output of simulation were compared with the real plant effluent data.

Table 2.2 Design avarage influent values of Bursa Doğu STP

Parameter	Unit	Concentration
TSS	mg/l	267
COD	mg/l	533
BOD	mg/l	267
TN	mg/l	63
TP	mg/l	11
SO_4^-	mg/l	96
Tmin	˚C	10
Tave	˚C	20
Tmax	˚C	25

2.3 Consolidation of Mainstream Deammonification Set-up For Pilot Plant in BioWin® 6.0 Software

BioWin® 6.0 software was used as simulation tool in this study. Biowin is a wastewater treatment simulator which is a product of EnviroSim Associates Ltd (https://envirosim.com).

The steps for building an MBBR type deammonification configuration in BioWin® software is schematically described in Figure 2.2. These steps might change based on the selected configuration for any other deammonification systems.

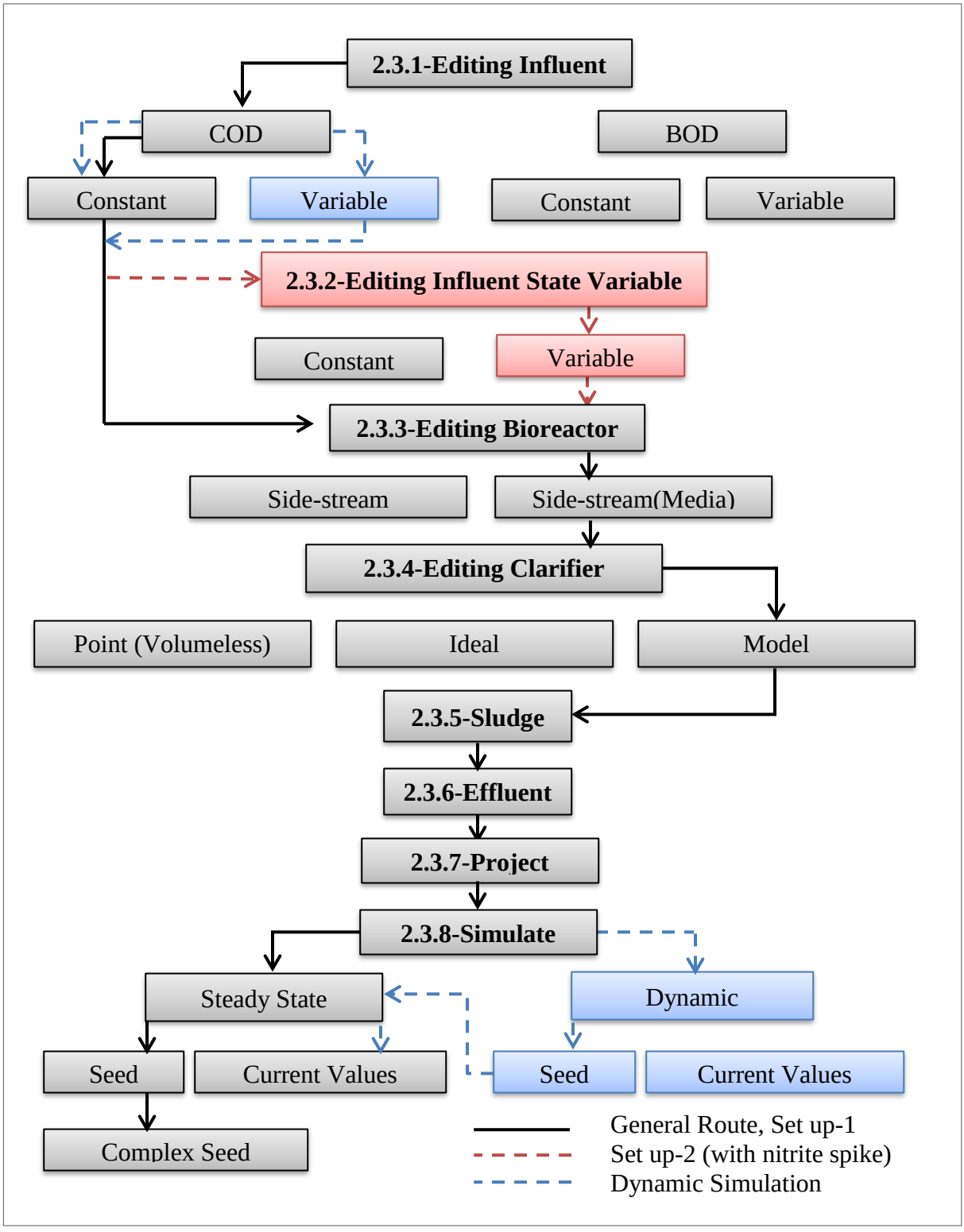

Figure 2.2 General description of MBBR deammonification configuration set-up consolidation in BioWin® 6.0.

2.3.1 Editing influent

The influent type can be chosen as COD or BOD (Figure 2.3). After choosing the influent type, BioWin® 6.0 provides two options for input type in influent editor. It can be either constant input that considers the influent as fixed or variable input which allows the user to simulate variations in the influent.

In this study, inlet flow was fixed as 108 m^3/d.

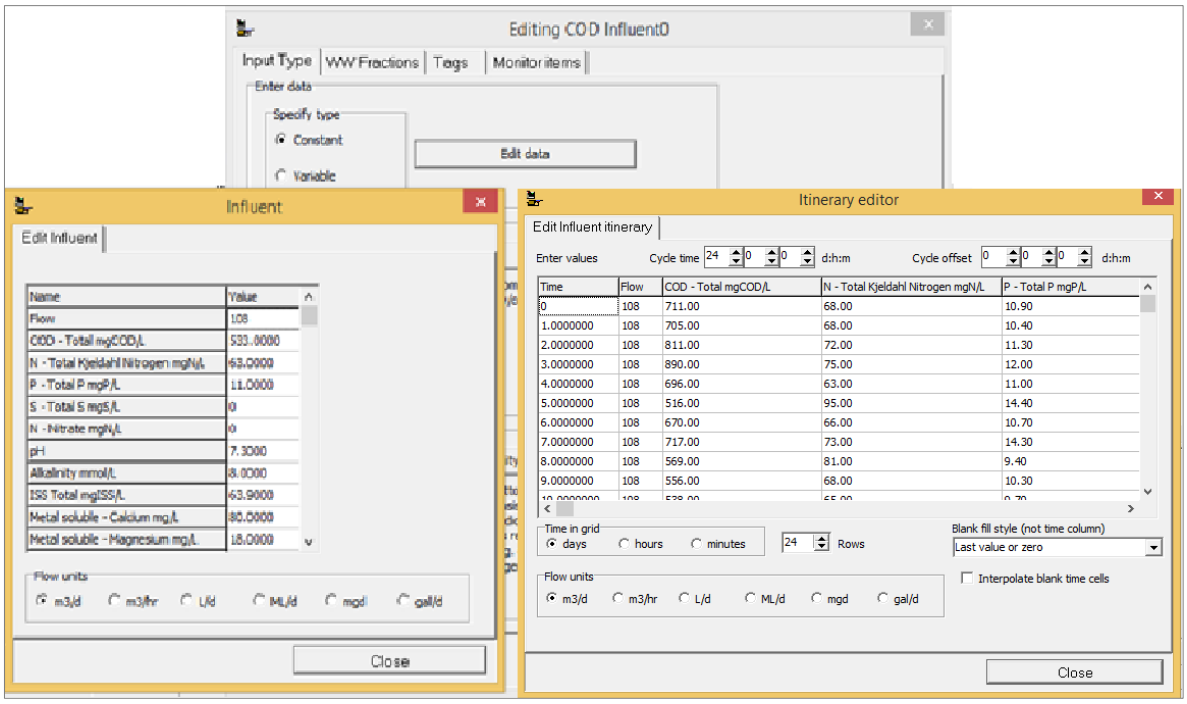

Figure 2.3 Editing influent in BioWin® 6.0.

2.3.2 Editing influent state variable

This choice is necessary for chemical addition (Figure 2.4). In this study, nitrite spike which was done only in Set-up 2 simulations requires nitrite addition from sidestream. Concentration of nitrite is used as input value in side-stream editor page. However, simulation requires addition of opposite charged ion for the balance of water chemistry in this case. Therefore, a cation should be added as equivalent opposite charged ion. Influent state variable element has the same options for input type as influent element. Input can be

constant or variable. In this study, variable option has been selected for Set-up 2 simulations in order to simulate nitrite spike which is done only during anoxic periods.

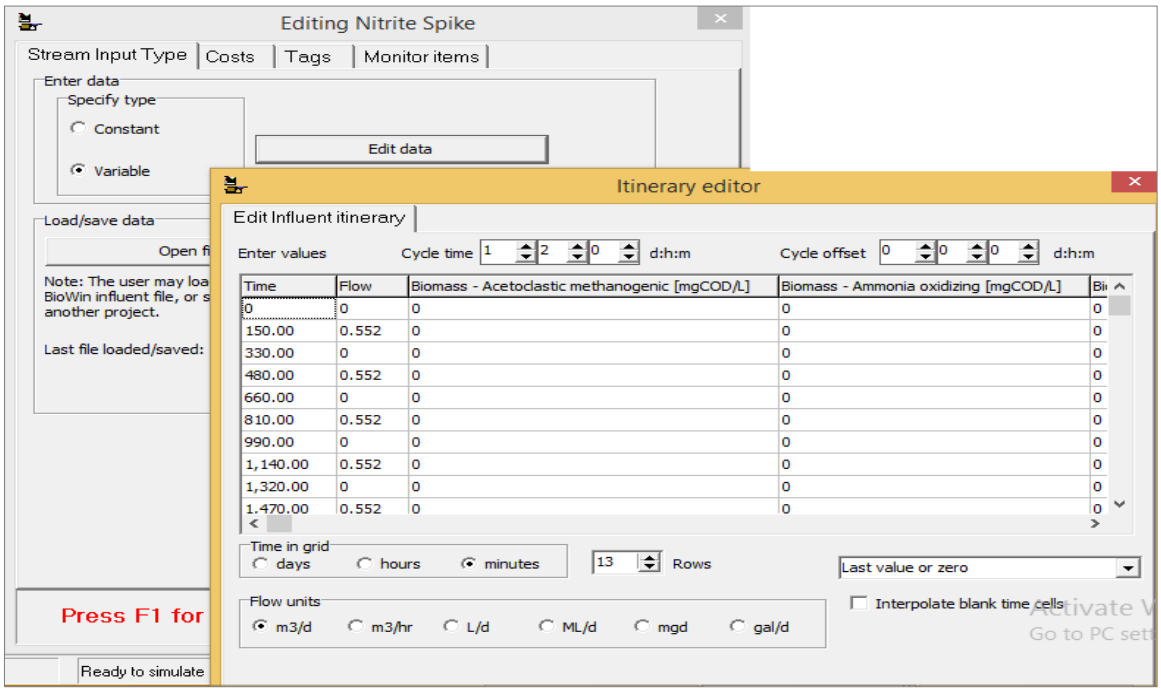

Figure 2.4 Editing influent state variable element in BioWin® 6.0

2.3.3 Editing bioreactor

Available bioreactor types for deammonification configurations in BioWin® 6.0 software are side-stream bioreactor and side-stream (Media) bioreactor. The only difference between them is growth type of biological system in the tank. The side-stream reactor has suspended growth system while side-stream (Media) bioreactor has attached-growth system. In this study side-stream media bioreactor has been chosen based on the existing pilot plant.

The details of bioreactor such as volume and dimensions, filling ratio, specific surface area of media are input in dimensions page of bioreactor editor (Figure 2.5). Aeration method and aeration pattern are input in operation page of bioreactor editor (Figure 2.5). Aeration method can be selected as DO setpoint, air flow rate or un-aerated. If it is selected as DO setpoint then there are two options to set the DO in the tank. It can be simulated as constant DO or scheduled DO. In this study, it was selected as scheduled DO in order to simulate aeration

pattern in single-stage deammonification reactor. Aeration pattern input is done in itinerary editor page by considering the anoxic and oxic durations in the reactor. It is possible to simulate the time grid as days, hours or minutes.

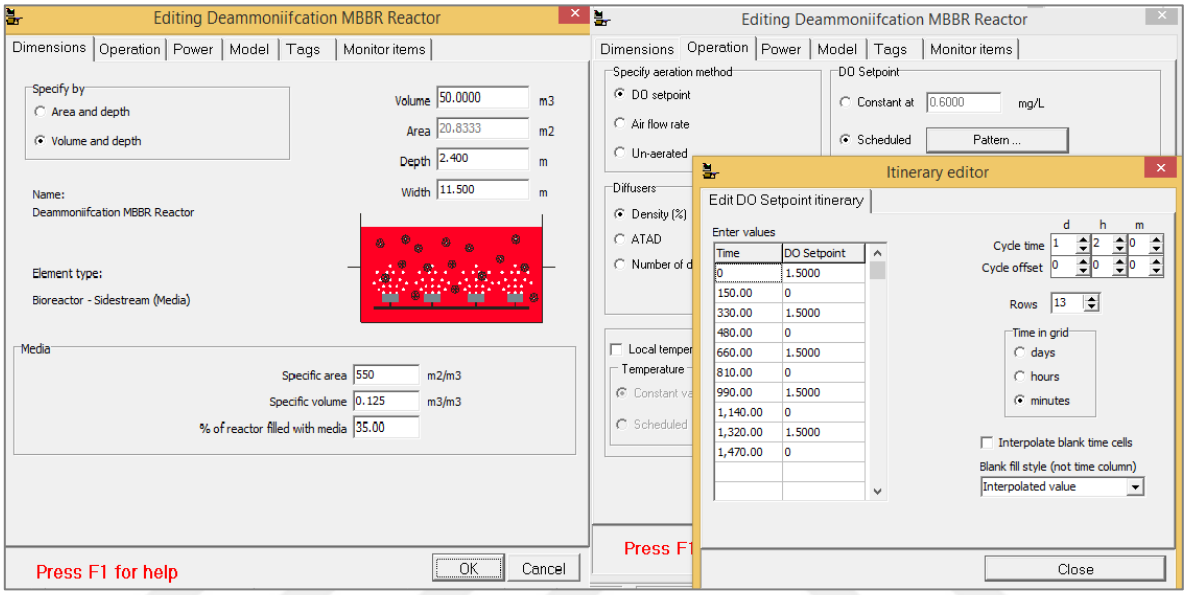

Figure 2.5 Editing side-stream (media) bioreactor element in BioWin® 6.0

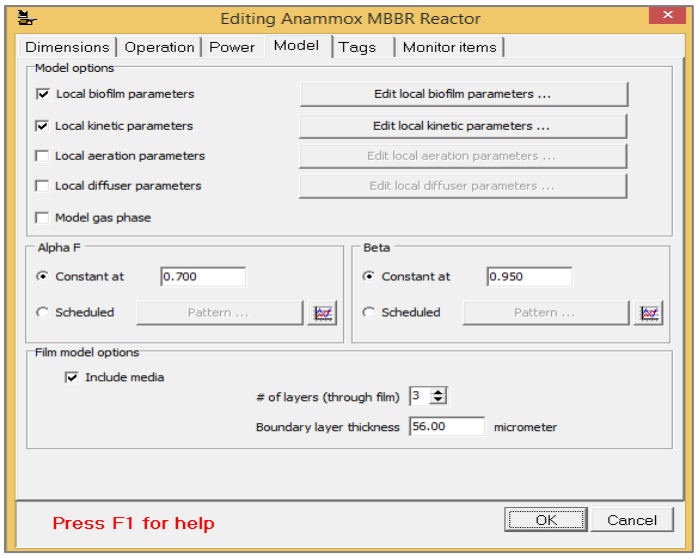

Figure 2.6 Editing model page of side-stream bioreactor element in BioWin® 6.0

In this study, volume of the reactor, specific area of media carrier, biofilm thickness and

filling ratio of the reactor were fixed based on the pilot plant information which is given in section 2.1.

2.3.4 Editing clarifier

Adding clarifier element to the configuration is optional based on the desired configuration of deammonification system such as IFAS or to have regular sludge removal component in the configuration. There are 3 options for clarifier type: point, ideal and model. Ideal (secondary) clarifier is suitable for settling of solid material in a sewage water from activated sludge liquor that is founded on an idealized particulate separation model. It is possible to fix the flow split methods, biological reaction, solids separation model and the physical properties of the ideal clarifier element. Point clarifier is similar to ideal clarifier. The greatest difference is that this element is without a volume and modelling of the biological reactions in the clarifier is not possible. The model (secondary) clarifier element (Figure 2.7) has the same features as ideal (secondary) clarifier except it is based on one-dimensional flux model.In this study, model clarifier was selected for the set-ups. Volume and depth values of clarifier were entered in dimensions section of clarifier editor page. Waste activated sludge (WAS) flow rate was entered in flow split section of clarifier editor page.

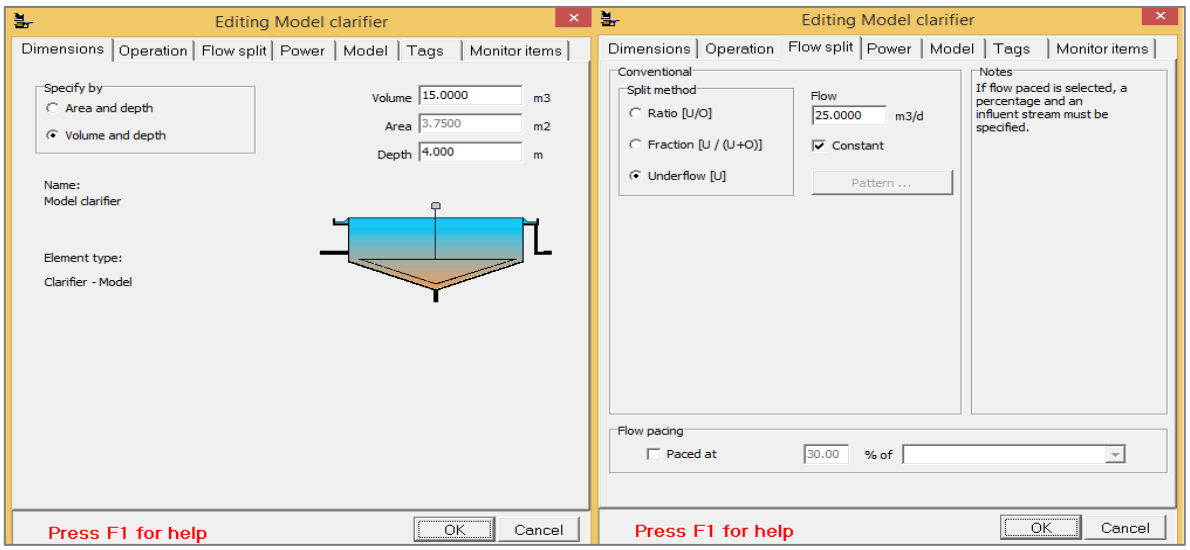

Figure 2.7 Editing model clarifier element in BioWin® 6.0.

2.3.5 Sludge

Sludge element (Figure 2.8) does not include model in it. It is an end point for the line which comes from upstream element. There is no specific input needed for sludge element.The input of WAS flowrate is done in clarifier element.

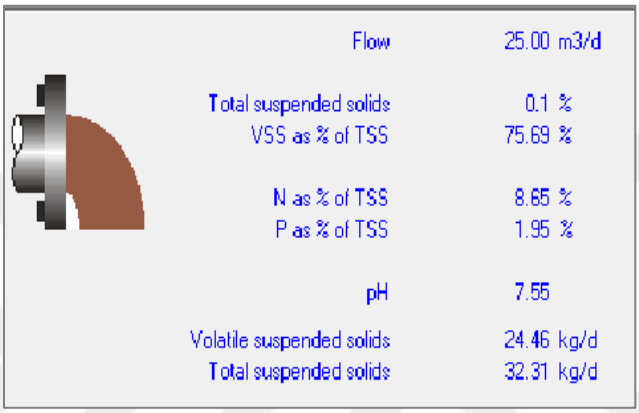

Figure 2.8 Screenshot of sludge element in BioWin® 6.0

2.3.6 Effluent

There is no model related in the effluent element. As such, it is a conduit and the final element in the chain used in a configuration. It shows the effluent results which is coming from the upstream element (Figure 2.9). In this study it shows the results after model clarifier.

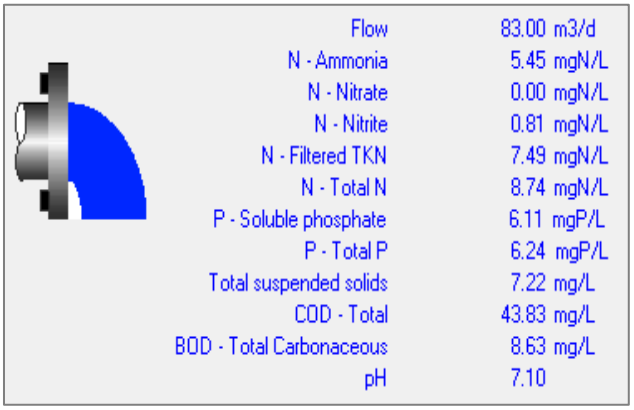

Figure 2.9 Screenshott od effluent element in BioWin® 6.0

2.3.7 Project

Parameters, liquid temperature and current project options are set from project button in BioWin® 6.0 window.

Adjustable parameters in BioWin® 6.0 are aeration/mass transfer (Figure 2.10), kinetic (Figure 2.11), stichiometric (Figure 2.11), settling (Figure 2.12), biofilm (Figure 2.12), physical/chemical (Figure 2.13) and other general parameters (Figure 2.13). Software uses default values unless user change it. In this study, default parameters were used for set-up 1 and set-up 2 simulations.

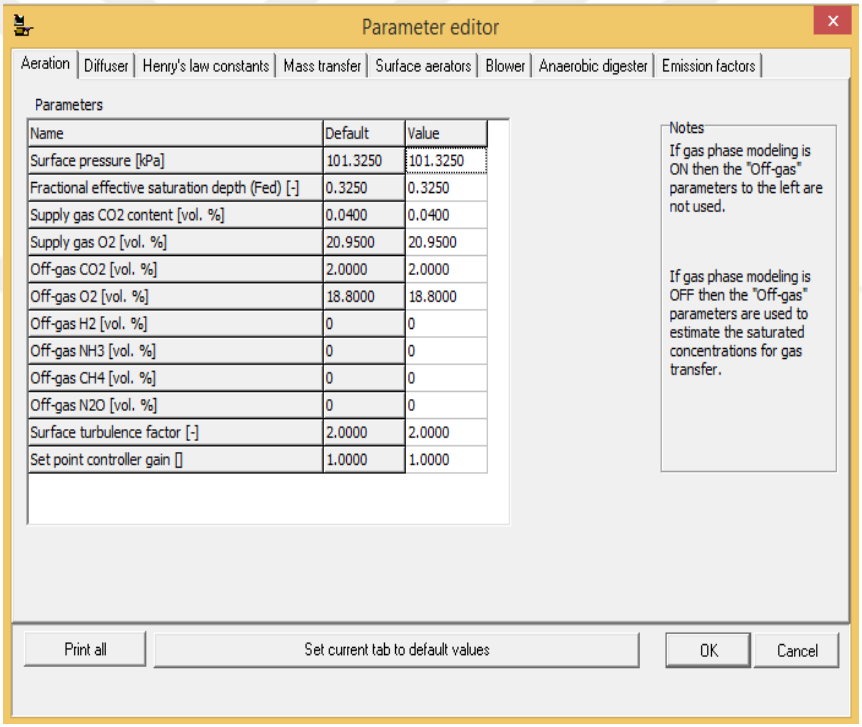

Figure 2.10 Aeratiom/mass transfer parameter editor

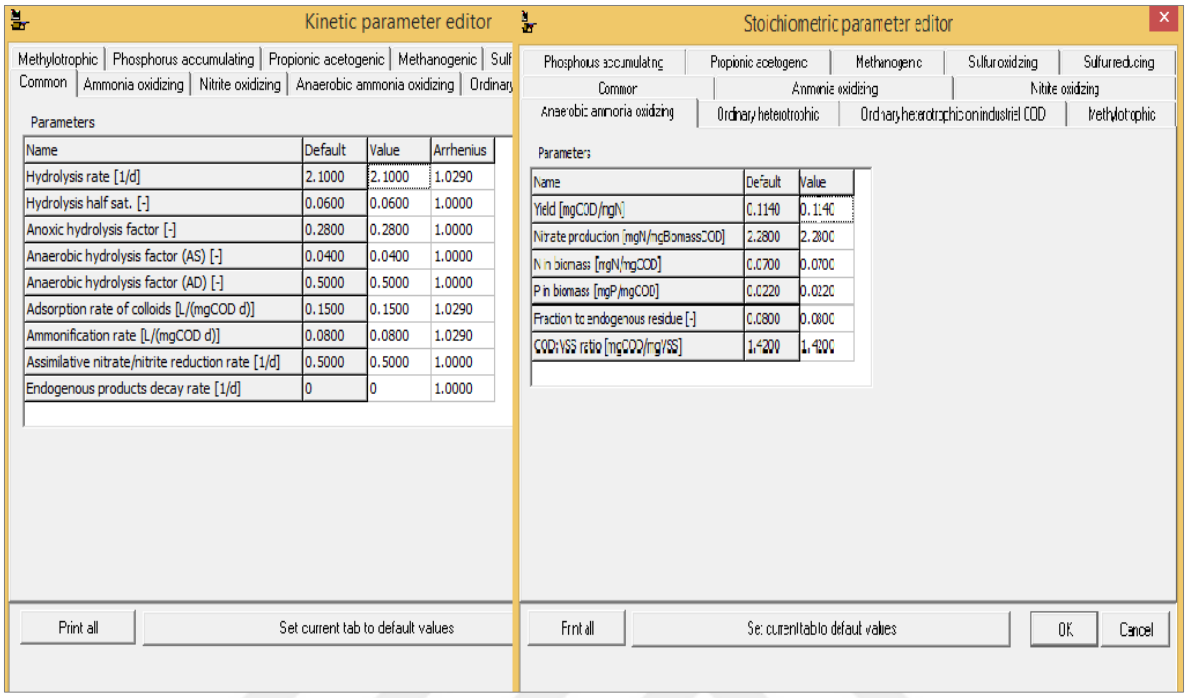

Figure 2.11 Kinetic parameters and Stoichiometric parameter editors in BioWin® 6.0

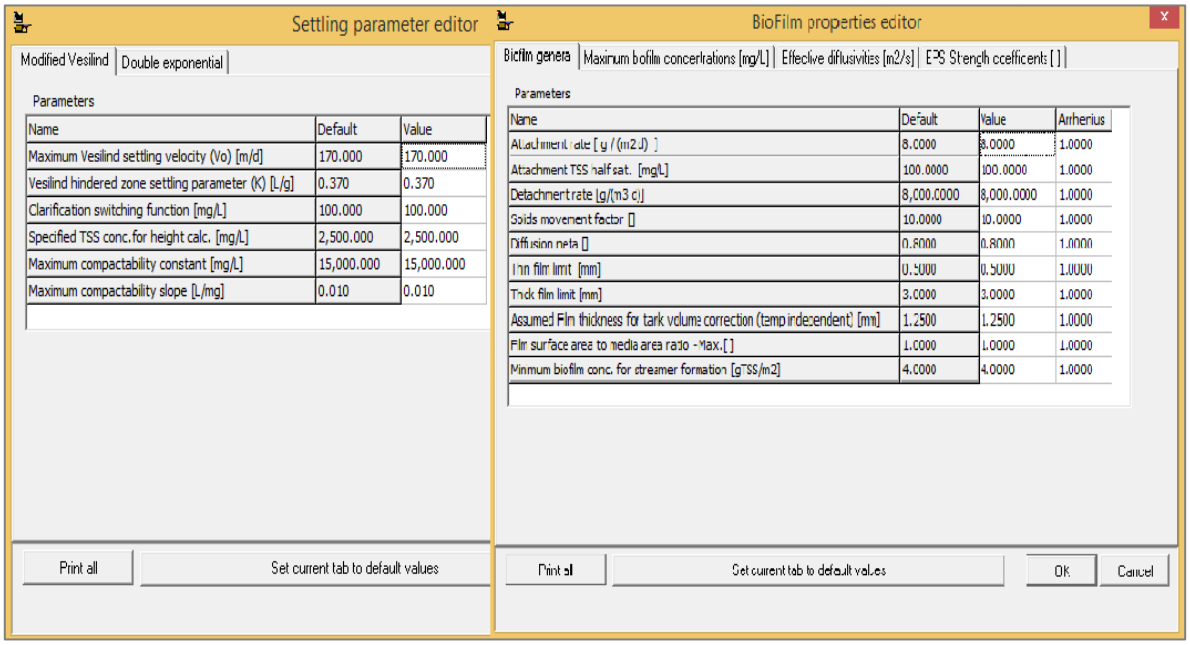

Figure 2.12 Settling parameter and Biofilm properties editors in BioWin® 6.0.

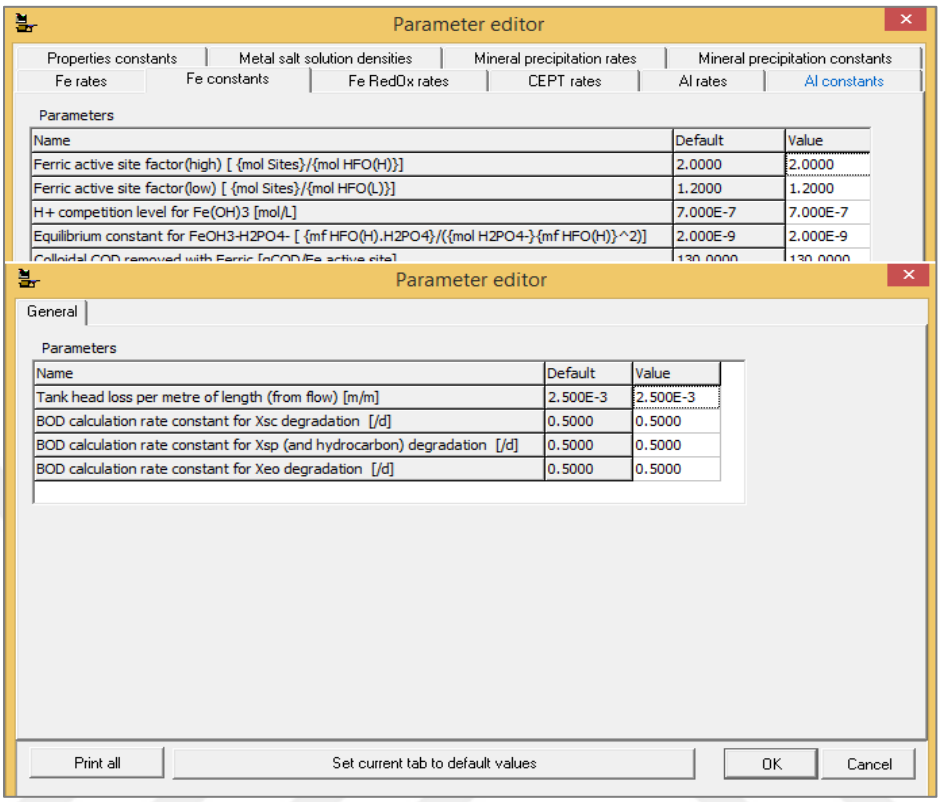

Figure 2.13 Physical/chemical parameter and other parameters editors in BioWin® 6.0.

Liquid temperature can be set as constant or scheduled under the subitem of *plant* which is in *project* menu. In this study, scheduled option is used only for dynamic simulations (Figure 2.14). However it is possible to define local temperature to specific bioreactors if needed.

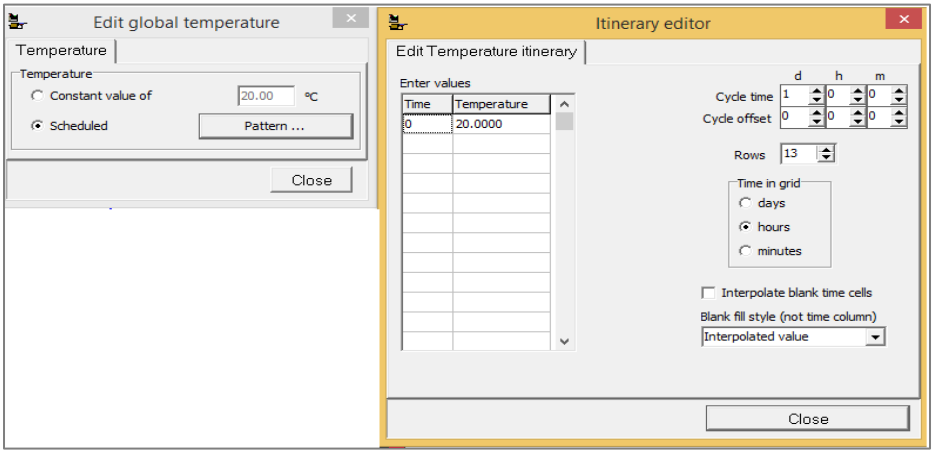

Figure 2.14 Temperature editing in BioWin® 6.0

The adjustable items in current project options editor (Figure 2.15). are related to more detalied settings in the model. Model page allows the user to include or exlude available model options in the simulation. In numerical parameters page, the user can choose the numerical solver type and the specific ranges of numerical solvers by clicking options button (Figure 2.16).

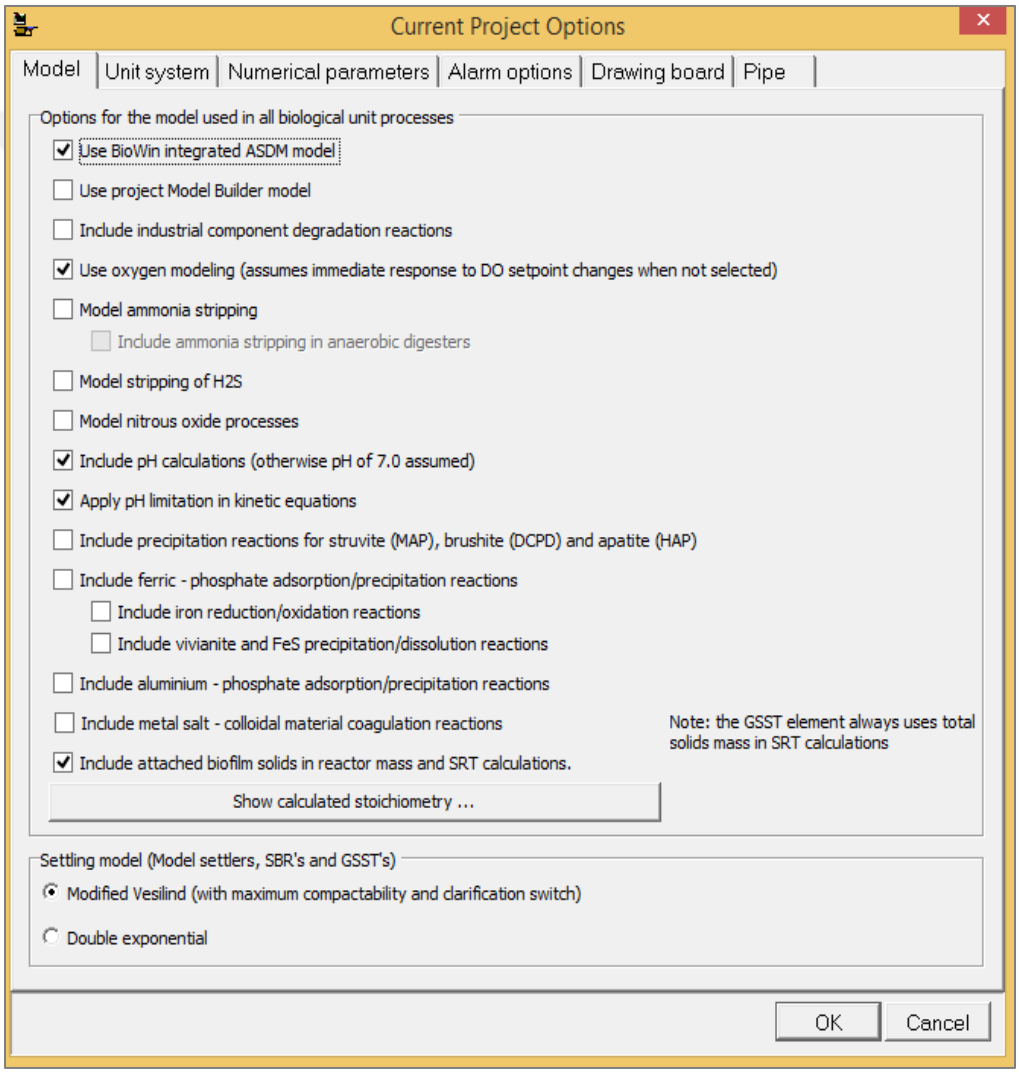

Figure 2.15 Project options page in BioWin® 6.0

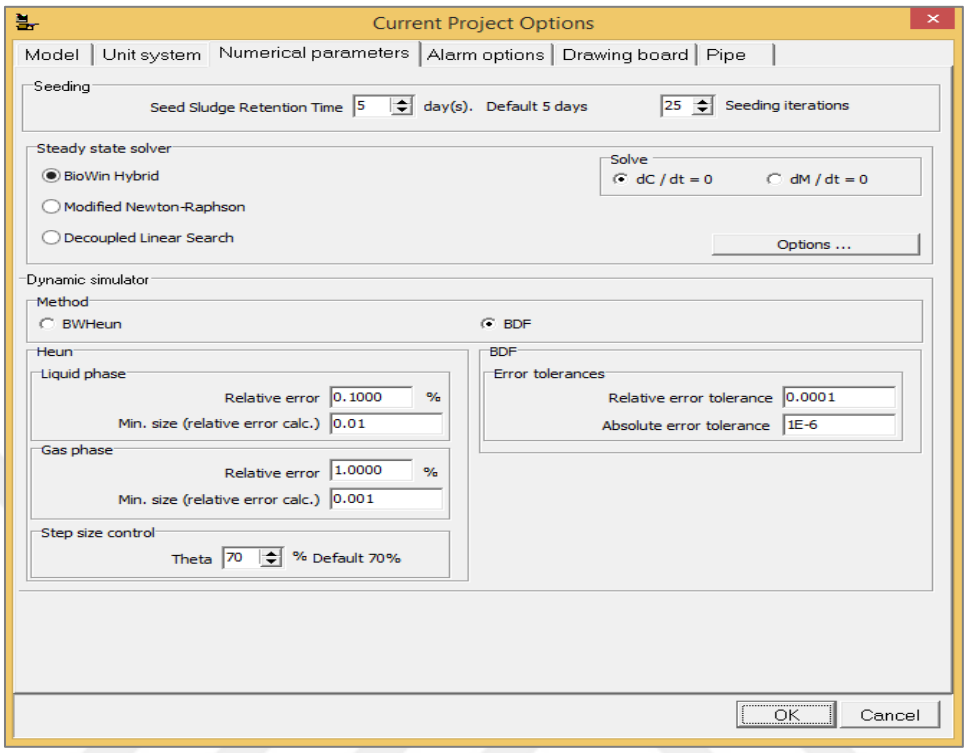

Figure 2.16 Numerical parameters page in BioWin® 6.0

2.3.8 Simulate

Last step is running the simulation as either steady-state condition or dynamic condition. Before simulating the model, it is suggested to check the data by clicking check data button. This button informs the user whether the configuration is ready to simulate or not.

In steady-state condition there is no change in time broadly. In order to simulate the model in steady-state conditions (Figure 2.17), user should choose one of the options for start of the simulation such as seed, current values and complex seed. If seed values is selected, an algorithm is used to give numerical seed values for the elements in a model. If current values is selected, current numerical values are used as initial values for the steady-state solver. The complex seeding runs the simulation dynamically within the steady-state model and it is used for usually the complex systems which has difficulties finding the solution (BioWin Help Manual, 2019). After experiencing the difficulties for finding a solution in simulations, it is decided to use only complex seed for the steady-state simulations in this study.

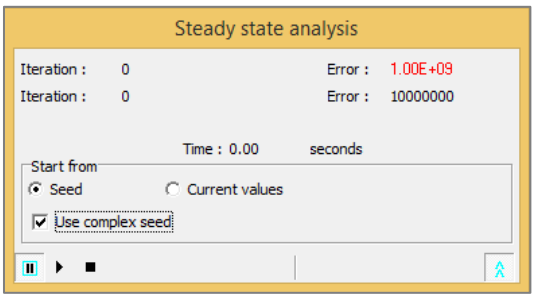

Figure 2.17 Steady-state simulation box in BioWin® 6.0

Dynamic condition considers changes in time in the system. The simulation start conditions contain options similar to ones related to steady state simulations metioned earlier. If seed values is selected, the model will use seeding with default state variables. If current values is selected, the seeding is done with the state variables in current situation. If a steady state simulation has been done earlier, the software will provide another option as last steady state. With this option seeding is completed with the values from the last steady state solution. (BioWin Help Manual, 2019). While simulating the system dynamically, few settings are needed which are available in dynamic simulation box (Figure 2.18). The user can define the simulation start date and simulation duration in days. As final step, user should choose one of the simulation start conditions which are previously mentioned and then click the simulate button.

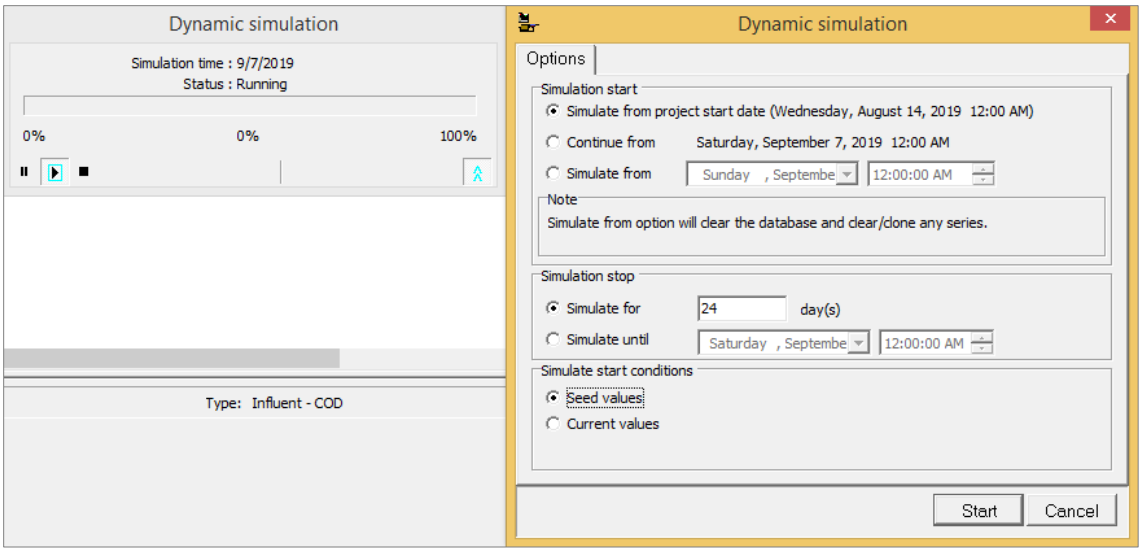

Figure 2.18 Dynamic simulation box in BioWin® 6.0

2.4 Steady State Simulations

2.4.1 Description of Set-up 1

Set-up 1 (Figure 2.19) includes a deammonification MBBR reactor followed by a settling tank. This set-up was consolidated in order to evaluate different set DO, intermittent aeration pattern (i.e., oxic/anoxic periods) and temperature on both effluent quality and distribution of microbial population. The procedure followed to run Set-up 1 is described in detail in section 2.3.

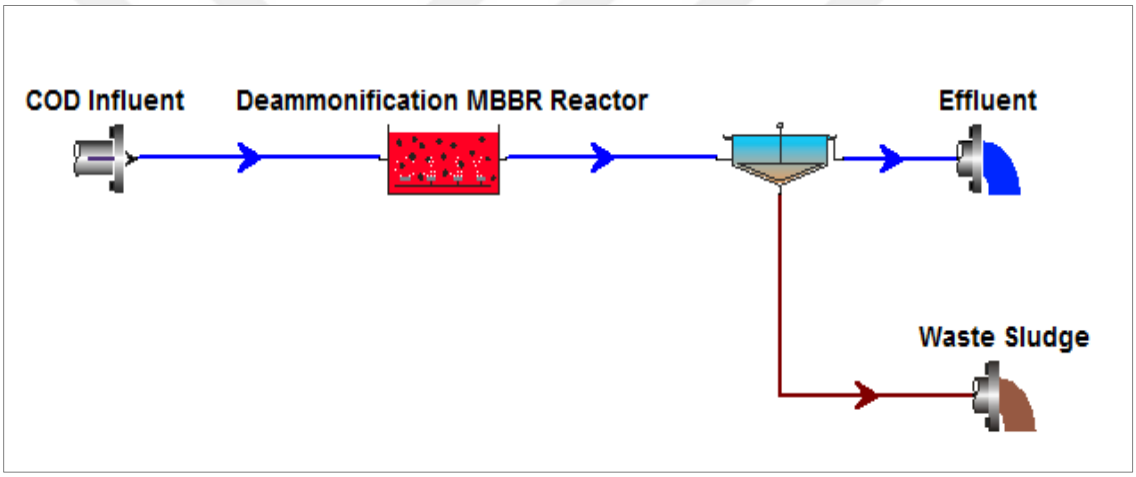

Figure 2.19. Set-up 1 flow diagram in BioWin® 6.0.

All elements were selected in order to build a most reliable model of the deammonification MBBR pilot plant. Kinetic, stoichiometric and general biofilm parameters as constant input values are shown in Annex 1- Table 1. The variable input parameters in Set-up 1 simulations were set DO, oxic/anoxic periods and temperature. Set DO values were ranged between 0.5-2.0 mg/l. In oxic/anoxic patterns, total oxic periods were ranged between 25% - 82% in a day. The output values obtained from each simulation were evaluated based on EU sensitive zone discharge limits (91/271/EEC).

Bursa Dogu STP influent design parameters which are shown in Table 2.2, have been used as influent parameters in set up-1 simulations.

2.4.2 Description of Set-up 2

Similar to the Set-up 1, Set-up 2 (Figure 2.20) includes deammonification MBBR followed by settling tank. In addition to set-up 1 configuration, set-up 2 configuration includes a sidestream for nitrite spike (0,55 m^3/d, 2000-8000 mg/l,) to the tank during anoxic periods. The concentration and flow of nitrite spike during anoxic periods were defined through ''state variable input'' menu as shown in Figure 2.4. As per personal contact with Envirosim, to maintain electroneutral conditions and to balance the charge of NO_2^- with a cation other than hydrogen (H^+) ion, magnesium (Mg^{+2}) was added as equivalent opposite charged ion as 3000-12000 mg/l concentrations. In order to simulate the system based on intermittent aeration, nitrite spike has been added as side stream element and influent type is selected as variable (Figure 2.4). Desired unaerated periods in minutes used as nitrite addition periods in variable influent editor in each simulation.

This set-up was consolidated in order to evaluate the effect of nitrite spike on the enrichment of Anammox species (AAO) during start-up phase of the reactor. In other words, this set-up allowed us to evaluate the enrichment of Anammox species under mainstream conditions independent from the efficiency of partial nitritation. Different conditions such as DO set point, water temperature and time setting of aerated and unaerated periods in intermittent aeration have been simulated. Bursa Dogu STP influent design average influent values which are shown in Table 2.2, have been used as influent parameters in Set-up 2 simulations. Kinetic, stoichiometric and general biofilm parameters as constant input values are shown in Annex 1- Table 1. The variable input parameters in Set-up 2 simulations were set DO, oxic/anoxic periods and temperature. Set DO values were ranged between 0.5-2.0 mg/l. In oxic/anoxic patterns, total oxic periods were ranged between 25% - 64% in a day.

The output values obtained from each run was mainly evaluated based on population of Anammox species on the carriers since the aim of this set-up was enrich the Anammox species during start-up phase of the deammonification system.

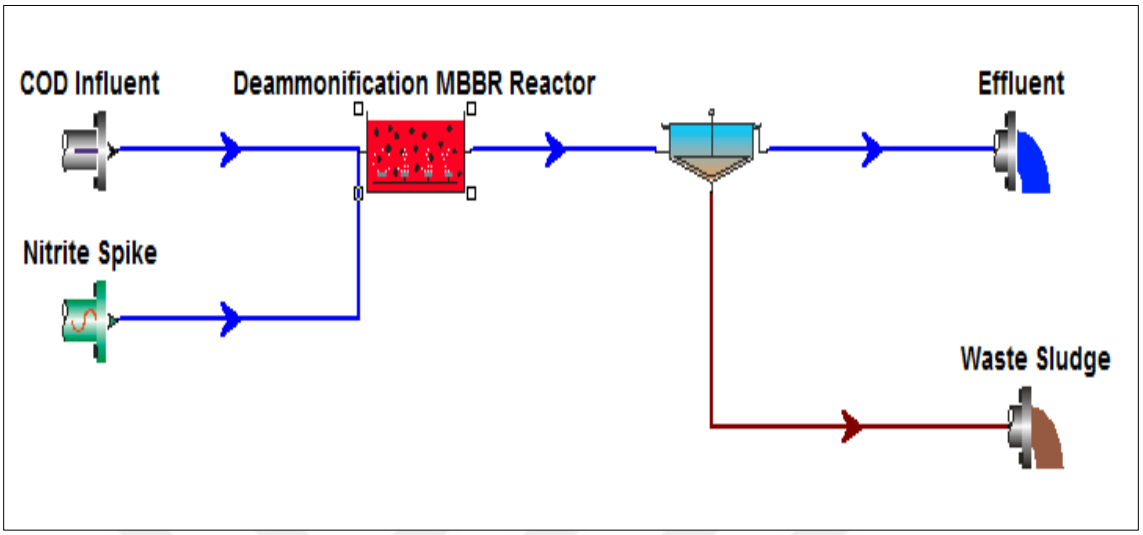

Figure 2.20. Set-up 2 flow diagram in BioWin® software.

2.5 Dynamic Simulations

It is important to be able to predict the reaction of the treatment plant in case of fluctuations in influent quality. There is no fluctuations hydraulicly in the studied pilot plant because of continuous feeding via pump but there is fluctuation in incoming wastewater characteristics. The laboratory analyses for influent characteristics are done with the composite samples which are taken from downstream of grit and grease chambers. The data received from the laboratory have been used as input for Set-up 2 dynamic simulations.

2.5.1 Set-up 2 dynamic simulation

Dynamic simulations of Set-up 2 were done using flow diagram shown in Figure 2.20 for 21 days with the wastewater temperature ranging between 23-26 ˚C. Similar to steady-state set-up 2 simulations, nitrite spike (0,55 m^3/d, 8000 mg/l) to the tank was added to the flow diagram thtough a side-stream with variable input based on anoxic periods in the tank. The influent data for Set-up 2 dynamic simulations were received from pilot plant and it is given in Table 2.4.

Table 2.3. Influent data for dynamic simulation of Set-up 2.

Date	Time	Flow	TSS	COD	TN	TP	SO_4^- (as S^{2-})	pH	DO	T
day	day	m^3/d	mg/l	mg/l	mg/l	mg/l	mg/l	-	mg/l	˚C
10/10/18	0	108	508	711	68	11	32	8.3	0.5	25
11/10/18	1	108	400	705	68	10	32	8.2	0.5	25
12/10/18	2	108	435	811	72	11	32	8.3	0.5	25
13/10/18	3	108	473	890	75	12	32	8.1	0.5	25
14/10/18	4	108	442	696	63	11	32	8.1	0.5	25
15/10/18	5	108	250	516	95	14	32	8.1	0.5	25
16/10/18	6	108	382	670	66	11	32	8.0	0.5	25
17/10/18	7	108	402	717	73	14	32	7.7	0.5	25
18/10/18	8	108	268	569	81	9	32	8.1	0.5	25
19/10/18	9	108	266	556	68	10	32	8.0	0.5	25
20/10/18	10	108	263	538	65	10	32	7.9	0.5	25
21/10/18	11	108	258	525	55	8	32	7.9	0.5	26
22/10/18	12	108	328	640	60	10	32	8.4	0.5	25
23/10/18	13	108	308	524	59	10	32	7.9	0.5	25
24/10/18	14	108	444	596	62	10	32	7.9	0.5	25
25/10/18	15	108	330	550	42	9	32	8.3	0.5	24
26/10/18	16	108	369	628	65	11	32	8.2	0.5	24
27/10/18	17	108	430	764	66	11	32	8.2	0.5	23
28/10/18	18	108	377	690	42	10	32	8.1	0.5	22
29/10/18	19	108	384	732	67	12	32	8.1	0.5	22
30/10/18	20	108	346	402	63	9	32	8.5	0.5	22
31/10/18	21	108	308	463	66	10	32	8.2	0.5	22

Nitrite spike is considered as same amount of nitrite for each day. As mentioned in previous section 2.4.2, it is required to enter equivalent ion mass as input for water chemisrtry. Therefore magnesium is also added as input to the influent state variable page.

2.6 Sensitivity Analysis

Sensitivity analysis was performed in order to define sensitive kinetic, stoichiometric and biofilm general parameters of BioWin® software on output parameters. For this purpose 120 kinetic, 10 biofilm and 112 stoichiometric parameters belonging to BioWin® 6.0 deammonification MBBR configuration were changed one by one using the Set-up 1

simulation identified as the optimum case in terms of effluent quality and microbial population distribution. One parameter has been analyzed at a time. Totally 242 different simulations have been done for sensitivity analysis. All analyzed 242 parameters are provided in Annex 1- Table 1 with their default values in BioWin® 6.0.

Normalized Sensitivity Coefficient (EPA, 1997) was used as sensitivity analysis method in this study.

$$S_{ij} = \frac{[\Delta yi/yi]}{[\Delta xi/xi]} \quad (2.1)$$

S_{ij} = Normalized sensitivity coefficient

x_i = Input Parameter

y_i = Output Parameter

Δ_{xi} = Difference in input parameter (10%) (Default input – 10% increased input)

Δ_{yi} = Difference in output parameter (Default output– result output)

Each input parameter has been increased up to 10 % and normalized sensitivity coefficient was calculated based on equation 2.1. The calculated S_{ij} values for effluent parameters of TN, NO^-_3-N, NO^-_2-N, TSS and COD were evaluated and their sensitivity level were classified in accordance with section 2.7.3.

2.7 Data Evaluation

2.7.1 Methodology of naming the simulations

The complexity of the study with significant amount of simulations requires simplification and methodology for the file numbering system and data storage. Therefore, a methodology is generated for naming the simulations since there has been approximately 400 simulations performed in the scope of this study. All the simulations were named due to their features as shown in Figure 2.21.

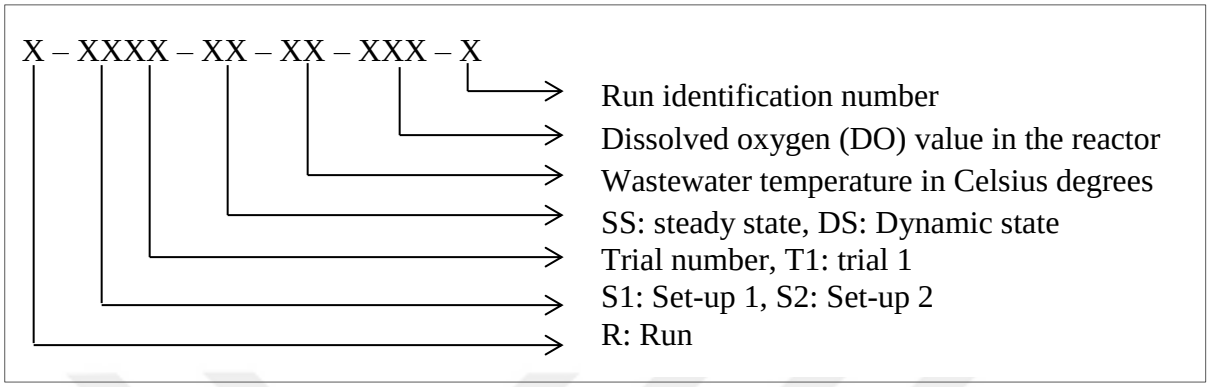

Figure 2.21 Methodology of naming BioWin® simulations

2.7.2 Steady-state simulations

Simulations performed under steady-state conditions were evaluated based on effluent discharge values obtained from the simulations and distribution of microbial population through the layers of biofilm as well as bulk liquid. The effluent discharge values were always evaluated due to EU discharge limits for sensitive areas with more than 100 000 p.e. (without phosphorus removal) is shown in Table 2.5.

Table 2.4. European Legislation discharge limits for sensitive areas (without P removal) (91/271/EEC).

Parameter	Unit	Concentration
TSS	mg / l	35
COD	mg / l	125
BOD	mg / l	25
TN	mg / l	10
TP	mg / l	NA

BioWin® allows the user to plot the end results from simulation as chart from album page as shown in Figures 2.22 - 2.24 besides reporting the effluent values on the simulation window at the end of the simulations (Figure 2.8). Additionally, the detailed results through biofilm

layers are also reported under “Album menu as details” as table shown in Figure 2.22.

BioWin Album - R-S1T1-SS-20-DO1,5-1.bwc

Album Database View

Name	Biomass - Acetoclastic methanogenic	Biomass - Ammonia oxidizing	Biomass - Anaerobic ammonia oxidizing	Biomass - Endogenous products	Biomass - Hydrogenotrophic methanogenic	Biomass - Methylotrophic	Biomass - Nitrite oxidizing
Layer1	0.01	18.48	1.81	2,909.56	0.00	0.22	0.52
Layer2	0.08	70.56	3.36	2,813.35	0.01	0.49	2.01
Layer3	0.82	300.04	7.56	486.96	0.27	1.47	9.58
Bulk	0.03	1.90	0.05	11.27	0.02	0.05	0.05

BioWin Album - R-S1T1-SS-20-DO1,5-1.bwc

Album Database View

Name	Biomass - Ordinary heterotrophic	Biomass - Phosphorus accumulating	Biomass - Propionic acetogenic	Biomass - Sulfur oxidizing	Biomass - Sulfur reducing acetotrophic	Biomass - Sulfur reducing hydrogenotrophic	Biomass - Sulfur reducing propionic acetogen
Layer1	1,252.95	0.91	0.03	48.59	0.45	259.47	0.32
Layer2	3,571.27	2.25	0.12	111.40	0.71	538.74	0.61
Layer3	5,170.28	2.84	0.88	69.40	1.51	51.19	1.51
Bulk	130.74	0.08	0.04	1.66	0.05	1.14	0.05

BioWin Album - R-S1T1-SS-20-DO1,5-1.bwc

Album Database View

Name	CODs - Methanol	CODs - Propionate	CODs - Soluble hydrocarbon	CODs - Undegradable	Gas - Dissolved hydrogen	Gas - Dissolved methane	Gas - Dissolved nitrogen	Gas - Dissolved nitrous oxide	Gas - Dissolved oxygen	Gas - Dissolv
Layer1	0.00	0.03	0	27.72	0.00	0.00	16.37	0	0.00	8.19
Layer2	0.00	0.04	0	27.72	0.01	0.00	16.32	0	0.01	8.18
Layer3	0.00	0.06	0	27.72	0.10	0.00	16.06	0	0.14	8.16
Bulk	0.00	0.06	0	27.72	0.10	0.00	15.96	0	0.63	8.14

BioWin Album - R-S1T1-SS-20-DO1,5-1.bwc

Album Database View

Name	CODp - Slowly degradable colloidal	CODp - Slowly degradable particulate	CODp - Stored PHA	CODp - Undegradable cellulose	CODp - Undegradable non-cellulose	CODs - Acetate	CODs - Complex readily degradable	CODs - Degradable volat
Layer1	1.36	3,304.82	0.01	0.00	1,063.54	1.31	0.39	0
Layer2	1.50	2,727.28	0.16	0.00	1,400.25	1.26	0.88	0
Layer3	2.64	2,138.89	0.28	0.00	2,218.34	0.93	3.91	0
Bulk	3.32	109.63	0.01	0.00	74.62	0.99	5.25	0

Figure 2.22 Sample screen shot of BioWin® 6.0 album menu details.

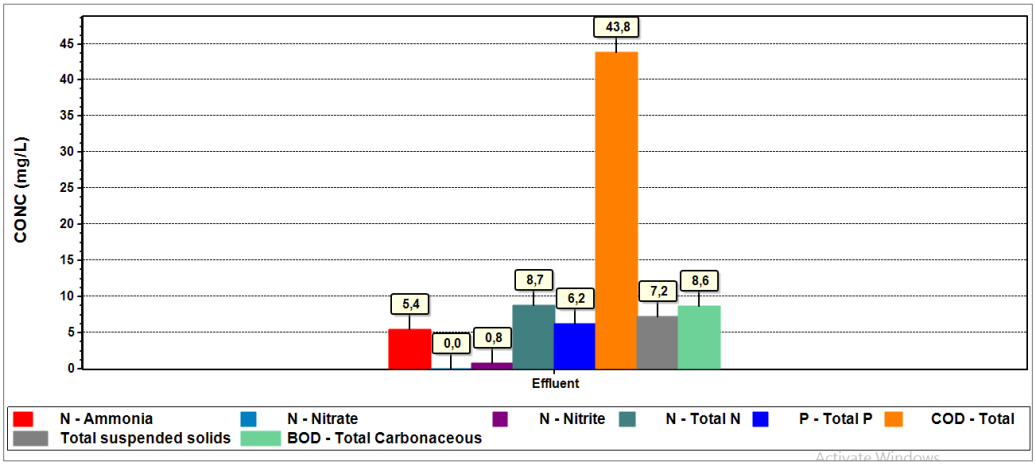

Figure 2.23. Sample screenshot of BioWin® 6.0 album showing effluent chart for a steady state simulation.

The simulator reports effluent values and biomass distribution in graphical format as shown

in Figure 2.23 and Figure 2.24 respectively. However, the broad data evaluation requires plotting of the data in different forms which allow comparson of simulations with each other. Hence, the effluent values and microbial population distribution in each biofilm layer reported in the summary table of each simulation group (i.e., Figure 3.1 and 3.2) was transferred to MS. Excel® and evaluated in detail by plotting the data in different forms of bar graphs as shown in section 3. The optimum simulations were identified as simulations resulting the effluent values very close or lower than the discharge limits together with the high Anammox species population through the entire depth of the biofilm. However, in Set-up 2 simulations allowing enrichment of Anammox species with nitrite spike, was mainly focused on the quantity of Anammox population through biofilm layers.

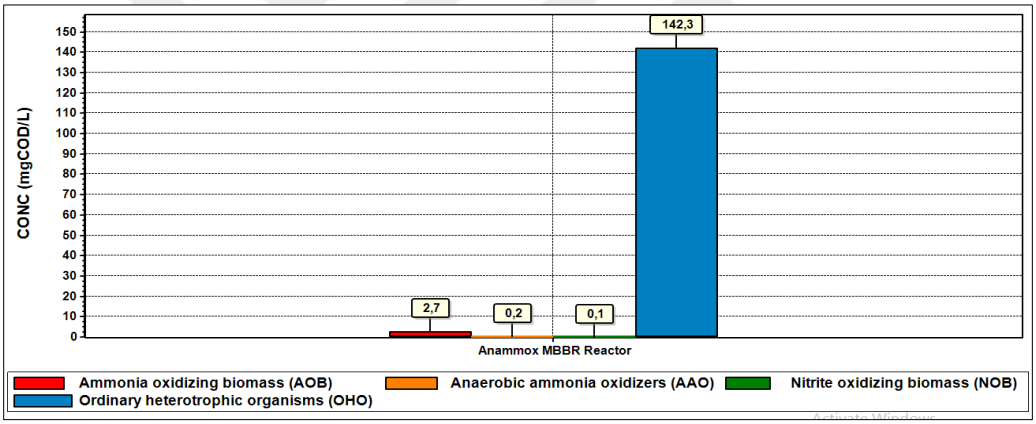

Figure 2.24. Sample screenshot of BioWin® 6.0 album showing the microbial population distribution as mg COD/l in bulk liquid of deammonification MBBR reactor.

2.7.3 Dynamic simulations

Effluent results of dynamic simulations were compared and evaluated with the actual effluent values of the pilot plant for the selected period.

The BioWin® 6.0 reports effluent results of dynamic simulations in the graphical format as shown in Figure 2.25. These results were compared with the actual pilot plant data by overlapping plant data onto the plotted chart from BioWin® 6.0.

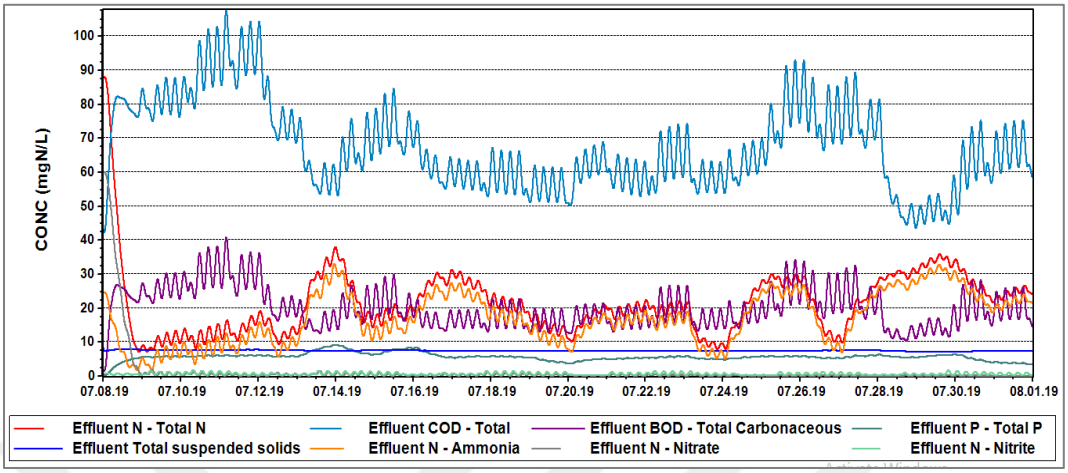

Figure 2.25. Sample screenshot of effluent chart for dynamic simulation in the album of BioWin® 6.0.

2.7.4 Sensitivity analysis

The normalized sensitivity coefficients (S_{ij}) calculated for 120 kinetic, 112 stoichiometric and 10 biofilm general parameters were evaluated based on the classification as described by Liwarska et al. (2010).

Group 1: $S_{ij} < 0.25$ Parameters having no significant Influence

Group 2: $0.25 \leq S_{ij} < 1$ Influential parameters

Group 3: $1 \leq S_{ij} < 2$ Very influential parameters

Group 4: $S_{ij} \geq 2$ Extremely influential parameters

3. RESULTS AND DISCUSSIONS

3.1. Set-up 1

Set-up 1 simulations were performed in 2 different stages. In the first stage, the simulations were done for the single-stage deammonification MBBR system model in an average wastewater temperature of 20˚C which mimics temperate environmental conditions. Second stage simulations were done for the extreme wastewater temperature conditions (minimum 10˚C and maximum 25˚C temperatures).

These simulations aimed to evaluate the possible use of wastewater simulators for the operation of single-stage deammonification MBBR systems. In other words, the use of simulators for setting the major operational parameters (DO set point, oxic/anoxic durations in a cycle) were studied. The simulation results were evaluated based on target effluent quality (TN <10 mg/l) together with the amount of Anammox (AAO) species in microbial consortia. Since the target effluent quality TN less than 10 mg/l can also be achieved by biological processes other than Anammox process, high amount of AAO population through biofilm layers was considered as an indicator of the prevelance of Anammox process.

Under 20˚C wastewater temperature condition, totally 29 simulations were performed using design average influent values of Bursa Dogu STP as described in Section-2.

The simulations were done for DO set points of 0.5, 1.0, 1.5 and 2.0 mg/l. Each DO set point was simulated with multiple options of oxic/anoxic periods in a cycle. Intermittent aeration patterns were adjusted by gradually changing cumulative oxic and cumulative anoxic durations in a cycle (~1440 minutes). To do this, duration of oxic period in a cycle was increased gradually at each simulation. For instance, an aeration pattern of 360 min oxic period and 180 min anoxic period corresponds to 75% oxic and 25% anoxic duration in a cycle.

The effluent quality and the population distribution of microbial species observed in the simulations performed for set DO 0.5 mg/l were summarized in Table 3.1 and Table 3.2, respectively.

Table 3.1 Set-up 1 effluent values at T=20 ˚C, DO=0.5 mg/l

SIMULATION NAME	AERATION PATTERN IN A CYCLE				EFFLUENT						
	Oxic	Anoxic	Oxic	Anoxic	SS	TP	NH_4^+-N	NO_3^--N	NO_2^--N	TN	COD
	min	min	%	%	mg/l	mg/l	mg/l	mg/l	mg/l	mg/l	mg/l
R-S1T1-SS-20-DO0,5-1	120	180	40%	60%	7.27	7.32	43.81	0	0	46.5	67.3
R-S1T1-SS-20-DO0,5-2	130	180	43%	60%	7.27	0.32	43.81	0	0	46.5	67.3
R-S1T1-SS-20-DO0,5-3	140	160	47%	53%	7.28	7.17	43.44	0	0	46.1	62.8
R-S1T1-SS-20-DO0,5-7	180	180	50%	50%	7.27	7.17	43.41	0	0	46.1	61.9
R-S1T1-SS-20-DO0,5-4	150	180	51%	49%	7.27	7.22	43.55	0	0	46.2	63.2
R-S1T1-SS-20-DO0,5-5	160	180	53%	47%	7.27	7.15	43.36	0	0	46.1	61.6
R-S1T1-SS-20-DO0,5-6	170	180	54%	46%	7.27	7.10	43.20	0	0	45.9	60.3
R-S1T1-SS-20-DO0,5-8	240	180	64%	36%	7.27	7.95	42.71	0	0	45.4	57.3
R-S1T1-SS-20-DO0,5-9	360	180	75%	25%	7.27	6.73	41.44	0	0	44.1	53.4
R-S1T1-SS-20-DO0,5-10	420	150	81%	19%	7.27	6.64	41.34	0	0	44.0	53.2

Table 3.2 Set-up 1 population distribution of microbial species at T=20 ˚C, DO=0.5 mg/l

SIMULATION NAME	OHO			AOB			NOB			AAO		
	L 1	L 2	L 3	L 1	L 2	L 3	L 1	L 2	L 3	L 1	L 2	L 3
R-S1T1-SS-20-DO0,5-1	501	1308	1762	0.3	1.2	6.8	0.2	0.7	4.9	0.7	1.4	5.6
R-S1T1-SS-20-DO0,5-2	501	1308	1762	0.3	1.2	6.8	0.2	0.7	4.9	0.7	1.4	5.6
R-S1T1-SS-20-DO0,5-3	474	1323	1985	0.4	1.5	8.3	0.2	0.8	4.9	0.8	1.5	5.7
R-S1T1-SS-20-DO0,5-7	459	1294	2006	0.4	1.6	8.9	0.2	0.8	4.9	0.8	1.5	5.7
R-S1T1-SS-20-DO0,5-4	473	1306	1926	0.4	1.5	8.3	0.2	0.8	4.9	0.7	1.5	5.7
R-S1T1-SS-20-DO0,5-5	455	1290	2032	0.4	1.7	9.2	0.2	0.8	4.9	0.8	1.5	5.7
R-S1T1-SS-20-DO0,5-6	442	1277	2122	0.5	1.9	10.1	0.2	0.8	4.9	0.8	1.6	5.7
R-S1T1-SS-20-DO0,5-8	415	1256	2392	0.7	2.6	13.5	0.2	0.8	4.9	0.9	1.7	5.9
R-S1T1-SS-20-DO0,5-9	392	1270	2899	1.3	5.2	25.4	0.2	0.9	5.0	1.1	2.0	6.2
R-S1T1-SS-20-DO0,5-10	485	1314	1863	0.4	1.4	7.8	0.2	0.7	4.9	0.7	1.4	5.6

All values are in mgCOD/l. L1:Layer 1, L2: Layer 2, L3: Layer 3

Among these simulations, the simulation resulting the lowest TN removal with minimum AAO population (*R-S1T1-SS-20-DO0.5-1*) was further demonstrated with bar charts in Figure 3.1 showing the removals and in Figure 3.2 showing the microbial population distribution.

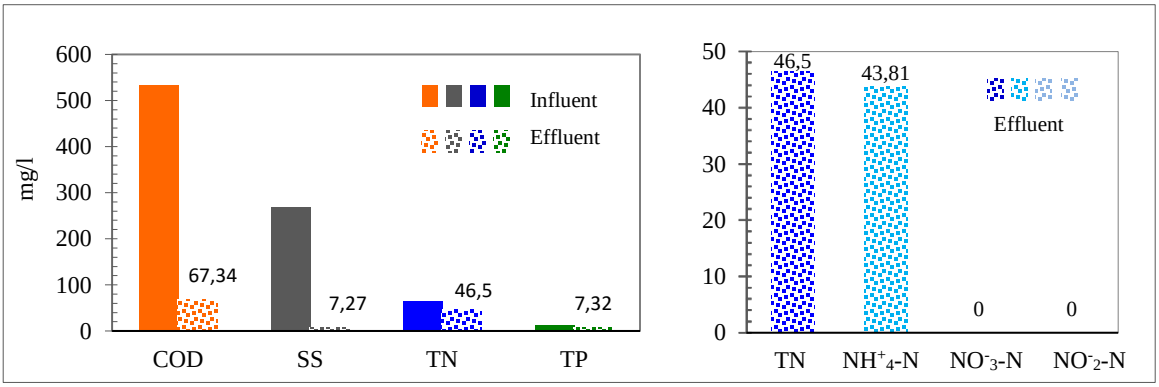

Figure 3.1. Influent and effluent charts of simulation R-S1T1-SS-20-DO0.5-1.

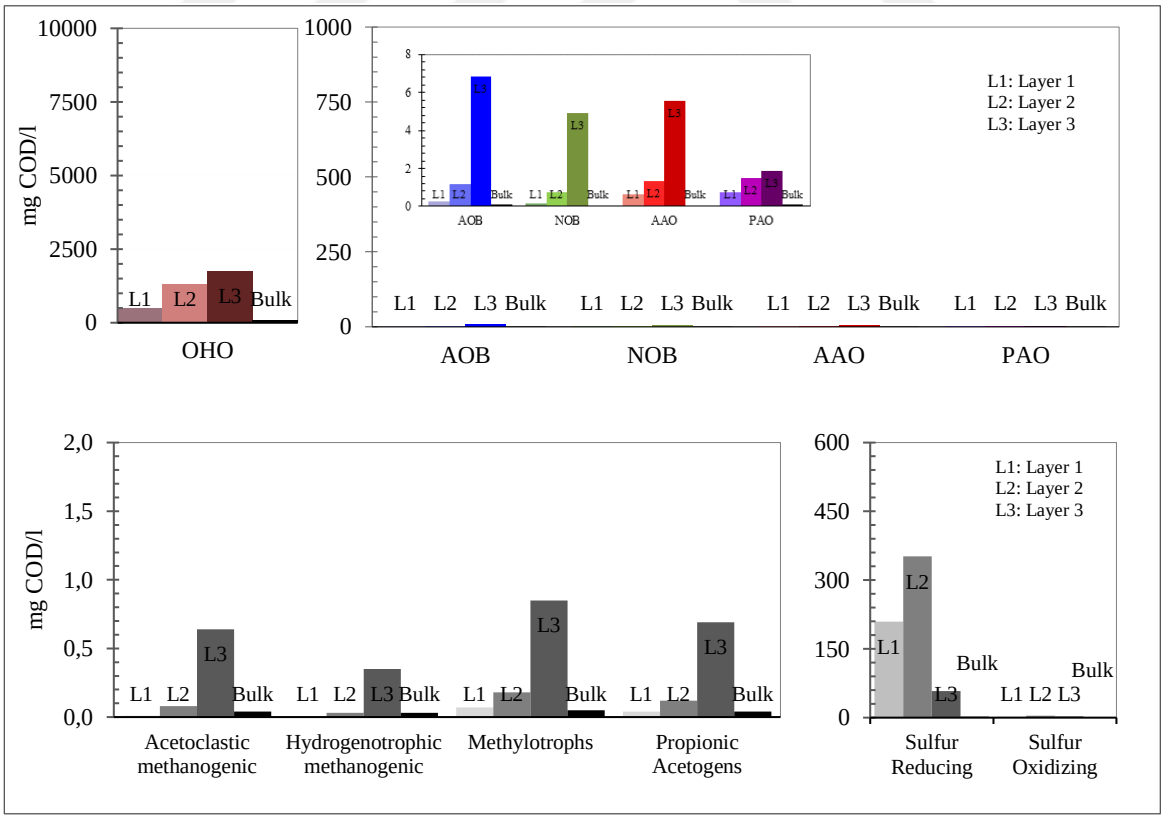

Figure 3.2. Microbial population distribution through biofilm layers of the simulation R-S1T1-SS-20-DO0.5-1.

The simulation resulting the highest TN removal with maximum AAO population (*R-S1T1-SS-20-DO0.5-10*) was also demonstrated with bar charts in Figure 3.3 showing the removals and in Figure 3.4 showing the microbial population distribution.

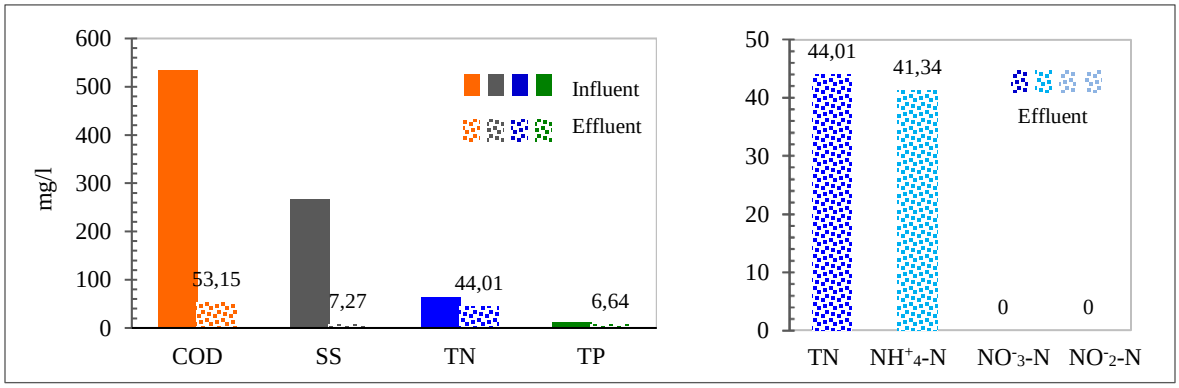

Figure 3.3 Influent and effluent charts of simulation R-S1T1-SS-20-DO0.5-10

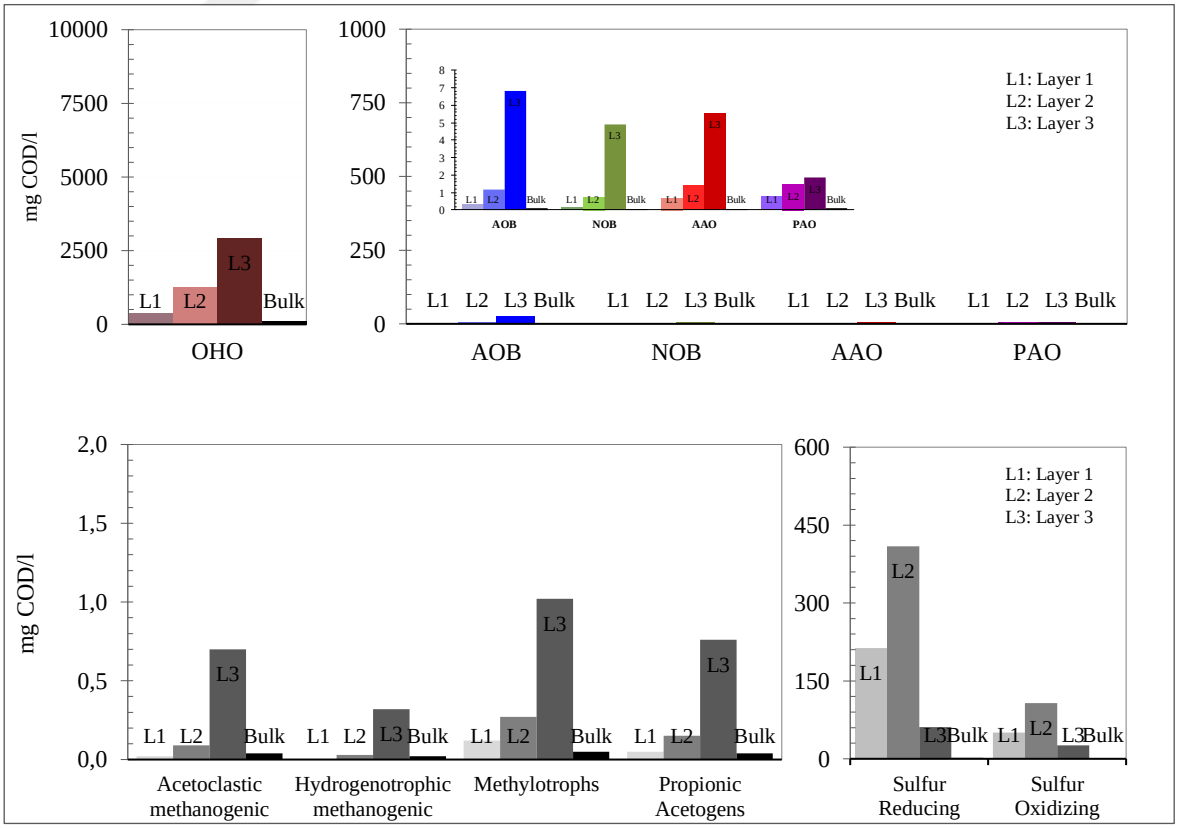

Figure 3.4 Microbial population distribution in biofilm layers of simulation R-S1T1-SS-20-DO0.5-10

L1 indicates first inner layer of the biofilm which is attached on the carrier, L2 indicates middle layer of the bofilm and L3 is the outer layer of the biofilm which in contact with bulk liquid.

Under set DO of 0.5 mg/l (Table 3.1) increasing oxic duration showed no significant influence on COD removal. In all simulations COD removal was observed around 90%. However, 0.5 mg/l DO set point was found insufficient for desired TN removal even under 81% oxic-19% anoxic aeration pattern. Neither partial nitritation nor full nitrification were observed. TN removal was 26% under 40% oxic-60% anoxic aeration pattern (Figure 3.1) while it was just increased to 30% under 81% oxic-19% anoxic aeration pattern (Figure 3.3). These results clearly demostrated the absence of both denitrification and Anammox activity due to lack of nitrification process. The low AAO population observed in all simulations (Table 3.2) indicate that the slight decrease in TN was mainly due to denitrification activity. The comparison of the microbial distribution observed under the lowest oxic duration aeration pattern (Figure 3.2) with the highest oxic duration aeration pattern (Figure 3.4) demonstrates that OHO and AOB population slightly increased with increasing oxic duration while there was no significant change in NOB and AAO population.

Figure 3.5 shows the DO concentration profile trough the biofilm (i.e. deepest layer: L1, mid layer: L2, outer layer: L3). Although the set DO value was very low (i.e., 0.5mg/l) in all simulations, the DO concentration in outer biofilm layer (L3) was significantly high (0.09-0.14 mg/l) while in the mid layer (L2) found 0.01 mg/l. These high DO values are not good for the growth of AAO species trough the biofilm depth.

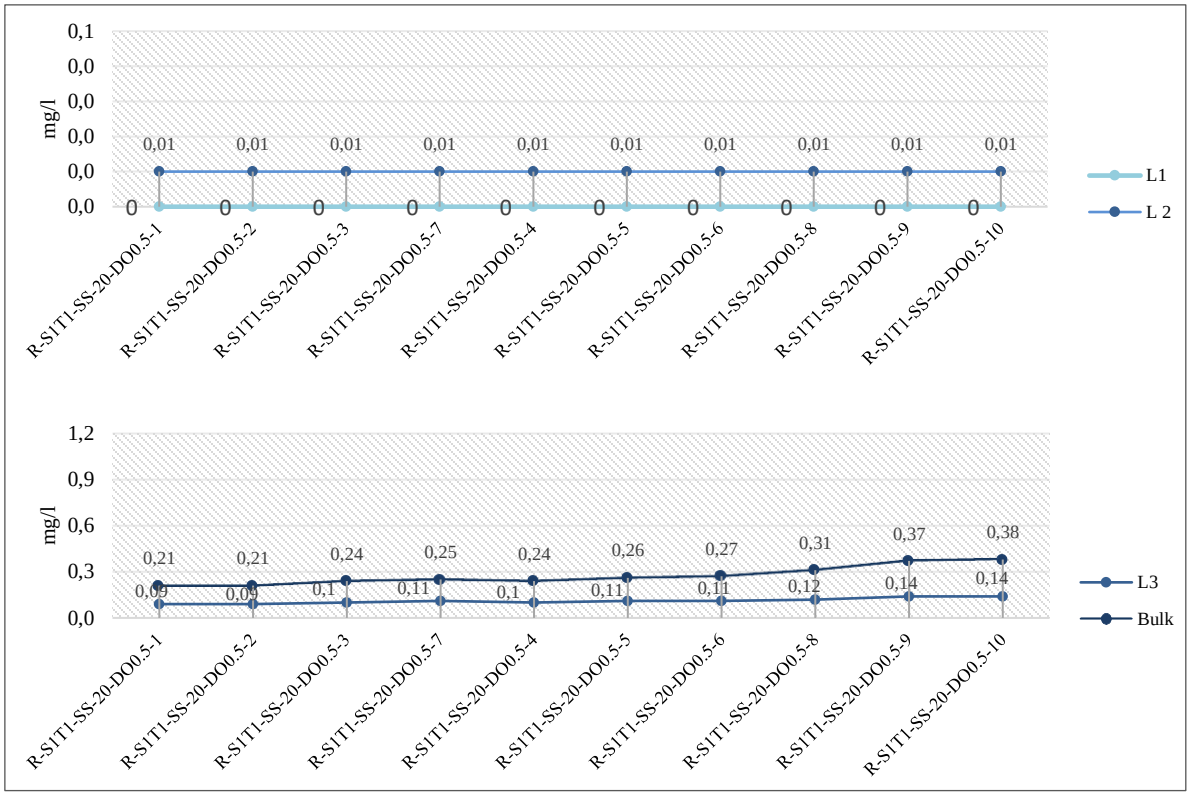

Figure 3.5 DO concentration profile through biofilm layers of simulations at DO set 0.5 mg/l and 20˚C wastewater temperature

The effluent quality and microbial population distribution of simulations done for set DO 1.0 mg/l were summarized in Table 3.3 and Table 3.4, respectively. Among these simulations, the simulation resulting the lowest TN removal with minimum AAO population (*R-S1T1-SS-20-DO1-1)* was further demonstrated with bar charts in Figure 3.6 showing the removals and in Figure 3.7 showing the microbial population distribution. The simulation resulting the highest TN removal with maximum AAO population (*R-S1T1-SS-20-DO1-7*) was also demonstrated with bar charts in Figure 3.8 showing the removals and in Figure 3.9 showing the microbial population distribution.

Under set DO of 1.0 mg/l (Table 3.3), no significant COD removal was observed in comparison to the 0.5 mg/l set DO simulations. In all simulations, COD removal was around 91%. Altough set DO of 1.0 mg/l provided better TN removal efficiency with respect to the removals observed for set DO 0.5 mg/l simulations, the minimum TN effluent was observed

as 12.64 mg/l which was still higher than the desired value of 10 mg/l. TN removal of 33% observed under 40% oxic-60% anoxic aeration pattern (Figure 3.6) increased to 80% under 81% oxic-19% anoxic aeration pattern (Figure 3.8).

Table 3.3 Set-up 1 effluent values at T=20 ˚C, DO=1.0 mg/l

SIMULATION NAME	AERATION PATTERN IN 1 CYCLE				EFFLUENT						
	Oxic	Anoxic	Oxic	Anoxic	SS	TP	NH_4^+-N	NO_3^--N	NO_2^--N	TN	COD
	min	min	%	%	mg/l	mg/l	mg/l	mg/l	mg/l	mg/l	mg/l
R-S1T1-SS-20-DO1-1	120	180	40%	60%	7.27	6.59	39.25	0	0.01	41.9	51.0
R-S1T1-SS-20-DO1-3	180	180	50%	50%	7.26	6.13	31.66	0	0.06	34.3	47.7
R-S1T1-SS-20-DO1-2	150	180	51%	49%	7.26	6.15	32.52	0	0.05	35.1	48.0
R-S1T1-SS-20-DO1-4	240	180	64%	36%	7.24	6.38	23.94	0	0.18	26.6	45.9
R-S1T1-SS-20-DO1-5	360	180	75%	25%	7.22	6.34	15.81	0	0.50	18.8	44.5
R-S1T1-SS-20-DO1-6	420	150	80%	20%	7.22	6.30	11.53	0	0.63	14.6	44.3
R-S1T1-SS-20-DO1-7	430	150	81%	19%	7.22	6.28	9.49	0	0.67	12.6	44.2

Table 3.4 Set-up 1 Population distribution of microbial species at T=20 ˚C, DO=1.0 mg/l

SIMULATION NAME	OHO			AOB			NOB			AAO		
	L 1	L 2	L 3	L 1	L 2	L 3	L 1	L 2	L 3	L 1	L 2	L 3
R-S1T1-SS-20-DO1-1	390	1324	3294	2.8	10.7	51.1	0.2	0.9	5.1	1.2	2.1	6.4
R-S1T1-SS-20-DO1-3	564	1964	4080	8.4	32.1	154.7	0.3	1.2	6.6	1.3	2.3	6.9
R-S1T1-SS-20-DO1-2	528	1842	3976	7.7	29.4	141.8	0.3	1.1	6.4	1.3	2.3	6.8
R-S1T1-SS-20-DO1-4	1113	3307	5002	16.4	62.7	277.8	0.5	1.8	9.2	1.6	3.0	7.5
R-S1T1-SS-20-DO1-5	1861	4179	6281	41.7	134.4	415.0	1.1	3.6	11.9	20.0	16.5	9.7
R-S1T1-SS-20-DO1-6	1843	4125	6577	45.0	146.8	457.3	1.2	3.9	13.1	142.5	95.4	24.1
R-S1T1-SS-20-DO1-7	1845	4097	6699	46.2	151.4	475.8	1.2	4.1	13.8	207.2	137.3	31.7

All values are in mgCOD/l. L1:Layer 1, L2: Layer 2, L3: Layer 3

The gradually increasing ammonium removals together with the slight nitrate accumulations indicate that TN decrease with increasing oxic period was mainly due to denitrification and/or

Anammox activities linked to the start of partial/full nitrification. The comparison of the microbial distribution observed under the lowest oxic duration aeration pattern (Figures 3.7) with the highest oxic duration aeration pattern (Figures 3.9) demonstrated that OHO and AOB population increased with increasing oxic duration.

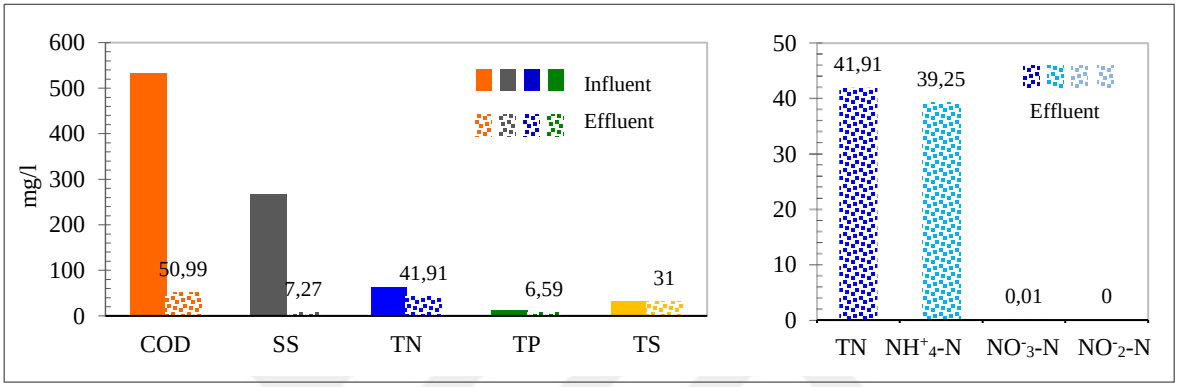

Figure 3.6 Influent and effluent charts of simulation R-S1T1-SS-20-DO1.0-1

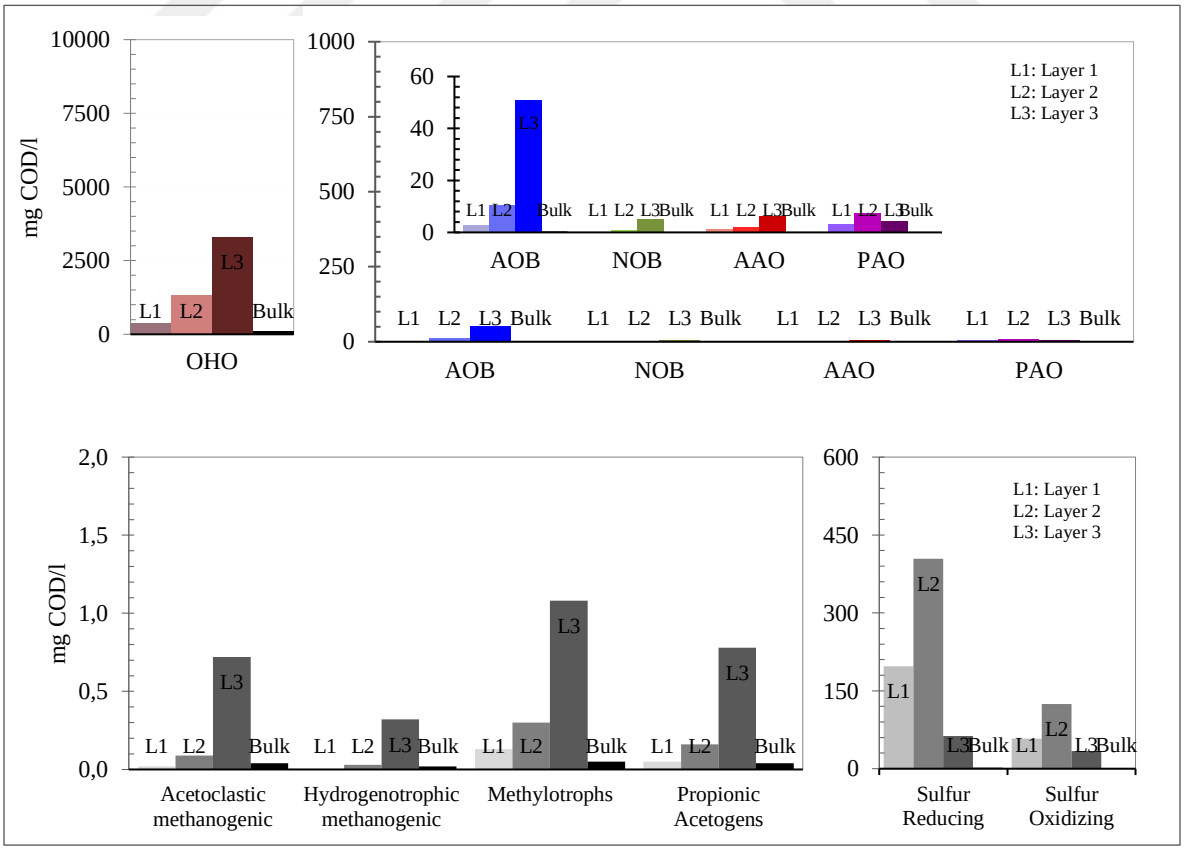

Figure 3.7 Microbial population distribution in biofilm layers of simulation R-S1T1-SS-20-DO1.0-1

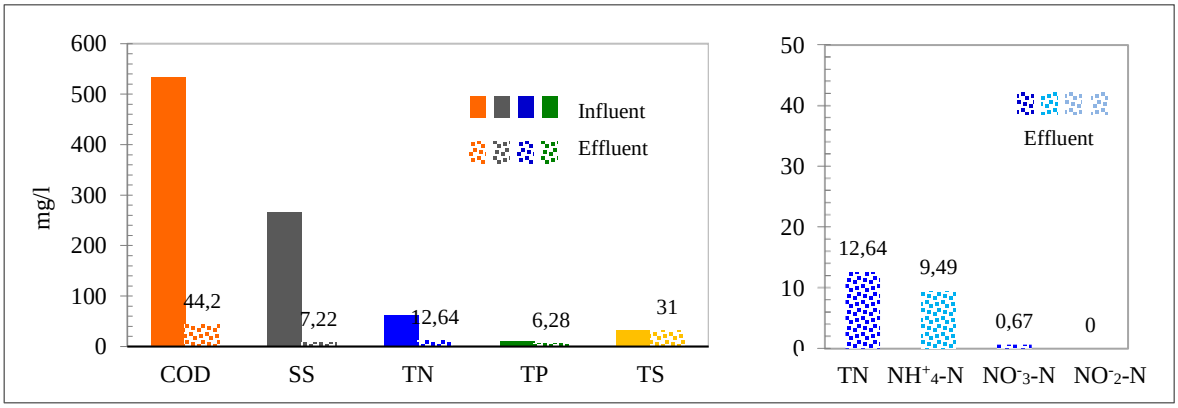

Figure 3.8 Influent and effluent charts of simulation R-S1T1-SS-20-DO1.0-7

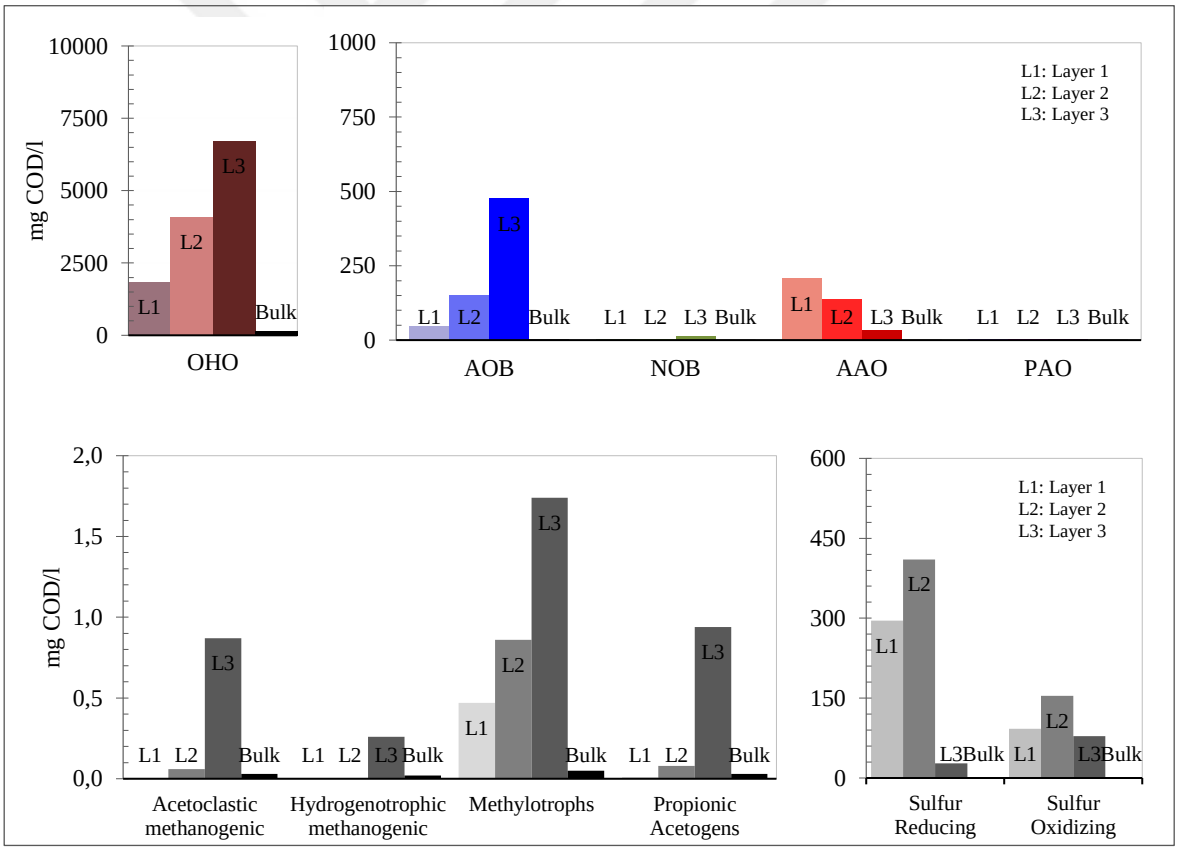

Figure 3.9 Microbial population distribution in biofilm layers of simulation R-S1T1-SS-20-DO1.0-7

However, DO increase from 0.5 mg/l to the 1.0 mg/l did not affect the NOB population significantly most probably due to high K_{DO} value of NOB species. Slight increase observed

in AAO population (Figure 3.9) was closely linked to the increasing activity of the AOB species without significant change in NOB activity. In other words, increasing set DO value from 0.5 mg/l to 1.0 mg/l resulted to observe partial nitritation in the system which favors the growth of AAO species. Figure 3.10 demonstrates the DO profile trough biofilm layers in all simulations performed at set DO 1.0 mg/l.

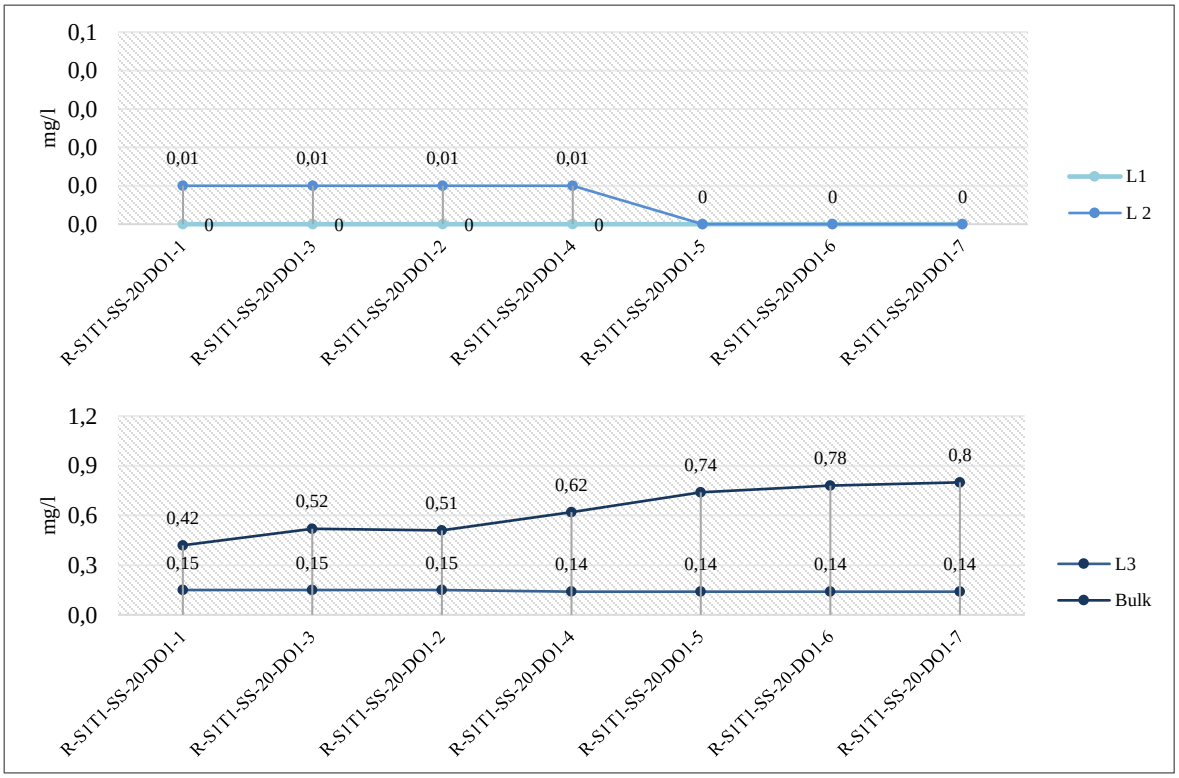

Figure 3.10 DO concentration profile through biofilm layers of simulations at DO set 1.0 mg/l and 20˚C wastewater temperature

This figure shows that increase of oxic duration in aeration pattrn resulted to accelrate AOB activity in the mid layer (L2) hence completely anaerobic conditions can be achieved in the deepest layer (L3) of biofilm. This situation is appearent in simulations *R-S1T1-SS-20-DO1-4* and *R-S1T1-SS-20-DO1-5.*

The effluent quality and microbial population distribution of simulations done for set DO 1.5 mg/l were summarized in Table 3.5 and Table 3.6, respectively. Among these simulations, the simulation resulting the lowest TN removal with minimum AAO population (*R-S1T1-SS-*

20-DO1.5-1) was further demonstrated with bar charts in Figure 3.12 showing the removals and in Figure 3.13 showing the microbial population distribution.

Table 3.5 Set-up 1 effluent values at T=20 ˚C, DO=1.5 mg/l

	AERATION PATTERN IN 1 CYCLE				EFFLUENT						
SIMULATION	**Oxic Duration**	**Anoxic Duration**	**Oxic**	**Anoxic**	**SS**	**TP**	**NH_4^+-N**	**NO_3^--N**	**NO_2^--N**	**TN**	COD
	minutes	minutes	%	%	mg/l	mg/l	mg/l	mg/l	mg/l	mg/l	mg/l
R-S1T1-SS-20-DO1.5-1	120	180	40%	60%	7.23	6.38	22.68	0	0.21	25.4	45.6
R-S1T1-SS-20-DO1.5-3	180	180	50%	50%	7.22	6.32	13.96	0	0.57	17.0	44.4
R-S1T1-SS-20-DO1.5-2	150	180	51%	49%	7.22	6.32	13.98	0	0.57	17.0	44.4
R-S1T1-SS-20-DO1.5-4	160	180	53%	47%	7.22	6.31	12.54	0	0.61	15.6	44.4
R-S1T1-SS-20-DO1.5-5	170	180	54%	46%	7.22	6.27	8.20	0	0.71	11.4	44.1
R-S1T1-SS-20-DO1.5-6	210	180	59%	41%	7.22	6.25	6.24	0	0.77	9.49	43.9
R-S1T1-SS-20-DO1.5-7	240	180	64%	36%	7.23	6.08	4.39	0.01	10.9	17.8	43.4
R-S1T1-SS-20-DO1.5-8	360	180	75%	25%	7.21	6.22	1.82	8.48	4.81	17.6	42.1
R-S1T1-SS-20-DO1.5-9	430	150	81%	19%	7.21	6.21	1.50	15.0	1.04	20.0	42.0

Table 3.6 Set-up 1 microbial distribution(as mgCOD/l) values at T=20 ˚C, DO=1.5 mg/l

	OHO			AOB			NOB			AAO		
SIMULATION	**L 1**	**L 2**	**L 3**	**L 1**	**L 2**	**L 3**	**L 1**	**L 2**	**L 3**	**L 1**	**L 2**	**L 3**
R-S1T1-SS-20-DO1.5-1	1253	3571	5170	18.5	70.6	300.0	0.5	2.0	9.6	1.8	3.4	7.6
R-S1T1-SS-20-DO1.5-3	1835	4151	6446	43.5	140.9	434.7	1.2	3.7	12.5	67.5	46.9	15.2
R-S1T1-SS-20-DO1.5-2	1835	4151	6445	43.5	140.8	434.5	1.1	3.7	12.5	66.9	46.5	15.1
R-S1T1-SS-20-DO1.5-4	1839	4136	6523	44.4	144.5	448.0	1.2	3.8	12.8	110.8	74.8	20.3
R-S1T1-SS-20-DO1.5-5	1841	4074	6793	46.9	154.0	487.7	1.3	4.2	14.3	249.0	164.0	36.6
R-S1T1-SS-20-DO1.5-6	1821	4023	6981	47.9	157.8	505.0	1.4	4.5	15.6	313.7	203.6	43.9
R-S1T1-SS-20-DO1.5-7	1479	4078	8023	62.1	200.0	598.5	2.4	7.9	26.0	0.2	0.8	3.5
R-S1T1-SS-20-D1.,5-8	1582	4399	7915	68.5	216.1	634.2	38.6	125.6	421.5	0.8	1.6	5.2
R-S1T1-SS-20-DO1.5-9	1522	4285	8010	69.9	220.3	632.7	48.2	157.3	526.0	5.1	5.4	7.8

All values are in mgCOD/l. L1:Layer 1, L2: Layer 2, L3: Layer 3

The simulation resulting the highest TN removal with maximum AAO population (*R-S1T1-SS-20-DO1.5-6*) was also demonstrated with bar charts in Figure 3.14 showing the removals and in Figure 3.15 showing the microbial population distribution. For simulations with DO set 1.5 mg/l, TN removal and microbial population distribution are also demonstrated for the *R-S1T1-SS-20-DO1.5-7* simulation in Figure 3.16 and 3.17 respectively to show a turning point in AAO population linked to applied aeration pattern in the operation.

As expected, increasing set DO value from 1.0 mg/l to the 1.5mg/l (Table 3.5) did not cause a significant change in COD removal efficiency. COD removal efficiency of around 92% was observed trough the simulations with oxic periods varying between 40% to 81%.

In contrast to the low set DO simulations (0.5 – 1.0 mg/l), the Anammox activity observed in the simulations with DO 1.5 mg/l were found heavily dependent on the aeration pattern, i.e., distribution of oxic/anoxic durations in a cycle. In the simulations with less than 60% oxic duration (*R-S1T1-SS-20-DO1.5-1, R-S1T1-SS-20-DO1.5-6*) (Tables 3.5-3.6, Figures 3.12 and 3.14), ammonium removal increased parallel to the increasing oxic duration. Slight nitrite accumulation was observed without any nitrate production indicating that possible partial nitritation in the system. TN removal gradually increased from 70% to 80% with increasing oxic period. This might be due to two mechanisms, denitrification and/or Anammox. The evaluation of these results together with microbial population distribution showed that under 60% oxic duration no significant change occurred in OHO, AOB and NOB population while AAO population was gradually increasing with increasing oxic duration.

As apparent from Figure 3.11 the DO profile through the biofilm layers, in these simulations DO concentration was 0 mg/l not only in the deepest layer of the biofilm (L1) but also in the middle layer (L2). These results demonstrated that AAO population increase is dependent on two major factors, low NOB population and 0 mg/l DO in the deeper layers (L1 and L2) of the biofilm.

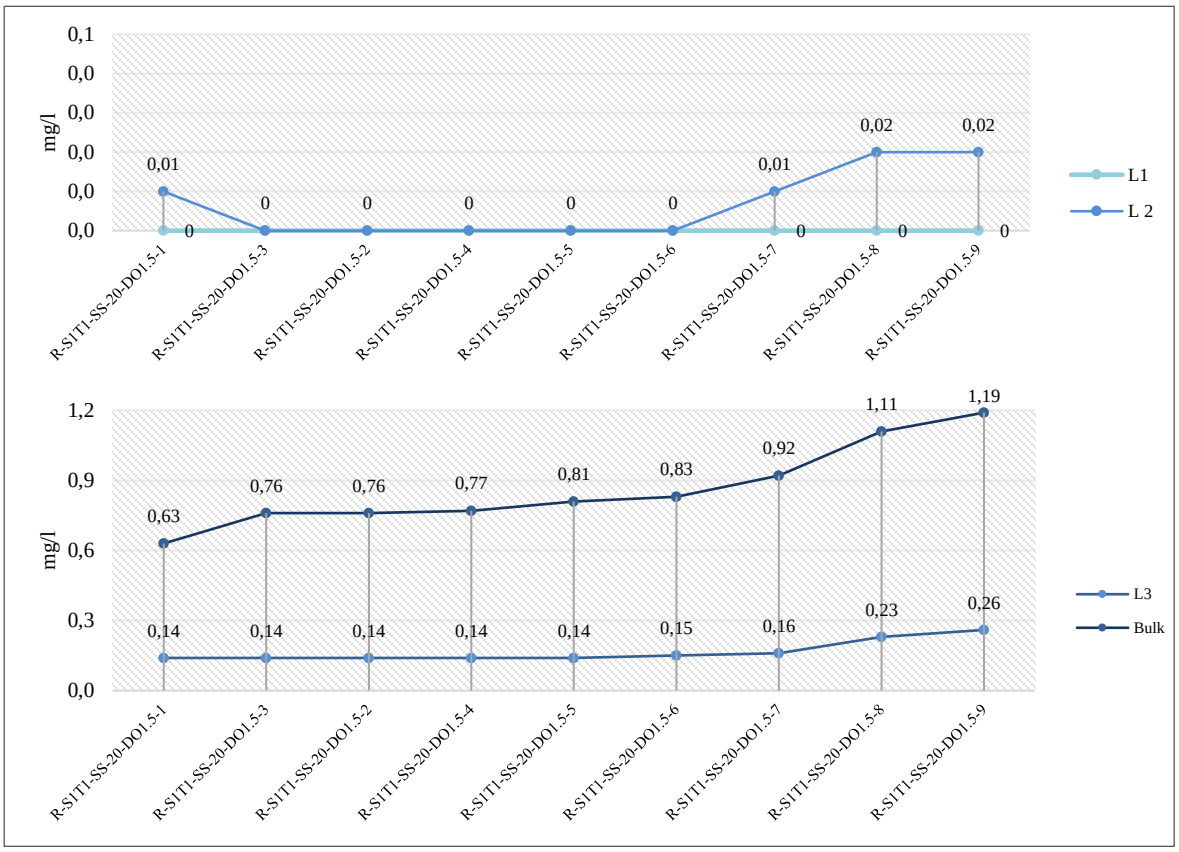

Figure 3.11 DO concentrations through biofilm layers of simulations at DO set 1.5 mg/l, 20˚C

In the simulations with greater than 59% oxic duration (*R- S1T1-SS-20-DO1.5-7*, *R- S1T1-SS-20-DO1.5-9*) (Tables 3.5-3.6) exhibited that with the increase of oxic duration from 59% (*R- S1T1-SS-20-DO1.5-6*) to 64% (*R-S1T1-SS-20-DO1.5-7*) caused a jump in nitrite effluent together with the start of nitrate production. Although the NOB population did not significantly increase, AAO population decreased drastically due to increasing oxygen penetration through the biofilm layers (Figure 3.11). With the increase of oxic duration from 59% (*R- S1T1-SS-20-DO1.5-6*) to 64% (*R- S1T1-SS-20-DO1.5-7*) TN removal decreased from 85% (Figure 3.14) to 68% (Figure 3.16) without significant change via further oxic duration increase. This finding clearly shows the decrease in TN removal with decreasing Anammox population. Table 3.7 summarizes microbial population distribution obtained for the simulation as optimum under set DO value of 1.5 mg/l.

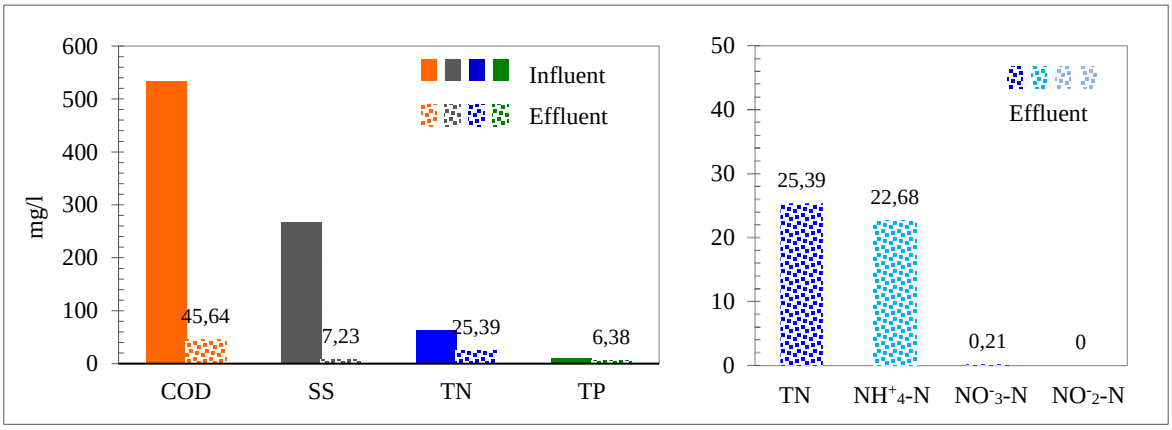

Figure 3.12. Influent and effluent charts of simulation R-S1T1-SS-20-DO1.5-1.

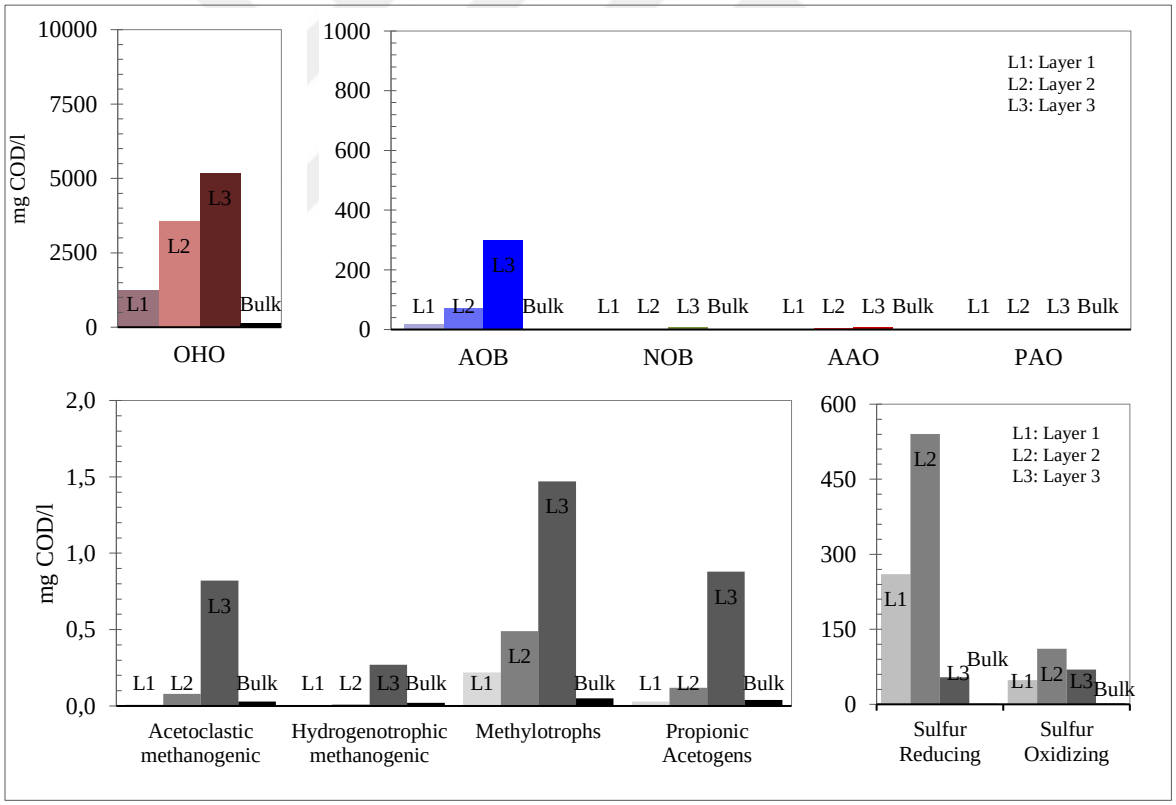

Figure 3.13. Microbial population distribution in biofilm layers of simulation R-S1T1-SS-20-DO1.5-1.

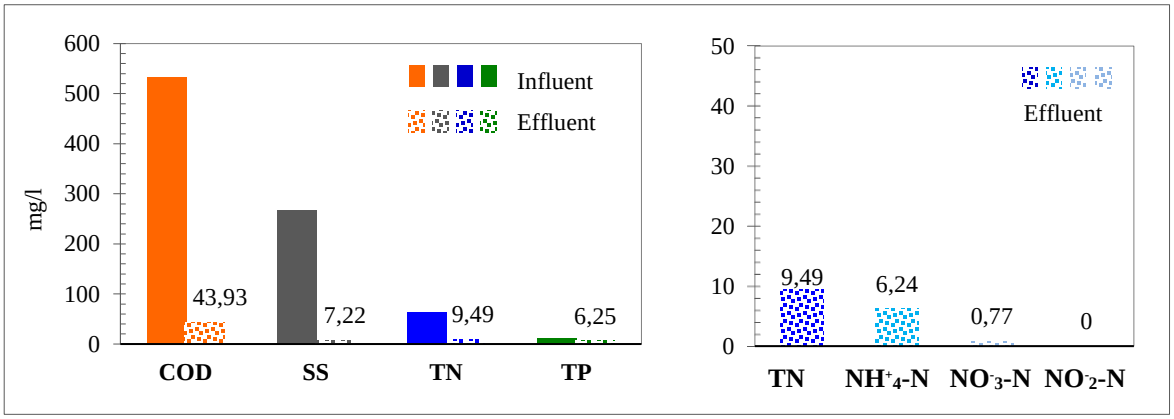

Figure 3.14. Influent and effluent charts of simulation R-S1T1-SS-20-DO1.5-6.

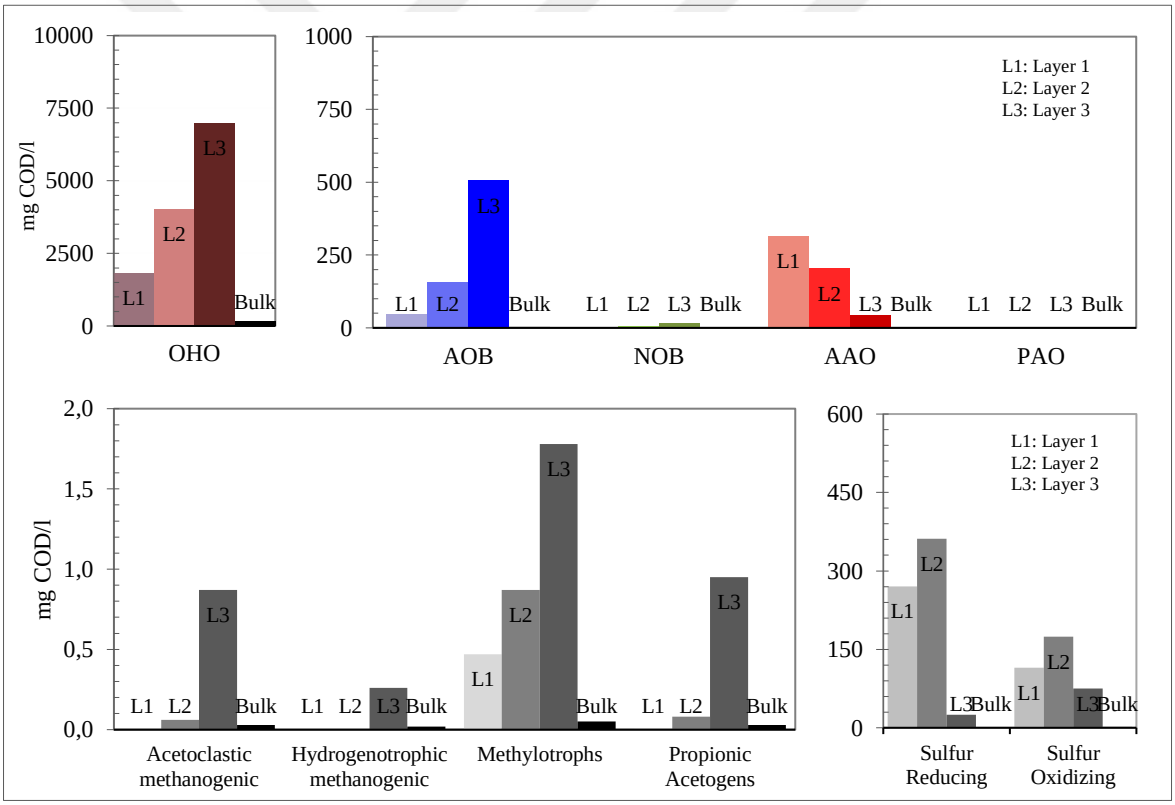

Figure 3.15. Microbial population distribution in biofilm layers of simulation R-S1T1-SS-20-DO1.5-6.

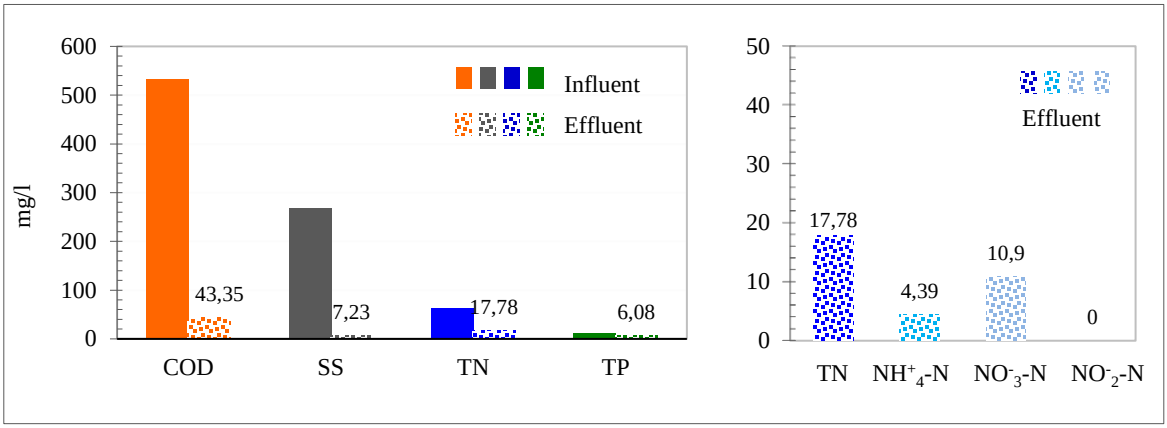

Figure 3.16 Influent and effluent charts of simulation R-S1T1-SS-20-DO1.5-7

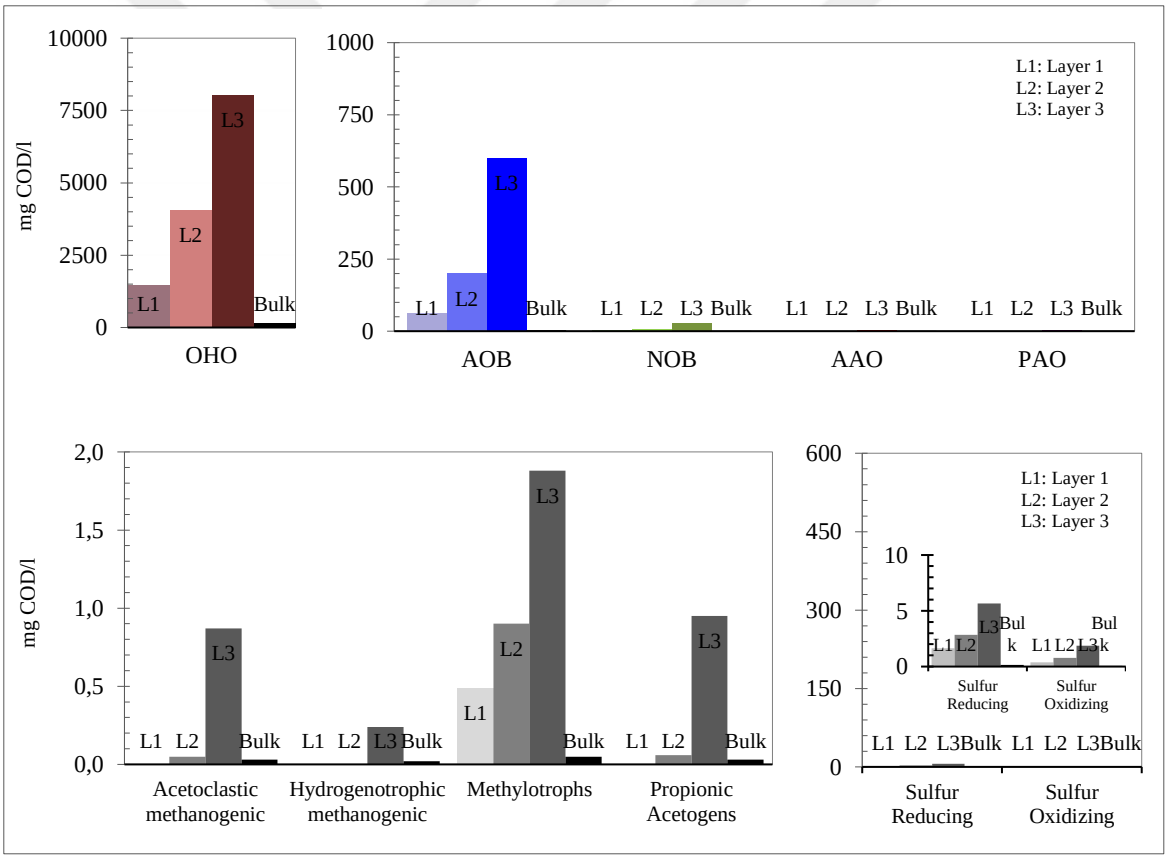

Figure 3.17 Microbial population distribution in biofilm layers of simulation R-S1T1-SS-20-DO1.5-7

The effluent quality and microbial population distribution of simulations done for set DO 2.0 mg/l are summarized in Table 3.7 and Table 3.8, respectively. Among these simulations, the simulation resulting the lowest TN removal with minimum AAO population (*R-S1T1-SS-20-*

DO2-4) was further demonstrated with bar charts in Figure 3.18 showing the removals and in Figure 3.19 showing the microbial population distribution. The simulation resulting the highest TN removal with maximum AAO population (*R-S1T1-SS-20-DO2-1*) was also demonstrated with bar charts in Figure 3.20 showing the removals and in Figure 3.21 showing the microbial population distribution. For simulations with DO set 2.0 mg/l, TN removal and microbial population distribution are also demonstrated for the *R-S1T1-SS-20-DO2-3* simulation in Figure 3.22 and 3.23 respectively to show a turning point in AAO population linked to applied aeration pattern in the operation.

COD removal efficiency of 92% observed under set DO value of 2.0 mg/l did not change in the simulations performed for set DO value of 2.0 mg/l with oxic periods varying between 25% to 51% (Table 3.8).

Similar to the simulations performed with set DO value 1.5 mg/l, the Anammox activity observed in the simulations with DO 2.0 mg/l were found heavily dependent on the aeration pattern, i.e., distribution of oxic/anoxic durations in a cycle. Additionally, these simulations clearly demonstrated the negative effect of high nitrite level (i.e.,FNA) on AAO bacteria. Table 3.7 summarizes microbial population distribution obtained for the simulation as optimum under set DO value of 1.5 mg/l.

Ammonium removal increased up to 89 % parallel to the increasing oxic duration. Slight nitrite accumulation was observed without any nitrate production indicating that possible partial nitritation in the system. However, the TN removal of 46% observed under 25% oxic duration (*R-S1T1-SS-20-DO2-4*) jumped to the 86% with a oxic duration increasing up to 40% (*R-S1T1-SS-20-DO2-5, R-S1T1-SS-20-DO2-1*). The AOB and NOB populations changes observed for 25% to 40% oxic duration (Table 3.9) demonstrate that the increasing oxic duration accelerated the activity of AOB species as well as slightly increased the activity of NOB species.

Table 3.7 Set-up 1 effluent values at T=20 ˚C, DO=2.0 mg/l

SIMULATION	AERATION PATTERN IN 1 CYCLE				EFFLUENT						
	Oxic Duration	**Anoxic Duration**	**Oxic**	**Anoxic**	**SS**	**TP**	**NH_4^+-N**	**NO_3^--N**	**NO_2^--N**	**TN**	COD
	minutes	minutes	%	%	mg/l	mg/l	mg/l	mg/l	mg/l	mg/l	mg/l
R-S1T1-SS-20-DO2-4	60	180	25%	75%	7.26	6.13	31.63	0	0.06	34.3	47.7
R-S1T1-SS-20-DO2-5	90	180	38%	63%	7.22	6.24	5.45	0	0.81	8.74	43.8
R-S1T1-SS-20-DO2-1	120	180	40%	60%	7.22	6.24	5.4	0	0.81	8.69	43.8
R-S1T1-SS-20-DO2-3	180	180	50%	50%	7.22	6.09	2.68	0.02	14.2	19.4	42.8
R-S1T1-SS-20-DO2-2	150	180	51%	49%	7.22	6.09	2.68	0.02	14.2	19.4	42.8
R-S1T1-SS-20-DO2-6	430	150	81%	19%	7.21	6.18	0.91	24.77	0.19	28.42	41.77

Table 3.8 Set-up 1 microbial distribution(as mgCOD/l) values at T=20 ˚C, DO=2.0 mg/l

	OHO			AOB			NOB			AAO		
SIMULATION	**L 1**	**L 2**	**L 3**	**L 1**	**L 2**	**L 3**	**L 1**	**L 2**	**L 3**	**L 1**	**L 2**	**L 3**
R-S1T1-SS-20-DO2-4	565	1968	4083	8.5	32.1	155.1	0.3	1.2	6.6	1.3	2.3	6.9
R-S1T1-SS-20-DO2-5	1805	3994	7084	48.2	159.2	512.1	1.4	4.7	16.3	340.9	219.1	46.8
R-S1T1-SS-20-DO2-1	1804	3992	7092	48.2	159.2	512.5	1.4	4.8	16.4	342.5	219.9	46.9
R-S1T1-SS-20-DO2-3	1357	4016	8224	66.7	211.9	622.5	5.4	17.6	57.5	0.1	0.4	3.0
R-S1T1-SS-20-DO2-2	1357	4016	8223	66.6	211.9	622.4	5.4	17.5	57.3	0.1	0.4	3.0
R-S1T1-SS-20-DO2-6	1383	3867	8379	91.1	269.0	598.3	54.8	173.5	518.6	4.0	5.4	8.5

All values are in mgCOD/l. L1:Layer 1, L2: Layer 2, L3: Layer 3

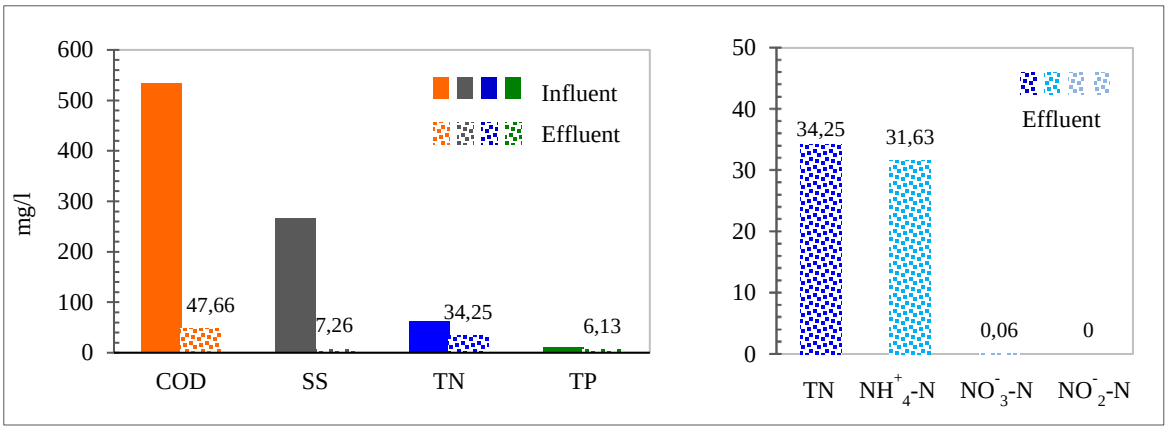

Figure 3.18 Influent and effluent charts of simulation R-S1T1-SS-20-DO2-4

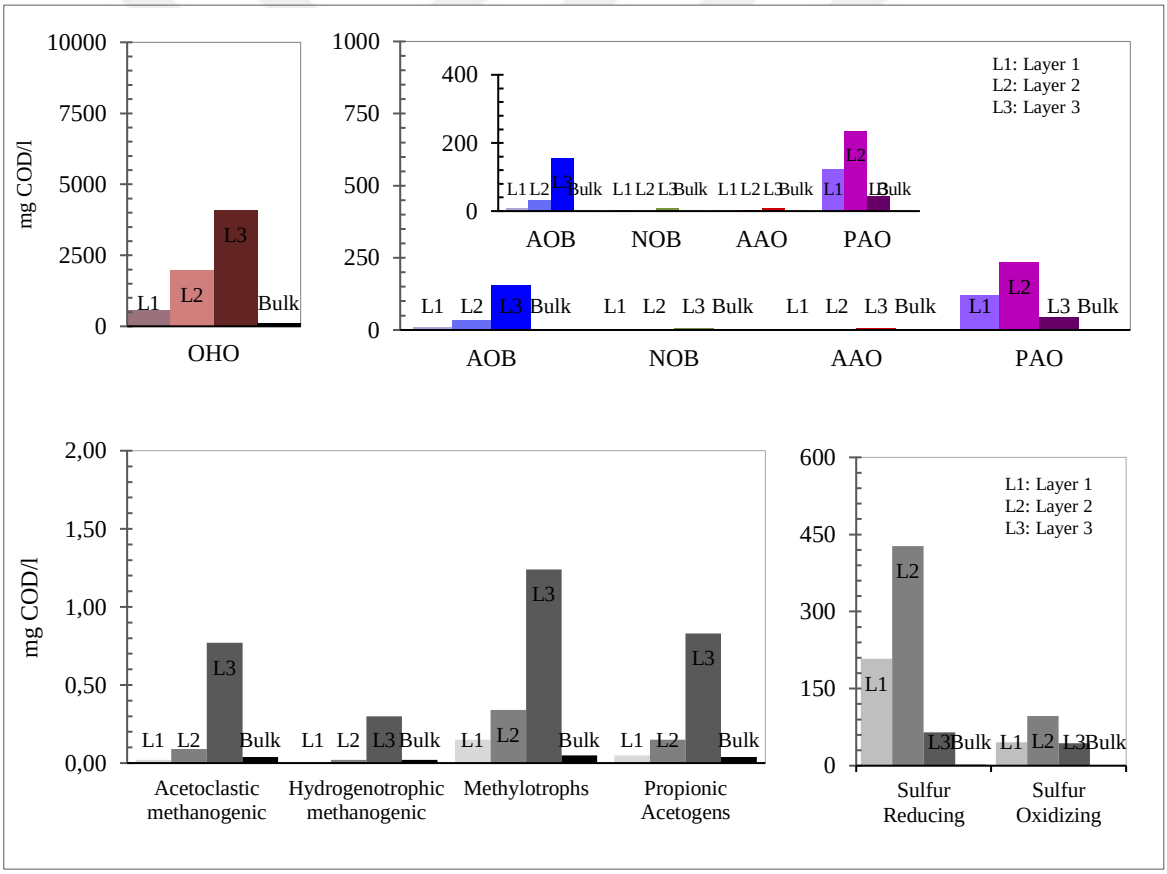

Figure 3.19 Microbial population distribution in biofilm layers of simulation R-S1T1-SS-20-DO2-4

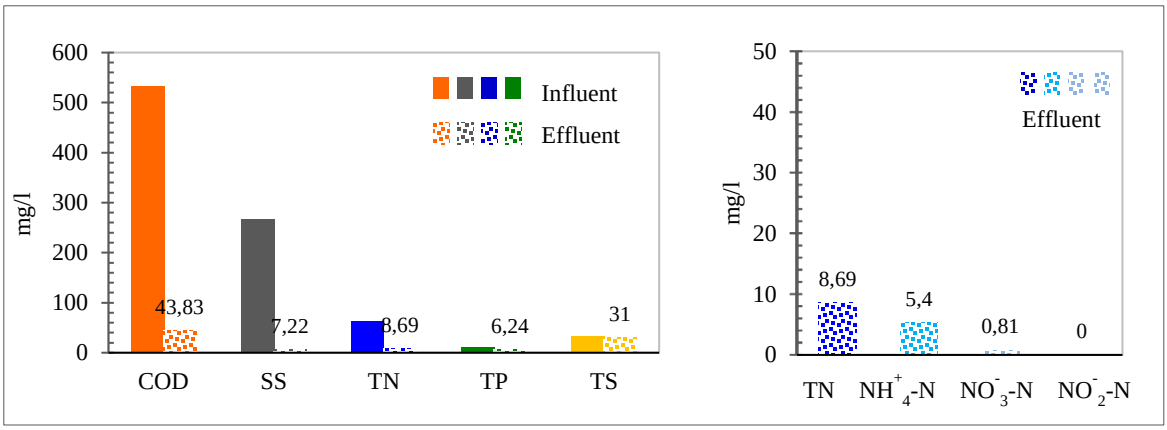

Figure 3.20 Influent and effluent charts of simulation R-S1T1-SS-20-DO2-1

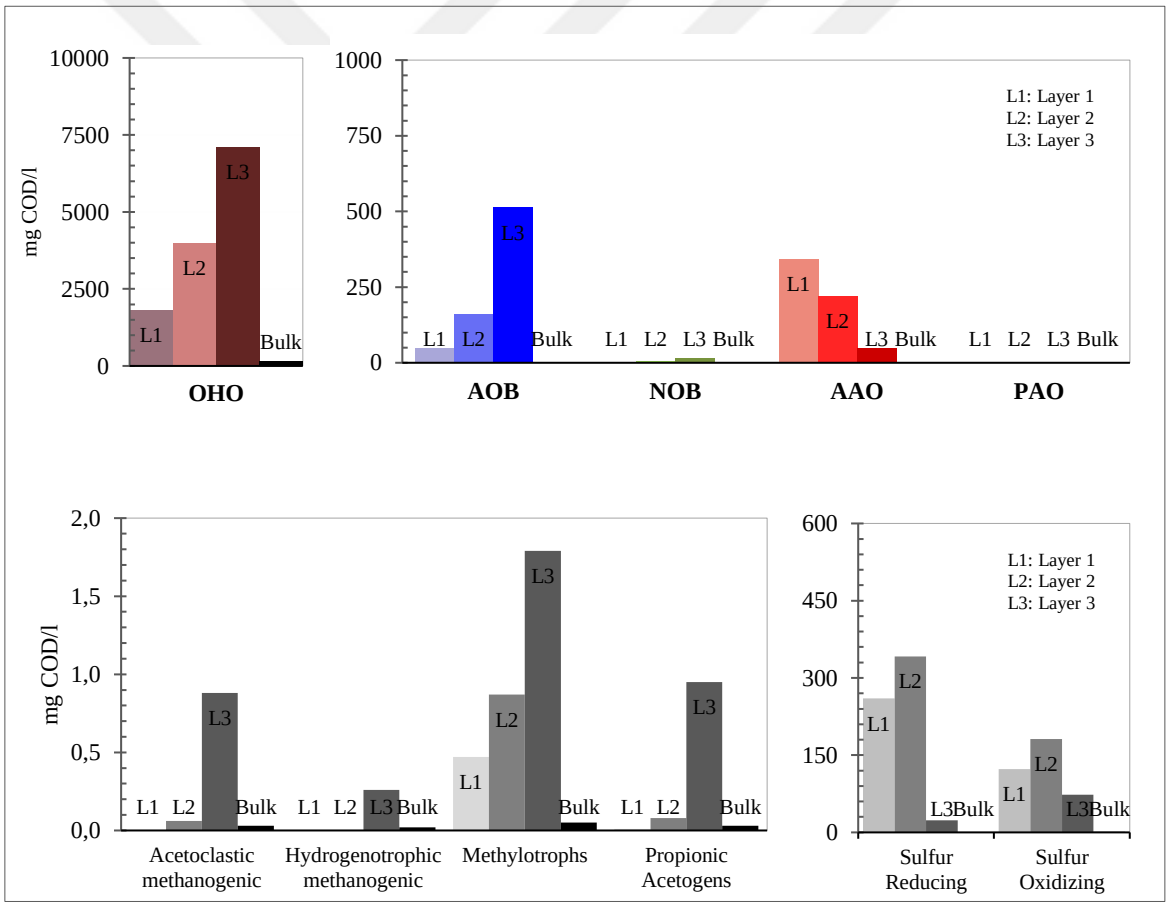

Figure 3.21 Microbial population distribution in biofilm layers of simulation R-S1T1-SS-20-DO2-1

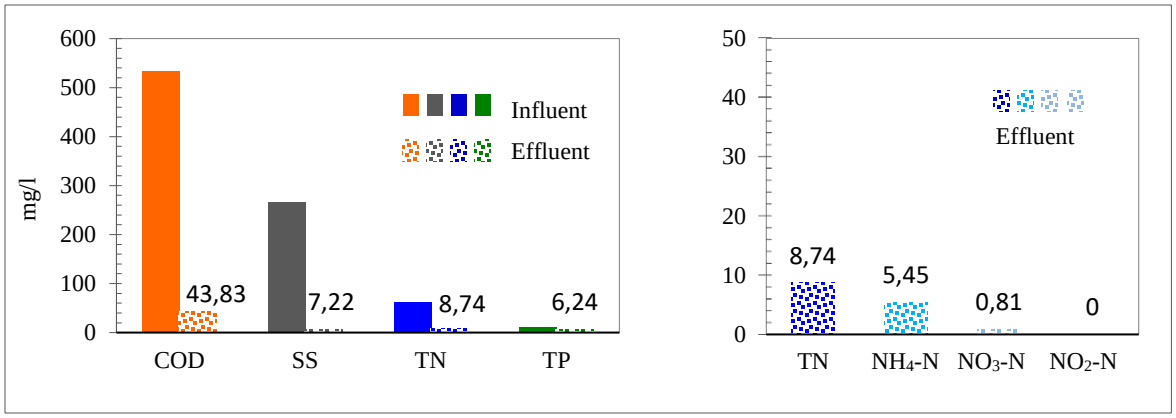

Figure 3.22. Influent and effluent charts of simulation R-S1T1-SS-20-DO2-5.

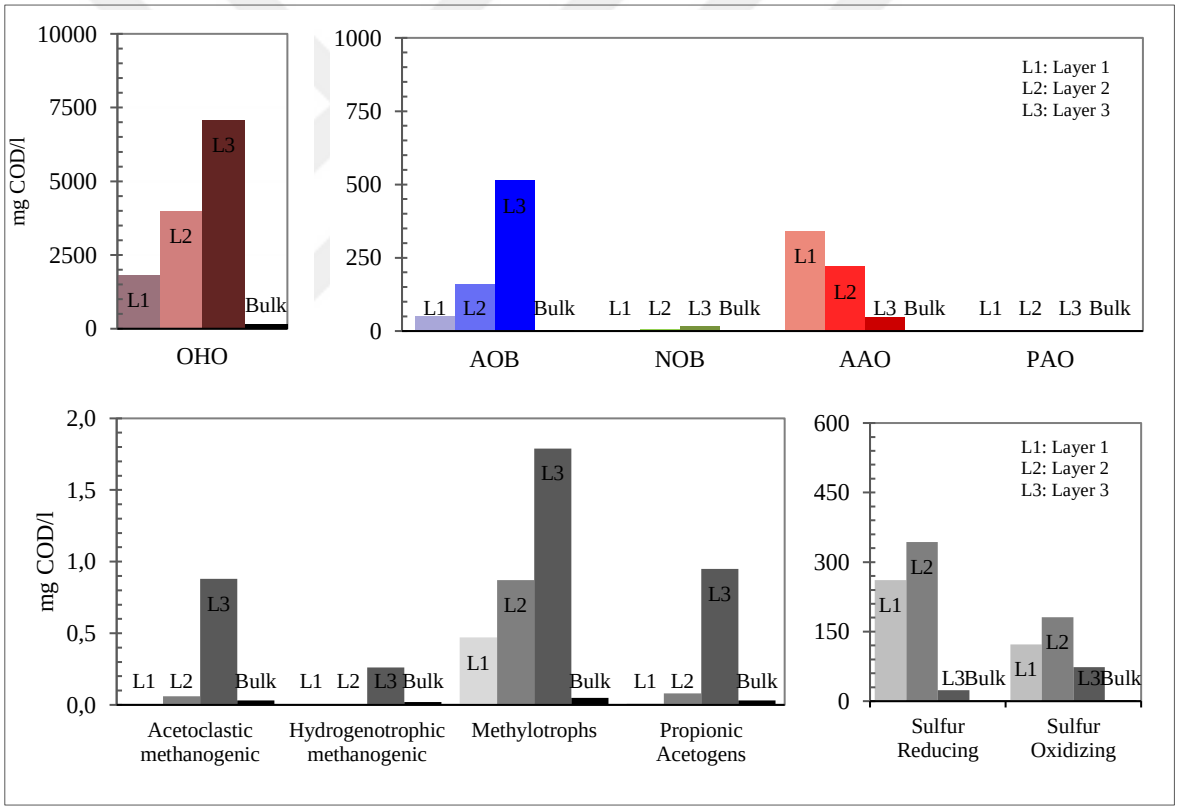

Figure 3.23. Microbial population distribution in biofilm layers of simulation R-S1T1-SS-20-DO2-5

Further increase of oxic period to the 50% increase ammonium removal efficiency to the 95 % together with high nitrite accumulation (14.2 mg/l) and slight nitrate formation. Increasing nitrite level together with increase in DO value to the level of 0.01 mg/l in the mid layer of the biofilm caused a drastic decrease in AAO population (Table 3.8, Figure 3.25).

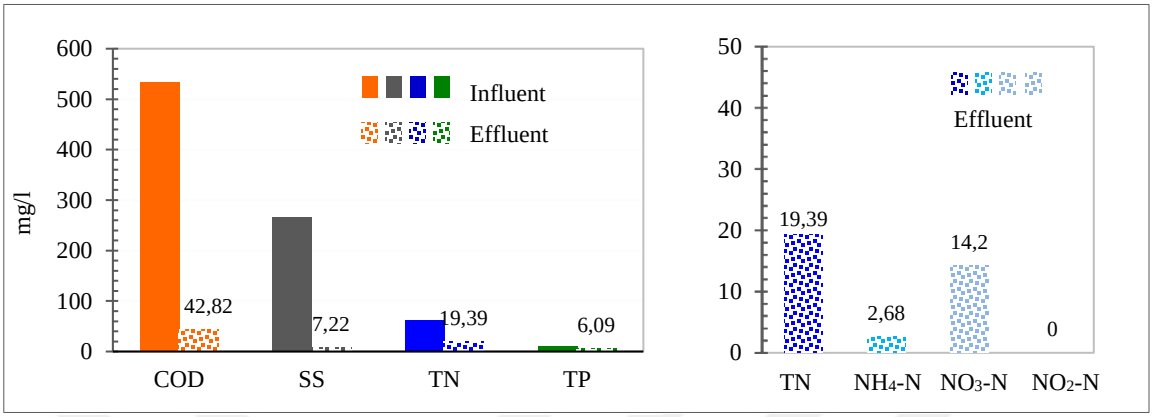

Figure 3.24 Influent and effluent charts of simulation R-S1T1-SS-20-DO2-3

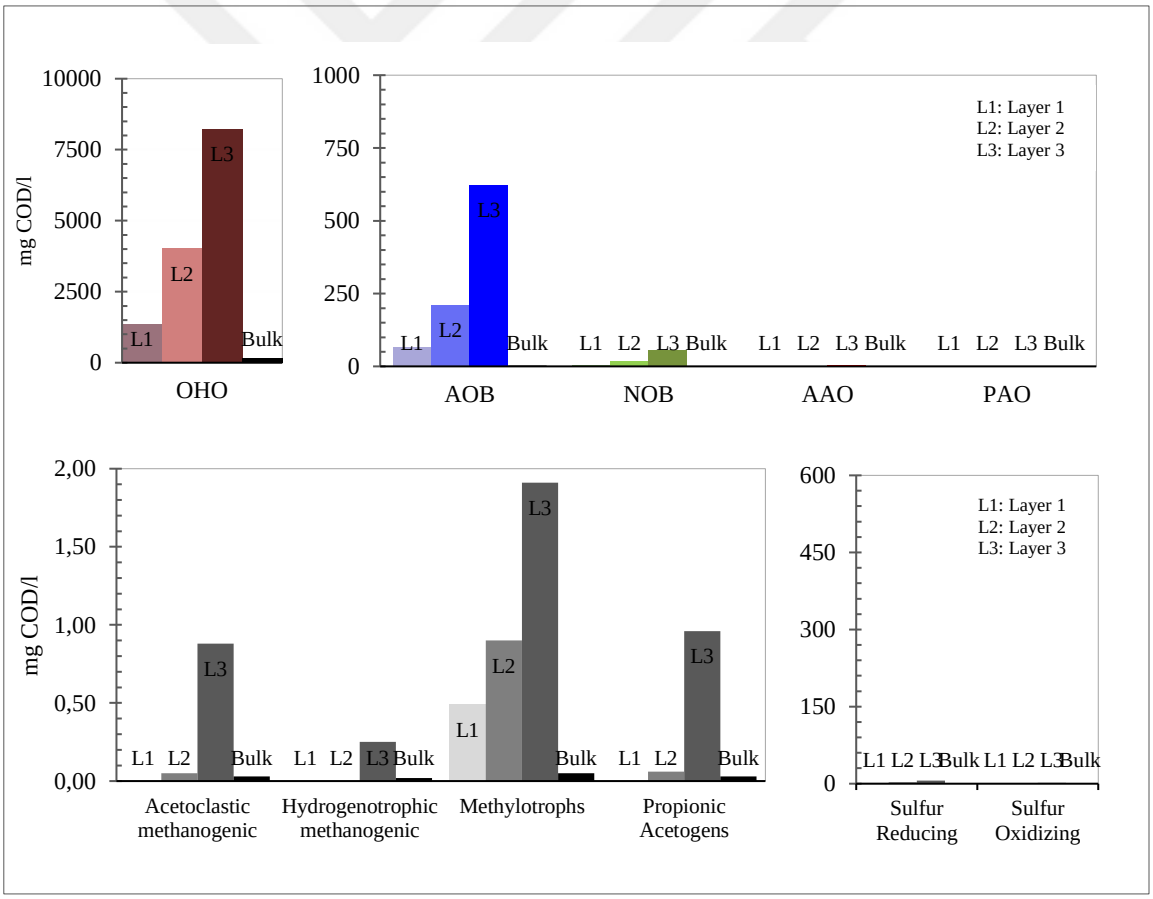

Figure 3.25 Microbial population distribution in biofilm layers of simulation R-S1T1-SS-20-DO2-3

The DO profile through the biofilm (Figure 3.27) shows that with the increase of oxic duration from 25% to 40 % DO level of 0.01 mg/l in the mid layer of the biofilm (L2) under

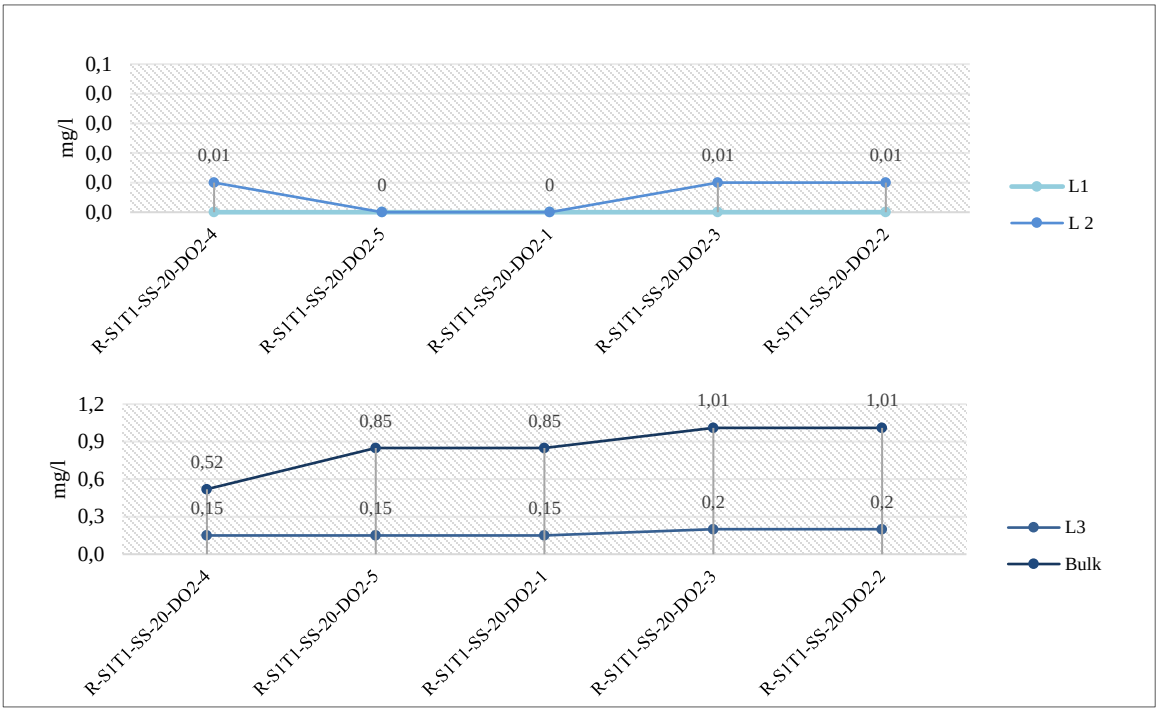

Figure 3.26 DO concentrations trough biofilm layers of simulations at DO set 2.0 mg/l, 20˚C.

25 % oxic period sharply decreased to 0 mg/l with the accelerating activity of AOB species. Accumulating nitrite together with the 0 mg/l DO through the biofilm thickness favored the growth of AAO species (Table 3.8, Figure 3.21).

In addition to the first stage simulations performed under average wastewater temperature of 20˚C, second stage of the Set-up 1 simulations were done for extreme wastewater temperatures of maximum 25˚C and minimum 10˚C (Table 3.9-3.10). The aim of these simulations was to identify a rough logic to operate mainstream deammonification systems under different seosonal conditions. At each temperature conditions, various simulations were performed starting from the lowest oxic duration 25% to the highest oxic duration 75% oxic in order to find minimum TN effluent together with maximum AAO population. These simulation results were evaluated together with the the results obtained under 20˚C (average temperature conditions) (Table 3.9-3.10). Tables 3.9 and 3.10 summarize the most optimum simulations identified at each wastewater temperature under DO set levels of 0.5, 1.0, 1.5 and 2.0 mg/l. Effluent values and microbial population distribution (just in the deeper layer of biofilm, L1) were also presented graphically in Figures 3.28 and 3.29, respectively.

Table 3.9 Effluent values of optimum simulations for DO set values 0.5, 1.0, 1.5 and 2.0 mg/l at 10˚C, 20˚C and 25˚C wastewater temperature.

					EFFLUENT							
T	**DO**		**Oxic**	**Anoxic**	**SS**	**TP**	**NH_4^+-N**	**NO_3^--N**	**NO_2^--N**	**TN**	**COD**	**TN %R**
˚C	mg/l	**SIMULATION NAME**	%	%	mg/l	mg/l	mg/l	mg/l	mg/l	mg/l	mg/l	%
10	0.5	*R-S1T1-SS-10-DO0.5-2*	81%	19%	7.28	6.5	43.41	0	0	46.18	62.19	27%
	1.0	*R-S1T1-SS-10-DO1-2*	81%	19%	7.28	3.35	41.51	0	0	44.17	47.82	30%
	1.5	*R-S1T1-SS-10-DO1.5-3*	81%	19%	7.24	6.11	29.44	0	0.23	32.31	45.1	49%
	2.0	*R-S1T1-SS-10-DO2-3*	78%	22%	7.24	6.08	10.31	9.48	3.86	26.28	43.99	58%
20	0.5	*R-S1T1-SS-20-DO0,5-10*	81%	19%	7.27	6.64	41.34	0	0	44.01	53.15	30%
	1.0	*R-S1T1-SS-20-DO1-7*	81%	19%	7.22	6.28	9.49	0	0.67	12.64	44.2	80%
	1.5	*R-S1T1-SS-20-DO1,5-6*	59%	41%	7.22	6.25	6.24	0	0.77	9.49	43.93	85%
	2.0	*R-S1T1-SS-20-DO2-5*	38%	63%	7.22	6.24	5.45	0	0.81	8.74	43.83	86%
25	0.5	*R-S1T1-SS-25-DO0.5-2*	78%	22%	7.25	6.63	26.94	0	0.1	29.54	48.39	53%
	1.0	*R-S1T1-SS-25-DO1-1*	78%	22%	7.2	6.27	1.68	0.01	0.94	5.06	42.62	92%
	1.5	*R-S1T1-SS-25-DO1.5-1*	54%	46%	7.21	6.26	1.54	0.01	1.05	5.03	42.48	92%
	2.0	*R-S1T1-SS-25-DO2-1*	25%	75%	7.22	6.24	5.4	0	0.81	8.69	43.83	86%

Table 3.10 Microbial population distribution of optimum simulations for DO set values 0.5, 1.0, 1.5 and 2.0 mg/l at 10˚C, 20˚C and 25˚C wastewater temperature.

			OHO			**AOB**			**NOB**			**AAO**		
T ˚C	**DO** mg/l	**SIMULATION NAME**	**L1**	**L 2**	**L3**	**L1**	**L 2**	**L3**	**L1**	**L 2**	**L3**	**L1**	**L 2**	**L3**
10	0.5	*R-S1T1-SS-10-DO0.5-2*	609	1556	2163	0.2	0.9	6.4	0.2	0.7	6.0	0.5	1.2	6.4
	1.0	*R-S1T1-SS-10-DO1-2*	531	1677	5384	1.4	4.9	25.4	0.3	1.1	6.3	1.7	2.7	8.5
	1.5	*R-S1T1-SS-10-DO1.5-3*	1525	4216	7324	16.8	61.1	236.0	1.1	4.1	17.4	2.8	4.8	9.2
	2.0	*R-S1T1-SS-10-DO2-3*	1916	5258	7868	77.7	231.6	539.8	40.4	128.6	412.2	0.6	1.6	6.0
20	0.5	*R-S1T1-SS-20-DO0,5-10*	391	1273	2931	1.4	5.5	26.6	0.2	0.9	5.0	1.1	2.0	6.2
	1.0	*R-S1T1-SS-20-DO1-7*	1845	4097	6699	46.2	151.4	475.8	1.2	4.1	13.8	207.2	137.3	31.7
	1.5	*R-S1T1-SS-20-DO1,5-6*	1821	4023	6981	47.9	157.8	505.0	1.4	4.5	15.6	313.7	203.6	43.9
	2.0	*R-S1T1-SS-20-DO2-5*	1805	3994	7084	48.2	159.2	512.1	1.4	4.7	16.3	340.9	219.1	46.8
25	0.5	*R-S1T1-SS-25-DO0.5-2*	699	2227	3295	10.6	40.2	196.9	0.3	1.1	6.4	1.0	1.9	6.2
	1.0	*R-S1T1-SS-25-DO1-1*	1615	3677	7517	52.4	167.0	529.3	2.2	6.9	23.3	350.2	216.9	50.0
	1.5	*R-S1T1-SS-25-DO1.5-1*	1580	3650	7650	52.4	167.1	529.6	2.6	8.4	28.3	349.1	210.8	48.5
	2.0	*R-S1T1-SS-25-DO2-1*	1804	3992	7092	48.2	159.2	512.5	1.4	4.8	16.4	342.5	219.9	46.9

All values are in mgCOD/l. L1:Layer 1, L2: Layer 2, L3: Layer 3

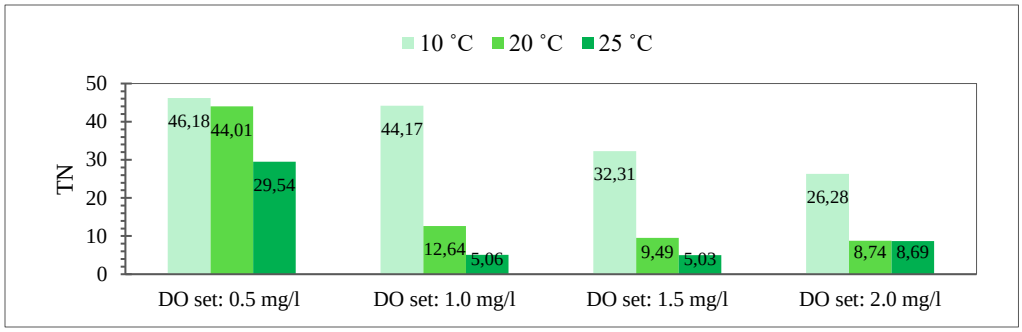

All values are in mg/l.

Figure 3.27 TN effluent values in optimum simulations for DO set values of 0.5, 1.0, 1.5 and 2.0 mg/l at 10˚C, 20˚C and 25˚C wastewater temperatures.

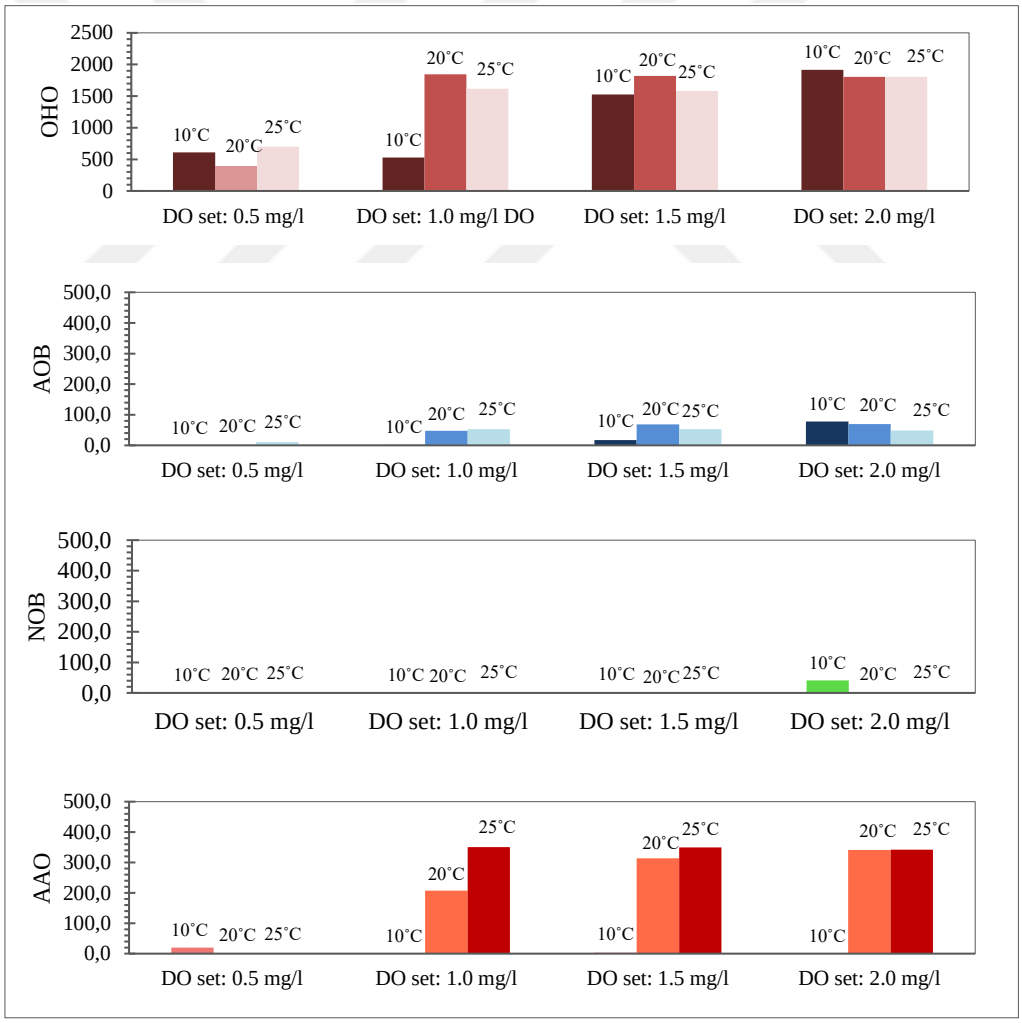

All values are in mgCOD/l.

Figure 3.28 Microbial population distribution in the deeper layer (L1) of biofilm of optimum simulations for DO set values of 0.5, 1.0, 1.5 and 2.0 mg/l at 10˚C, 20˚C and 25˚C.

The results clearly demostrated that under average and high wastewater temperature (20-25˚C) the desired TN removal efficiency can be achieved either keeping DO level high with short oxic-long anoxic operation or keeping DO level low with high oxic-short anoxic periods. Temperature effect on TN removal efficiency and microbial population distribution in 0.5, 1.0, 1.5 and 2.0 mgl/l set DO values, elaborated as charts in Figures 3.28 and 3.29, respectively. On the other hand, under low temperature (10˚C) conditions the optimum operation scheme was identified as keeping the set DO value as low as possible while keeping the oxic periods significantly longer with respect to the anoxic periods. But, under the studied HRT value (9 hrs) which is the existing HRT value of Bursa Dogu STP deammonification pilot plant, it is not possible to achieve desired TN removal and AAO population. In view of this finding, the operation of deammonification systems under low temperature conditions was further studied for different HRT. HRT values were as-is HRT (9 hrs) and five times greater than the as-is HRT. Set DO values were 0.5, 1.0 and 1.5 mg/l. In view of the previous simulations, the highest and lowest oxic-anoxic period distributions were chosen around 81% oxic-19% anoxic and 54% oxic-46% anoxic, respectively. The Tables 3.11 and 3.12 demonstrate the effluent values and microbial population distribution of these simulations. Although the increase of HRT from 9 to 47.7 hours resulted same/better TN removal efficiency under studied set DO and oxic-anoxic aeration patterns, it is obvious that increasing set DO value did not result a significant change in TN effluent either high oxic – low anoxic or low oxic – high anoxic aeration pattern. However if the DO level is kept low, it is possible to achieve the desired TN effluent (< 10 mg/l) with long oxic – short anoxic aeration pattern. Unfortunately, at extremely low wastewater temperature (10˚C) AAO population was significantly low compared to the optimum simulations found in Set-up 1 simulations under 20˚C average wastewater temperature (Table 3.12). This low AAO population demonstrates that the effluent TN level from a single-stage deammonification system under extremely low wastewater temperature can be achieved mainly denitrification-partial denitrification processes due to different growth kinetics of AOB, NOB an AAO species.

Table 3.11 Effluent results of simulations performed under 10˚C wastewater temperature.

					EFFLUENT						
DO		**HRT**	**Oxic**	**Anoxic**	**SS**	**TP**	**NH_4^+-N**	**NO_3^--N**	**NO_2^--N**	**TN**	**COD**
mg/l	**SIMULATION NAME**	h	%	%	mg/l	mg/l	mg/l	mg/l	mg/l	mg/l	mg/l
0.5	*R-S1T1-SS-10-DO0.5-2*	9	81%	19%	7.3	6.5	43.4	0.0	0.0	46.2	62.2
	R-S1T1-SS-10-DO0.5-9	47.7	81%	19%	7.0	7.2	2.9	4.7	0.0	9.8	37.8
	R-S1T1-SS-10-DO0.5-15	9	54%	46%	7.3	7.5	44.1	0.0	0.0	47.0	77.5
	R-S1T1-SS-10-DO0.5-14	47.7	54%	46%	7.1	0.6	45.5	0.0	0.0	47.9	44.4
1.0	*R-S1T1-SS-10-DO1-2*	9	81%	19%	7.3	3.4	41.5	0.0	0.0	44.2	47.8
	R-S1T1-SS-10-DO1-13	47.7	81%	19%	7.0	7.4	0.8	0.2	20.7	24.0	37.2
	R-S1T1-SS-10-DO1-1	9	54%	46%	7.3	2.8	42.7	0.0	0.0	45.4	52.4
	R-S1T1-SS-10-DO1-15	47.7	54%	46%	7.0	7.4	1.2	0.7	7.6	11.7	37.2
1.5	*R-S1T1-SS-10-DO1.5-3*	9	81%	19%	7.2	6.1	29.4	0.0	0.2	32.3	45.1
	R-S1T1-SS-10-DO1.5-22	47.7	81%	19%	7.0	7.4	0.6	0.1	31.8	34.8	37.2
	R-S1T1-SS-10-DO1.5-1	9	54%	46%	7.3	3.4	41.2	0.0	0.0	43.8	47.3
	R-S1T1-SS-10-DO1.5-24	47.7	54%	46%	7.0	7.4	0.7	0.2	22.4	25.6	37.2

Table 3.12 Microbial population distribution of simulations performed under 10˚C wastewater temperature.

DO		**OHO**			**AOB**			**NOB**			**AAO**		
mg/l	**SIMULATION NAME**	**L 1**	**L 2**	**L 3**	**L 1**	**L 2**	**L 3**	**L 1**	**L 2**	**L 3**	**L 1**	**L 2**	**L 3**
0.5	*R-S1T1-SS-10-DO0.5-2*	609	1556	2163	0.2	0.9	6.4	0.2	0.7	6.0	0.5	1.2	6.4
	R-S1T1-SS-10-DO0.5-9	652	1883	5198	47.3	115.0	279.3	1.7	4.4	12.3	0.2	0.7	2.5
	R-S1T1-SS-10-DO0.5-15	655	1584	1614	0.1	0.6	4.9	0.2	0.7	6.0	0.4	1.1	6.1
	R-S1T1-SS-10-DO0.5-14	315	891	2973	1.4	4.1	14.7	0.3	0.7	2.8	2.9	4.0	7.1
1.0	*R-S1T1-SS-10-DO1-2*	531	1677	5384	1.4	4.9	25.4	0.3	1.1	6.3	1.7	2.7	8.5
	R-S1T1-SS-10-DO1-13	686	1707	4630	71.2	135.0	224.8	40.4	87.0	180.8	3.5	4.7	7.2
	R-S1T1-SS-10-DO1-1	566	1450	3343	0.4	1.7	10.9	0.2	0.9	6.1	1.0	1.7	7.4
	R-S1T1-SS-10-DO1-15	822	1905	4672	57.5	126.3	262.9	33.9	80.7	196.3	2.1	3.2	5.8
1.5	*R-S1T1-SS-10-DO1.5-3*	1525	4216	7324	16.8	61.1	236.0	1.1	4.1	17.4	2.8	4.8	9.2
	R-S1T1-SS-10-DO1.5-22	547	1541	4599	91.9	139.8	179.4	55.8	93.3	141.7	4.1	5.2	7.7
	R-S1T1-SS-10-DO1.5-1	542	1721	5710	1.7	6.1	31.0	0.3	1.1	6.4	1.8	2.9	8.7
	R-S1T1-SS-10-DO1.5-24	666	1681	4625	73.8	136.2	218.6	41.7	87.8	176.5	3.6	4.8	7.3

All values are in mgCOD/l. L1:Layer 1, L2: Layer 2, L3: Layer 3

3.2. Set-up-2

In Set-up 2 simulations, the effect of nitrite spike on enrichment of Anammox species in the single-stage deammonification MBBR systems was studied. Hence, different than the Set-up 1 simulations, Set-up 2 simulations results were majorly evaluated based on the Anammox species in the microbial consortia with the lowest TN effluent values as much as possible.

The simulations were done for DO set points of 0.5, 1.0, 1.5 and 2.0 mg/l with same aeration patterns of Set-up 1 optimum simulations in order to study the difference of AAO population and TN effluent values. Each DO set point was simulated with multiple options of oxic/anoxic periods in a cycle. However, only the simulations resulting the maximum AAO population were discussed under this section. The effluent values and microbial population distribution of Set-up 2 simulations are summarized together with the results of Set-up 1 simulations (Tables 3.1-3.8) in Tables 3.14 and 3.15, respectively. Among the Set-up 2 simulations the one resulting the maximum AAO population with highest TN removal efficiency (*R-S2T1-SS-20-DO1.5-1*) was further presented graphically to demonstrate the microbial population distribution (Figure 3.32) and effluent values (Figure 3.31).

Except extremely low DO condition (i.e. 0.5 mg/l), nitrite spike to the pilot plant increased AAO population significantly.with respect to the Set-up 1 simulations. The max AAO population was obtained under set DO 2.0 mg/l with 37% oxic- 63% anoxic aeration pattern conditions. The increase in AAO population under DO 1.0, 1.5 and 2.0 mg/l resulted effluent TN values lower than Set-up 1 simulations indicating the major role of Anammox process in TN removal.

Figure 3.29 compares the AAO populations in Set-up 2 with the corresponding Set-up 1 AAO populations graphically. Based on the results, there has been a slight increase on AAO population in the simulations performed under set DO 0.5 mg/l with nitrite spike due to inefficient nitrification process. The significant increase on AAO observed under 1.0, 1.5 and 2.0 mg/l set DO values which demonstrates the successful enrichment of Anammox species with nitrite spike as aimed. The highest increase on AAO population was acquired from the simulation *R-S2T1-SS-20-DO2-3* as 1224.6 mgCOD/l in the deepest layer.

Table 3.13 Comparison table of Set-up 1 and Set-up 2 simulations under 20 ˚C wastewater temperature with 0.5, 1.0, 1.5 and 2.0 mg/l set DO.

					EFFLUENT						
DO			**Oxic**	**Anoxic**	**SS**	**TP**	**NH_4^+-N**	**NO_3^--N**	**NO_2^--N**	**TN**	**COD**
mg/l	**SIMULATION NAME**	**Nitrite Spike**	%	%	mg/l	mg/l	mg/l	mg/l	mg/l	mg/l	mg/l
0.5	*R-S1T1-SS-20-DO0.5-10*	-	81%	19%	7.3	6.6	41.3	0.0	0.0	44.0	53.2
	R-S2T1-SS-20-DO0.5-3	√	78%	22%	7.3	6.0	39.8	0.0	0.1	42.4	48.6
1.0	*R-S1T1-SS-20-DO1-7*	-	81%	19%	7.2	6.3	9.5	0.0	0.7	12.6	44.2
	R-S2T1-SS-20-DO1-6	√	81%	19%	7.2	6.2	3.6	0.0	1.4	7.4	43.6
1.5	*R-S1T1-SS-20-DO1.5-2*	-	51%	49%	7.2	6.3	14.0	0.0	0.6	17.0	44.4
	R-S2T1-SS-20-DO1.5-1	√	51%	49%	7.2	6.3	5.2	0.0	1.4	9.1	44.1
2.0	*R-S1T1-SS-20-DO2-5*	-	37%	63%	7.2	6.2	5.5	0.0	0.8	8.7	43.8
	R-S2T1-SS-20-DO2-3	√	37%	63%	7.3	6.3	8.2	0.0	1.4	12.2	44.5

Table 3.14 Microbial population distribution of simulations performed under 20˚C wastewater temperature.

	OHO			**AOB**			**NOB**			**AAO**		
SIMULATION NAME	**L 1**	**L 2**	**L 3**	**L 1**	**L 2**	**L 3**	**L 1**	**L 2**	**L 3**	**L 1**	**L 2**	**L 3**
R-S1T1-SS-20-DO0.5-10	391	1273	2931	1.4	5.5	26.6	0.2	0.9	5.0	1.1	2.0	6.2
R-S2T1-SS-20-DO0.5-3	564	1904	3688	2.7	10.1	49.7	0.3	1.1	6.3	1.2	2.1	6.7
R-S1T1-SS-20-DO1-7	1845	4097	6699	46.2	151.4	475.8	1.2	4.1	13.8	207.2	137.3	31.7
R-S2T1-SS-20-DO1-6	1979	4322	7524	51.2	165.2	484.7	2.0	6.7	22.2	561.8	313.0	62.4
R-S1T1-SS-20-DO1.5-2	1835	4151	6445	43.5	140.8	434.5	1.1	3.7	12.5	66.9	46.5	15.1
R-S2T1-SS-20-DO1.5-1	2505	4935	7074	44.4	136.3	383.9	1.8	5.8	18.8	950.0	561.5	110.3
R-S1T1-SS-20-DO2-5	1805	3994	7084	48.2	159.2	512.1	1.4	4.7	16.3	340.9	219.1	46.8
R-S2T1-SS-20-DO2-3	2853	5355	6698	45.0	135.7	380.3	1.6	5.1	16.5	1224.6	770.0	150.8

All values are in mgCOD/l. L1:Layer 1, L2: Layer 2, L3: Layer 3

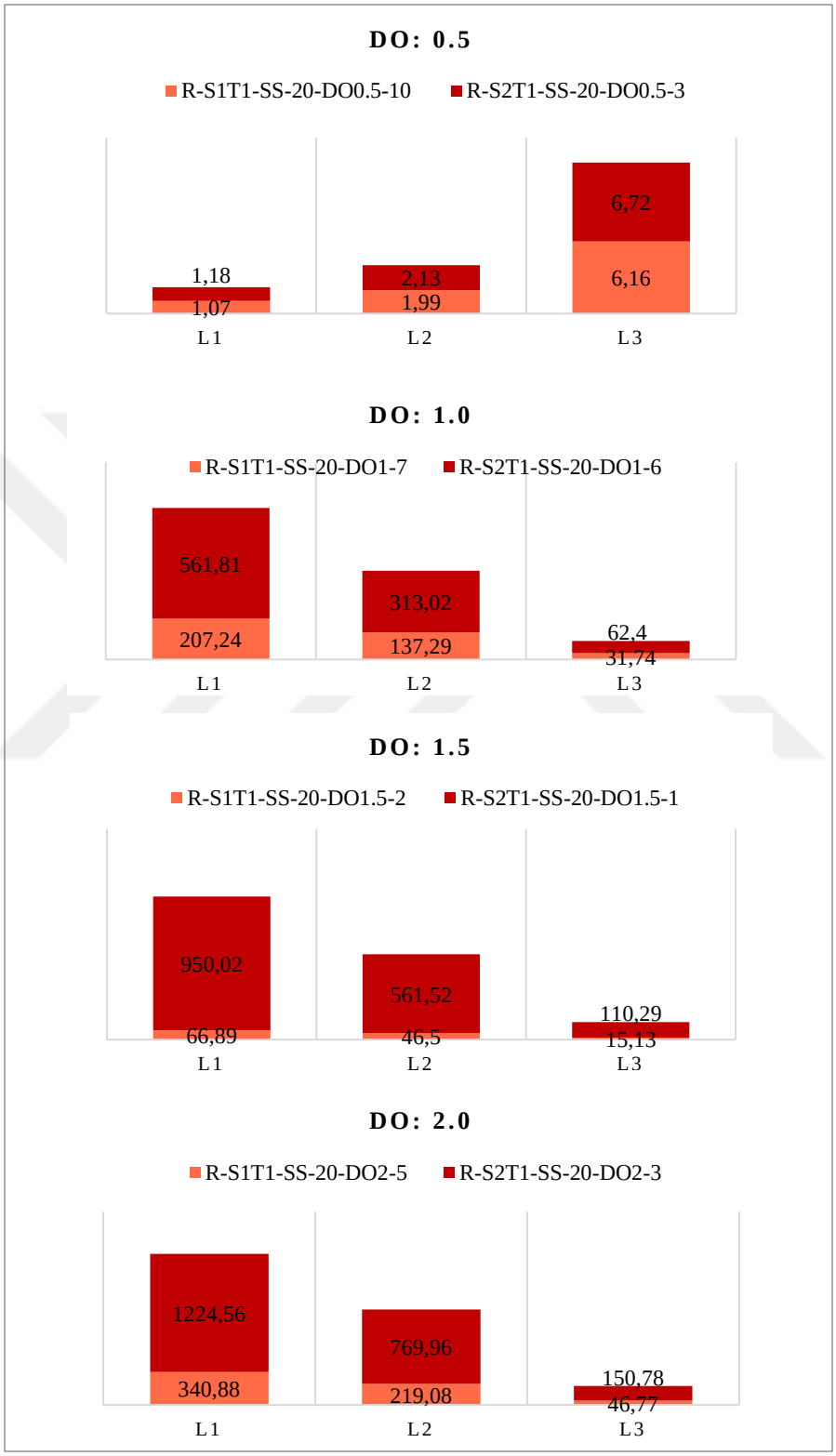

Figure 3.29 AAO populations trough biofilm layers in Set-up 1 and Set-up 2 simulations at 20˚C with DO set 0.5, 1.0, 1.5 and 2.0 mg/l.

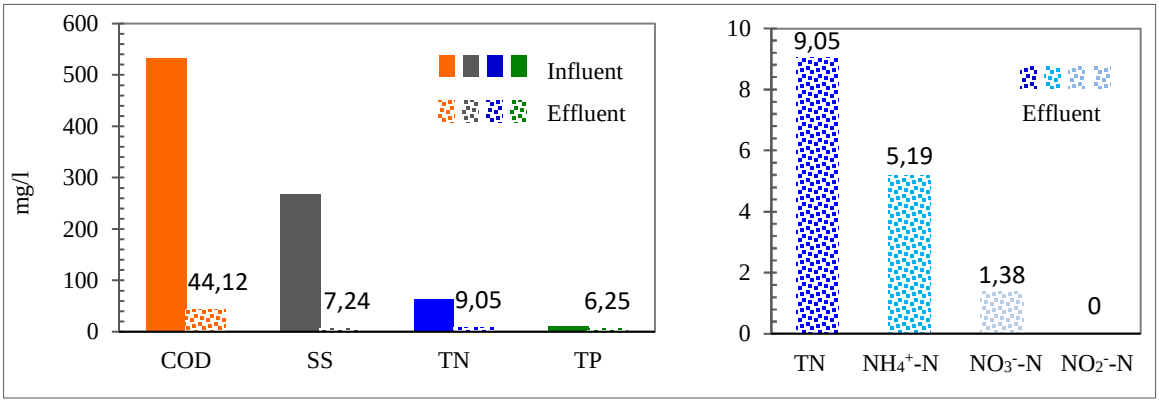

Figure 3.30 Influent and effluent charts of simulation R-S2T1-SS-20-DO1.5-1.

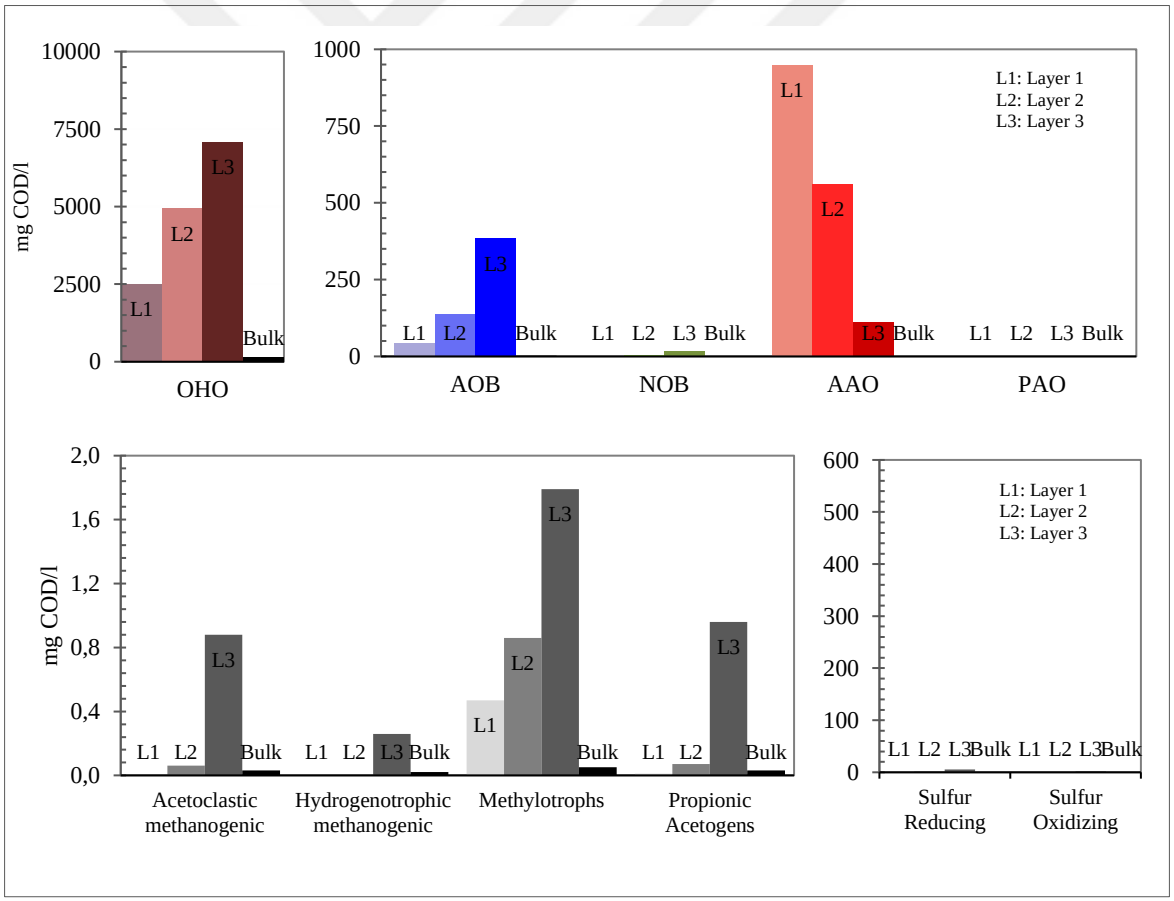

Figure 3.31. Microbial population distribution in biofilm layers of simulation R-S2T1-SS-20-DO1.5-1.

In addition to the Set-up 2 simulation resulting the maximum AAO population with highest TN removal efficiency (*R-S2T1-SS-20-DO1.5-1*), the simulation resulting the lowest AAO

population was also presented graphically to demonstrate the microbial population distribution (Figure 3.34) and effluent values (Figure 3.33).

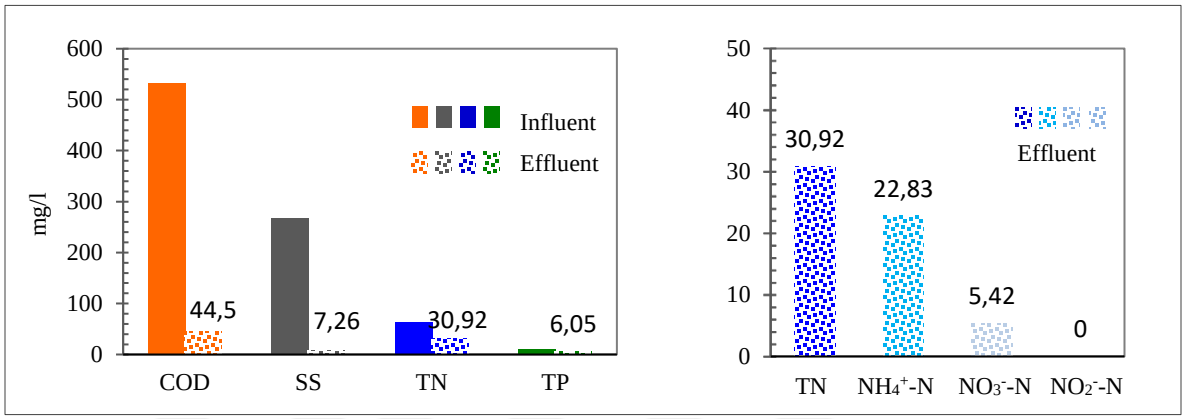

Figure 3.33. Influent and effluent charts of simulation R-S2T1-SS-10-DO2-4.

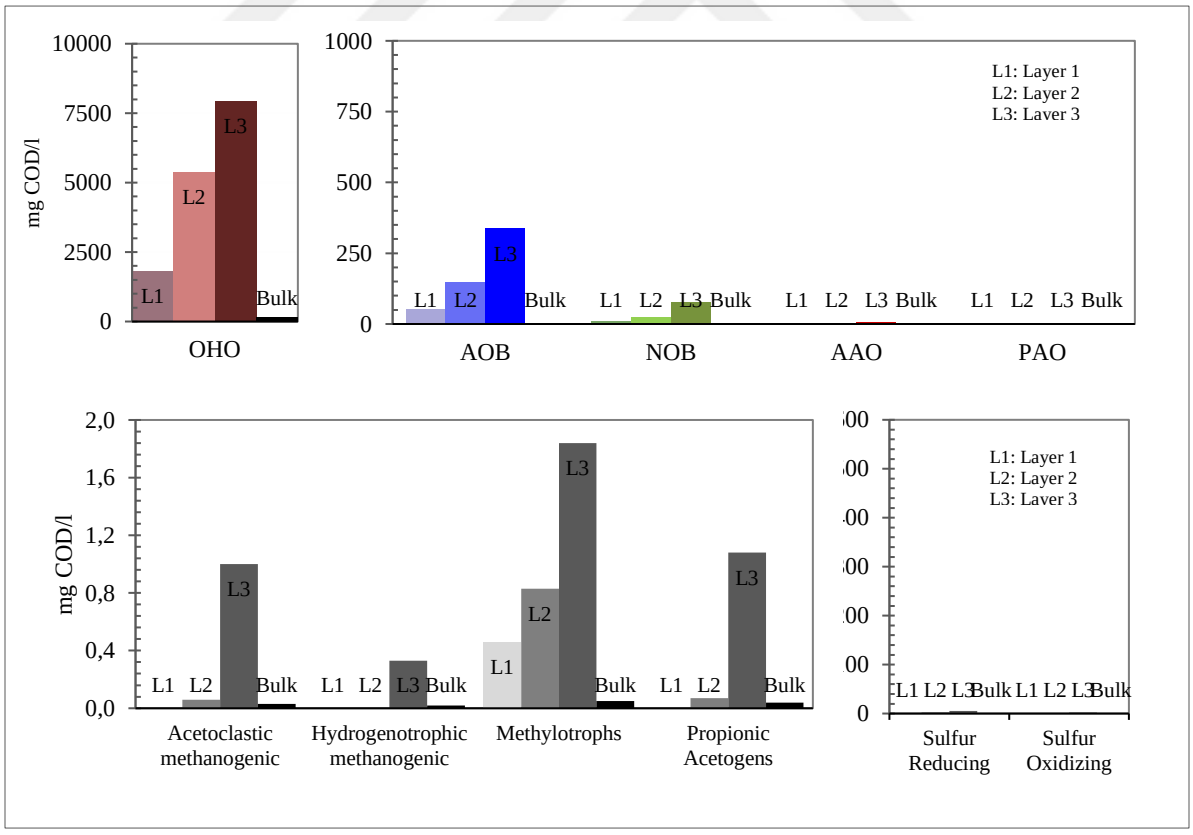

Figure 3.32 Microbial population distribution in biofilm layers of simulation R-S2T1-SS 10-DO2-4

3.3. Sensitivity Analysis

Sensitivity analysis were done for kinetic, stoichiometric and general biofilm parameters using the most optimum set-up 1 simulation (*R-S1T1-SS-20-DO2-5*) which identified in Section 3.1. Influential, very influential and extremely influential parameters were identified based on calculated normalized sensitivity coefficient (S_{ij}) as described in section 2.5.

The overall results for effluent parameters: TN, NO^-_3-N, NO^-_2-N, TSS and COD showed that among 242 kinetic/stoichiometric/biofilm general parameters, 14 parameters were identified as influential ($0{,}25 \leq S_{ij} < 1$, Table 3.18) 2 parameters identified as very influential ($1 \leq S_{ij} < 2$**,** Table 3.19**)** and 19 parameters were identified as extremely influential ($S_{ij} \geq 2$, Table 3.20).

Table 3.15 Influential Parameters - $0{,}25 \leq S_{ij} < 1$

RUN NO	R-S1T1-SS-20-DO2-5 $S_{i,j} = \lvert \Delta Y / Y_i \rvert / \lvert \Delta X / X_i \rvert$				S_{ij} Values for Effluent Parameters															
					TN				NH_4^+-N				NO_3^--N				NO_2^--N			
	PARAMETERS	X_i	ΔX	New	Y_i	Y_e	ΔY	S_{ij}	Y_i	Y_e	ΔY	S_{ij}	Y_i	Y_e	ΔY	S_{ij}	Y_i	Y_e	ΔY	S_{ij}
	KINETIC PARAMETERS																			
	General Parameters																			
2	Hydrolysis half sat. [-]	0.06	1.1	0.07	8.74	8.52	0.22	0.25	5.45	5.21	0.24	0.44	0	0	0	-	0.81	0.82	0.01	0.12
3	Anoxic hydrolysis factor [-]	0.28	1.1	0.31	8.74	8.94	0.2	0.23	5.45	5.66	0.21	0.39	0	0	0	-	0.81	0.79	0.02	0.25
	AOB														0	-				
11	Substrate (NH4) half sat. [mgN/L]	0.7	1.1	0.77	8.74	9.07	0.33	0.38	5.45	5.79	0.34	0.62	0	0	0	-	0.81	0.79	0.02	0.25
	AAO															-				
24	Max. spec. growth rate [1/d]	0.2	1.1	0.22	8.74	8.7	0.04	0.05	5.45	5.46	0.01	0.02	0	0	0	-	0.81	0.75	0.06	0.74
25	Substrate (NH4) half sat. [mgN/L]	2	1.1	2.2	8.74	8.75	0.01	0.01	5.45	5.44	0.01	0.02	0	0	0	-	0.81	0.82	0.01	0.12
26	Substrate (NO2) half sat. [mgN/L]	1	1.1	1.1	8.74	8.77	0.03	0.03	5.45	5.43	0.02	0.04	0	0	0	-	0.81	0.86	0.05	0.62
27	Aerobic decay rate [1/d]	0.02	1.1	0.02	8.74	8.76	0.02	0.02	5.45	5.44	0.01	0.02	0	0	0	-	0.81	0.84	0.03	0.37
	OHO															-				
31	Max. spec. growth rate [1/d]	3.2	1.1	3.52	8.74	8.3	0.44	0.50	5.45	4.99	0.46	0.84	0	0	0	-	0.81	0.82	0.01	0.12
32	Substrate half sat. [mgCOD/L]	5	1.1	5.5	8.74	8.93	0.19	0.22	5.45	5.64	0.19	0.35	0	0	0	-	0.81	0.8	0.01	0.12
	SWITCHES																			
101	Ordinary heterotrophic DO half sat. [mgO2/L]	0.15	1.1	0.17	8.74	8.53	0.21	0.24	5.45	5.24	0.21	0.39	0	0	0	-	0.81	0.81	0	0.00
	BIOFILM GENERAL PARAMETERS																			
121	Attachment rate [g / (m2 d)]	8	1.1	8.8	8.74	8.36	0.38	0.43	5.45	5.08	0.37	0.68	0	0	0	-	0.81	0.8	0.01	0.12
123	Detachment rate [g/(m3 d)]	8000	1.1	8800	8.74	9.12	0.38	0.43	5.45	5.81	0.36	0.66	0	0	0	-	0.81	0.82	0.01	0.12
128	Assumed Film thickness for tank volume correction (temp independent) [mm]	1.25	1.1	1.38	8.74	8.98	0.24	0.27	5.45	5.7	0.25	0.46	0	0	0	-	0.81	0.79	0.02	0.25
	STOICHIOMETRIC PARAMETERS																			
	OHO																			
182	Yield acetic (aerobic) [-]	0.6	1.1	0.66	8.74	8.53	0.21	0.24	5.45	5.23	0.22	0.40	0	0	0	-	0.81	0.81	0	0.00

Table 3.16 Very Influential Parameters - $1 \leq S_{ij} < 2$

R-S1T1-SS-20-DO2-5					Sij Values for Effluent Parameters															
$S_{i,j} = \lvert \Delta Y / Y_i \rvert / \lvert \Delta X / X_i \rvert$					TN				NH_4^+-N				NO_3^--N				NO_2^--N			
RUN	PARAMETERS KINETIC PARAMETERS *General Parameters* *AOB*	X_i	ΔX	New	Y_i	Y_e	ΔY	S_{ij}	Y_i	Y_e	ΔY	S_{ij}	Y_i	Y_e	ΔY	S_{ij}	Y_i	Y_e	ΔY	S_{ij}
16	Aerobic decay rate [1/d]	0.17	1.1	0.19	8.74	9.42	0.68	0.78	5.45	6.16	0.71	1.30	0	0	0	-	0.81	0.77	0.04	0.49
17	Anoxic/anaerobic decay rate [1/d]	0.08	1.1	0.09	8.74	9.29	0.55	0.63	5.45	6.03	0.58	1.06	0	0	0	-	0.81	0.78	0.03	0.37

Table 3.17 Extremely Influential Parameters - $S_{ij} \geq 2$

R-S1T1-SS-20-DO2-5					S_{ij} Values for Effluent Parameters															
$S_{i,j} = \lvert \Delta Y / Y_i \rvert / \lvert \Delta X / X_i \rvert$					TN				NH_4^+-N				NO_3^--N				NO_2^--N			
RUN NO	PARAMETERS KINETIC PARAMETERS *General Parameters*	X_i	ΔX	New	Y_i	Y_e	ΔY	S_{ij}	Y_i	Y_e	ΔY	S_{ij}	Y_i	Y_e	ΔY	S_{ij}	Y_i	Y_e	ΔY	S_{ij}
1	Hydrolysis rate [1/d]	2.1	1.1	2.31	8.74	9.84	1.1	1.26	5.45	6.64	1.19	2.18	0	0	0	-	0.81	0.73	0.08	0.99
7	Ammonification rate [L/(mgCOD d)]	0.08	1.1	0.088	8.74	15.4	6.68	7.64	5.45	7.19	1.74	3.19	0	0	0	-	0.81	5.81	5	61.73
	AOB														0	-				
10	Max. spec. growth rate [1/d]	0.9	1.1	0.99	8.74	6.82	1.92	2.20	5.45	3.36	2.09	3.83	0	0	0	-	0.81	0.98	0.17	2.10
	NOB															-				
20	Substrate (NO2) half sat. [mgN/L]	0.1	1.1	0.11	8.74	14.8	6.09	6.97	5.45	6.92	1.47	2.70	0	0	0	-	0.81	5.43	4.62	57.04
	AAO															-				

30	Nitrite sensitivity constant [L / (d mgN)]	0.016	1.1	0.018	8.74	13.3	4.6	5.26	5.45	6.36	0.91	1.67	0	0	0	-	0.81	4.5	3.69	45.56
	OHO															-				
36	Anoxic decay rate [1/d]	0.233	1.1	0.256	8.74	14.3	5.53	6.33	5.45	6.65	1.2	2.20	0	0	0	-	0.81	5.12	4.31	53.21
	PAO															-				
48	Max. spec. growth rate [1/d]	0.95	1.1	1.045	8.74	7.57	1.17	1.34	5.45	4.05	1.4	2.57	0	0	0	-	0.81	1.04	0.23	2.84
	SWITCHES																			
104	Ammonia oxidizing DO half sat. [mgO2/L]	0.25	1.1	0.275	8.74	10.4	1.66	1.90	5.45	7.17	1.72	3.16	0	0	0	-	0.81	0.74	0.07	0.86
110	Anoxic NO3(->N2) half sat. [mgN/L]	0.05	1.1	0.055	8.74	15.4	6.68	7.64	5.45	7.15	1.7	3.12	0	0	0	-	0.81	5.79	4.98	61.48
	BIOFILM GENERAL PARAMETERS														0	-				
124	Solids movement factor []	10	1.1	11	8.74	15.4	6.69	7.65	5.45	7.16	1.71	3.14	0	0	0	-	0.81	5.8	4.99	61.60
125	Diffusion neta []	0.8	1.1	0.88	8.74	6.86	1.88	2.15	5.45	3.35	2.1	3.85	0	0	0	-	0.81	1.03	0.22	2.72
126	Thin film limit [mm]	0.5	1.1	0.55	8.74	7.46	1.28	1.46	5.45	3.95	1.5	2.75	0	0	0	-	0.81	1.03	0.22	2.72
129	Film surface area to media area ratio - Max.[ ]	1	1.1	1.1	8.74	8.25	0.49	0.56	5.45	3.1	2.35	4.31	0	0.01	0.01	-	0.81	2.69	1.88	23.21
	STOICHIOMETRIC PARAMETERS																			
	NOB																			
153	Yield [mgCOD/mgN]	0.09	1.1	0.099	8.74	15.5	6.79	7.77	5.45	7.18	1.73	3.17	0	0	0	-	0.81	5.87	5.06	62.47
	AAO																			
158	Yield [mgCOD/mgN]	0.114	1.1	0.125	8.74	15.5	6.78	7.76	5.45	7.19	1.74	3.19	0	0	0	-	0.81	5.85	5.04	62.22
	OHO																			
164	Yield (aerobic) [-]	0.666	1.1	0.733	8.74	14	5.25	6.01	5.45	4.36	1.09	2.00	0	0	0	-	0.81	7.18	6.37	78.64
177	Endogenous fraction - anaerobic [-]	0.184	1.1	0.202	8.74	15.5	6.71	7.68	5.45	7.16	1.71	3.14	0	0	0	-	0.81	5.82	5.01	61.85
179	Yield (anoxic) [-]	0.54	1.1	0.594	8.74	12.6	3.82	4.37	5.45	5.45	0	0.00	0	0	0	-	0.81	4.65	3.84	47.41
180	Yield propionic (aerobic) [-]	0.64	1.1	0.704	8.74	15.4	6.69	7.65	5.45	7.15	1.7	3.12	0	0	0	-	0.81	5.8	4.99	61.60

3.4. Dynamic simulation

Dynamic simulations of Set-up 2 were done using the influent data of Bursa Dogu STP influent values for 21 days between 11/10/2018 – 31/11/2018. Similar to the real plant operation data, the aeration pattern of %40 oxic- %60 anoxic with 0.5 mg/l set DO was identified in the simulatior BioWin® 6.0. The major difficulty faced at the beginning of the dynamic simulation was the lack of influent data to identify to the simulator before the start of the dynamic simulation. However, the dynamic simulation of the plant was tried with the avaliable data and the effluent results were obtained as shown in Figure 3.34. As a next step these result were compared with the real plant effluent data for the same time period. (Figure 3.35). Simulation results for COD followed a very similar pattern with actual plant COD results. This showed that in BioWin® 6.0 stoichiometric and kinetic constants belonging to the COD removal processes are already calibrated to the mainstream conditions. No further calibration is necessary for the kinetic and stoichiometric constants of the processes responsible from COD removal, i.e. aerobic organic carbon removal by OHO and denitrification by faculatative heterotrophs. However, the TN effluent results obtained from the simulator was matching roughly with the plant data while NH_4^+-N effluent results were completely different than the actual plant data. This observation was heavily related with the performing dynamic simulations with a simulator uncalibrated to the actual plant conditions. In other words, using the default stoichiometric and kinetic constant of the species responsible from ammonium removal especially, AAO species caused obtaining confusing results. Therefore, this trial clearly showed us the importanc eof calibration of the simulators before using them for dynamic simulations. The sensitivity analysis performed in the scope of this study (section-) will be quite helpful for future studies to be performed on calibration of simulators for MBBR type mainstream deammonification systems.

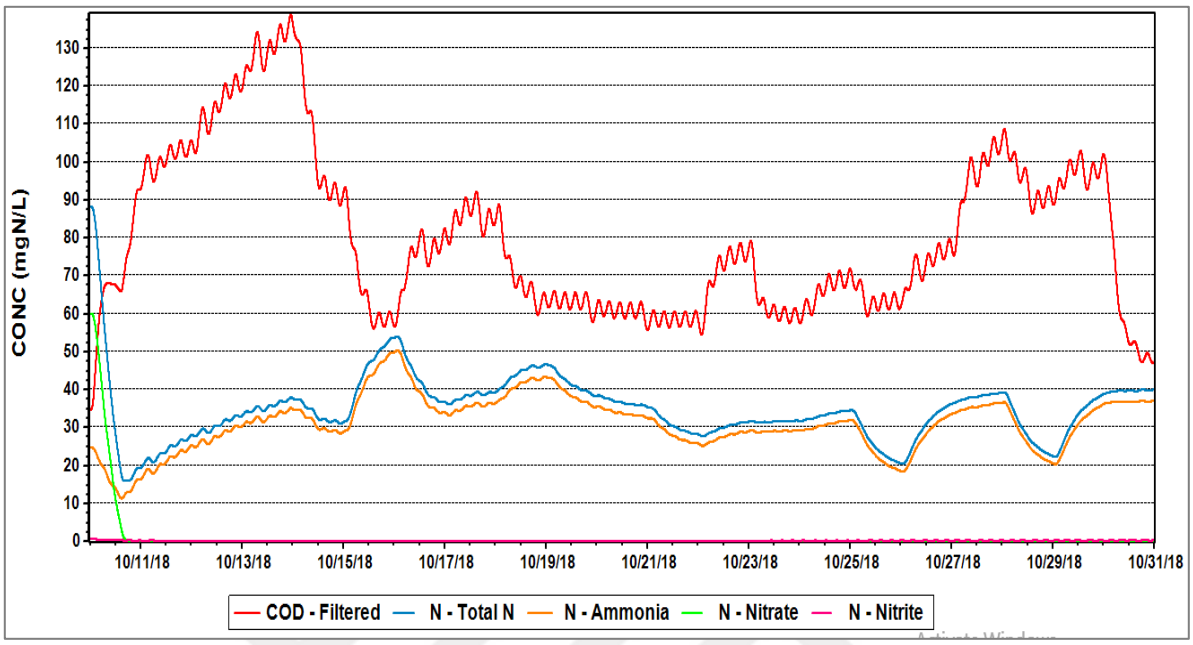

Figure 3.34 Dynamic simulation effluent results of deammonification MBBR model for 21 days.

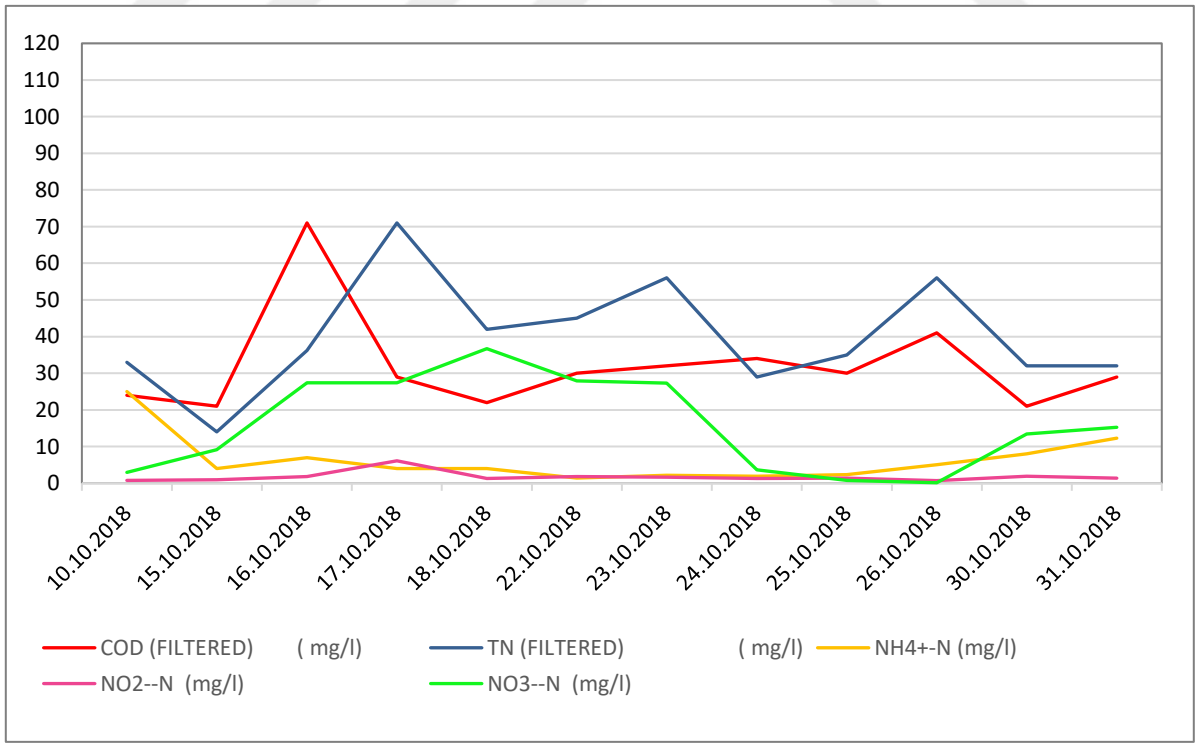

Figure 3.35 Actual effluent data of Bursa deammoification MBBR pilot plant for 21 days.

4. CONCLUSION

In this study, start-up phase of a single-stage mainstream MBBR deammonification system was studied using a real data from a pilot plant located in Bursa Dogu STP. The possible use of computer based wastewater simulators to identify and understand the processes occuring in a mainstream deammonification system was evaluated under mainly average wastewater temperature (20°C) conditions together with high and low wastewater temperature conditions (25°C- 10°C). As the simulator, BioWin® 6 of Envirosim (Canada) was used since it is the one having widest application in all over the World with user-friendly charactics and also the one having MBBR deammonification module.

In this study, start-up phase of a single-stage mainstream MBBR deammonification system was studied using a real data from a pilot plant located in Bursa Dogu STP. The possible use of computer based wastewater simulator for following the processes occuring in the system was evaluated under mainly average wastewater temperature (20˚C) conditions together with high and low wastewater temperature conditions (25˚C- 10˚C).

The effect of nitrite spike to the pilot to enrich Anammox species was also done with the use of simulator BioWin® 6.0. One sample dynamic simulation was done using the influent values of the real pilot in Bursa in order to evaluate the limitations of the simulator use without any calibration to estimate the effluent values. Sensitivity analysis was also done for totally 242 kinetic, stoichiometric and biofilm general parameters of BioWin® 6.0 to describe the significance of changing these parameters during calibration of simulators.

The major conclusions obtained from this study are as follows:

1. In the operation of single-stage deammonification systems, set DO value and oxic-anoxic aeration pattern are the major operation parameters that directly decide which processes (i.e., partial/full nitrification, partial/full denitrification, Anammox) will be prevalent and dominant in the system.

2. The wastewater simulators were found to be a useful tool to understand which processes occuring through the entire depth of the biofilm under different operational conditions and how these processes affecting effluent values.
3. Under average wastewater temperature of 20˚C, the operation methodology has to be adjusted in such a way that NOB population will not increase significantly and dissolved oxygen penetration to the deeper layer of the biofilm will be prevented. AOB population is very important for partial nitritation to occur. The lack of AOB will directly prevent the growth of AAO species.
4. Under 20˚C wastewater temperature, gradually increasing set DO value from 0.5 mg/l up to 2.0 mg/l favors the growth of AAO species due to increased partial nitritation activity in the system while keeping the aeration pattern constant. Oxic duration must be adjusted based on the applied set DO value.Under the studied plant conditions, the optimum operation scheme for 20˚C was identified as 2.0 mg/l set DO with 37% oxic-63% anoxic aeration pattern.
5. Under extreme temperature conditions (i.e. very low or very high temperature) different operational strategies are necessary since the growth kinetics of different group of bacteria (i.e., AOB, NOB and AAO) are affected from such extreme temperature changes differently.
6. Under high wastewater temperature conditions (e.g 25˚C), the desired TN removal efficiency can be achieved either keeping DO level high with short oxic-long anoxic operation or keeping DO level low with high oxic-short anoxic periods. Under the studied plant conditions, the optimum operation scheme for 25˚C was identified as 2.0 mg/l set DO with 25% oxic-75% anoxic aeration pattern.
7. Under low temperature conditions (e.g. 10˚C), if the HRT is proper, keeping the set DO value as low as possible with oxic periods longer than anoxic period will provide themaximum AAO growth. However under such a low wastewater temperature conditions, the main process responsible from TN removal will always be partial and/or full denitrification processes. Under the studied plant conditions, the simulations showed that as-is HRT is insusfficient to achieve desired TN removal efficiency. Almost five times increase in HRT is necessary to achieve TN effluent of

9.8 mg/ l. However, this increse will not result a significant increase in AAO population under 10°C conditions and the treatment will majorly be achieved by partial/full nitrification and partial/full denitrification processes.

8. Nitrite spike during the start-up phase of single-stage deammonification systems may accelerate the growth of AAO species.
9. A sample dynamic simulation performed with the pilot data in this study demonstrated that dynamic simulations of single-stage mainstream deammonification systems with simulators like BioWin® 6.0 without any calibration demonstrate good COD effluent correlations with real plants data but not with NH_4^+-N.
10. The use of simulators for dynamic simulations of single-stage mainstream deammonification MBBR systems definitely require calibration of the simulators since the default kinetic and stoichiometric constants of AAO species identified in the simulator program usually do not match with the real plant conditions.
11. Sensitivity analaysis of kinetic, stoichiometric and biofilm parameters is necessary in order to accelerate the calibration studies.
12. Sensitivity analysis performed for a single-stage mainstream deammonification system under 20°C wastewater temperature conditions demonstrated that the following 9 Kinetic parameters, 6 stoichiometric parameters and 4 biofilm general parameters are extremely influential: *Hydrolysis rate (1/d), Ammonification rate (L/(mgCOD d)), Max. spec. growth rate of AOB (1/d), Substrate (NO_2) half sat. For NOB (mgN/L), Nitrite sensitivity constant (L/(d mgN)) for AAO, Anoxic decay rate (1/d) for OHO, Max. spec. growth rate (1/d) for PAO, Ammonia oxidizing DO half sat. (mgO_2/L), Anoxic NO_3 (->N_2) half sat. (mgN/L), Yield (mgCOD/mgN) of NOB,Yield (mgCOD/mgN) of AAO, Yield (aerobic) of OHO, Endogenous fraction – anaerobic for OHO, Yield (anoxic) of OHO, Yield propionic (aerobic) of OHO, Solids movement factor, Diffusion neta, Thin film limit , Film surface area to media area ratio – max*

REFERENCES

Abma, W. R.; Schultz, C. E.; Mulder, J. W.; Van der Star, W. R. L.; Strous, M.; Tokutomi, T.; Van Loosdrecht, M. C. M. ‘’Full-Scale Granular Sludge Anammox Process’’, Water Sci. Technol., 55 (2007) 27–33.

Biasea, A.; Kowalskia, M.S.; Devlina, T.R.; Oleszkiewicza, Jan A. “Moving bed biofilm reactor technology in municipal wastewater treatment: A review” Journal of Environmental Management, 247 (2019) 849-866.

BioWin Help Manual, Envirosim ltd. (2019)
http://www.envirosim.com/downloads/BW5Manual.pdf

Boltz, J.; ‘’Moving Bed Biofilm Reactor Technology: Process Applications, Design, and Performance’’, Water Environment Research, 83 (2011) 560-575.

Boltz, J.; Johnson, B.R.; Daigger, G.T.; Sandino, J.; ‘’ Modeling Integrated Fixed-Film Activated Sludge and Moving-Bed Biofilm Reactor Systems I: Mathematical Treatment ‘’ Water Environment Research, 81 (2009) 555-575.

Butler C.S.; Boltz J.P.; Ajuha, S.; ‘’ Comprehensive Water Quality and Purification’’, Elsevier, USA, (2014) 90–107.

Chamorro, S.; Pozo, G.; Jarpa, M.; Hernandez, V.; Becerra, J.; Vidal, G.; ‘’Monitoring endocrine activity in Kraft mill effluent treated by aerobic moving bed bioreactor system’’ Water Sci. Technol., 62 (2010) 154-161.

Choubert, J.M.; Canler, J.P.; Pétrimaux, O.; Héduit, A.; Lessard, P.; ‘’A one dimensional moving bed biofilm reactor model for nitrification of municipal wastewaters’’, Bioprocess and Biosystems Engineering, 40 (2017) 1141-1149.

Christensson, M.; Ekstrom, S.; Andersson Chan, A.; Le Vaillant, E.; Lemaire, R.; '' Experience from Start-Ups of the First ANITA-Mox Plants'', Water Sci. Technol., 67 (2013) 2677–2684.

De Clippeleir, H.; Vlaeminck, S.E.; Wilde, F.; Daeninck, K.; Mosquera, M.; Boeckx, P.; Verstraete, W.; Boon, N.; ''One-stage partial nitritation/anammox at 15 °C on pretreated sewage: feasibility demonstration at lab-scale'', Applied Microbiology and Biotechnology, 97 (2013) 10199–10210.

Dongen, V.; Jetten, M.S.M.; Loosdrecht, M.C.M.; ''The SHARON®-Anammox® process for treatment of ammonium rich wastewater'', Water Science and technology, 44 (2001) 153-160.

Francis, C.A.; Beman, J.M.; Kuypers, M.M.; ''New processes and players in the nitrogen cycle: the microbial ecology of anaerobic and archaeal ammonia oxidation'' ISME (2007) 19-27.

Fux, C.; Siegrist, H.; ''Nitrogen removal from sludge digester liquids by nitrification/denitrification or partial nitritation/anammox: environmental and economical considerations'' Water Science and technology, 50 (2004) 19-26.

Growth and Metabolism of Anammox Bacteria, (2008) Wouter van der star, Delft University

Gruber, N.; Galloway, J.N.; '' An Earth-system perspective of the global nitrogen cycle'', Nature, 451 (2008) 293–296. Hendrickx, T.L.G.; Wang, Y.; Kampman, C.; Zeeman, G.; Temmink, H.;.Buisman, J.N.; ''Autotrophic nitrogen removal from low strength waste water at low temperature'' Water Research, 46 (2012) 2187-2193.

Henze, M.; Loosdrecht, M.C.M.; Ekama, G.A.; Brdjanovic, D.; ''Biological Wastewater Treatment Principles, Modelling and Design'' IWA Publishing, London, UK (2008).

Hu, Z.; Lotti, T.; Kreuk, M.; Kleerebezem, R.; Loosdrecht, M.; Kruit, J.; Jetten, M.S.M.;

Kartal, B.; ‘’Nitrogen Removal by a Nitritation-Anammox Bioreactor at Low Temperature’’, Applied and Environmental Microbiology, 79 (2015) 2807-2812.

Hung, C.; Yu F.; McFeters, G.; Stewart, P. ‘’Nonuniform spatial patterns of respiratory activity within biofilms during disinfection’’ Appl.Environ.Microbiol., 61 (1995) 22522256.

Jetten, M.S.; Strous, M.; van de Pas-Schoonen, K.T.; Schalk, J.; van Dongen, U.G.; et al. ‘’The anaerobic oxidation of ammonium’’ FEMS Microbiol. Rev, 22 (1998) 421-437.

Jonfelt, C.:’’An evaluation of an MBBR anammox model - sensitivity analysis and calibration’’, MSc Thesis, Uppsala Univ., Faculty of Science and Technology, Uppsala, Sweden, (2016).

Josef Trela ‘’Mainstream wastewater treatment in integrated fixed film activated sludge (IFAS) reactor by partial nitritation/anammox process’’, Bioresource Technology, 198 (2015) 478-487.

Kaldate, A.; Vlaeminck, S.E.; Gonzalez-Ospina, A.; Dyson, J.; Verstraete, W.; Graveleau, L.; ‘’Fast Start-Up of a Deammonification SBR Treating Sludge Digestate’’, WEFTEC, Orlando, FL, USA, October 10-14 (2009).

Kampschreur, M. J.; Poldermans, R.; Kleerebezem,R.; van der Star, W. R. L.; Haarhuis, R.; Abma, W. R.; Jetten, M. S. M.; van Loosdrecht, M. C. M.; ‘’Emission of nitrous oxide and nitric oxide from a full-scale single-stage nitritation-anammox reactor’’ Water Science and technology 60 (12) (2009) 3211-3217.

Kartal, B.; Loosdrecht, M.; Kuenen, J.G.; ‘’Sewage Treatment with Anammox’’, Science 328(5979) (2010) 702-703.

Kartal, B.; Vossenberg, K.J.; Woebken, D.; Maalcke, W.J.; Wessels, H.J. C. T.; Dutilh, B.D.; Janssen-Megens, E.M.; Roeselers, G.; Yan, J.; Speth, D.; Gloerich, J.; Geerts, W.; Biezen, E.; Pluk, W.; Francoijs, K.J.; Russ, L.; Lam, P.; Malfatti, S.; Tringe, S.G.; Haaijer, S.C.M.;

Camp, H.J.M.; Stunnenberg, H.G.; Amann, R.; Kuypers, M.M.M.; Jetten, M.S.M,; '' The metagenome of the marine anammox bacterium 'Candidatus Klaus, S.; Baumler, R.; Rutherford, B.; Thesing, G.; Zhao, H.; Bott, C.; ''Startup of a Partial Nitritation-Anammox MBBR and the Implementation of pH-Based Aeration Control'', Water Environment Research, 6 (2007) 500-508.

Kuenen, J. Gijs. "Anammox bacteria: from discovery to application" Nature reviews/ microbiology, 6 (2008)

Lackner, S.; Gilbert, E.; Vlaeminck, S.; Joss, A.; Horn, H.; van Loosdrecht, M. ''FullScale Partial Nitritation/Anammox Experiences, An Application Survey'' Water Research, 55 (2014) 292–303.

Laureni, M.; Weissbrodt, D.G.; Szivák, I.; Robin, O.; Nielsen, J.L.; Morgenroth, E.; Joss, A.; '' Activity and growth of anammox biomass on aerobically pre-treated municipal wastewater'', Water Research (2015) 325-36.

Magrí C.A.; López, H.; Campos, E.; Balaguer, M.; Colprim, J.; Flotats, X.; ''A model for the simulation of the Sharon process: pH as a key factor'', Environmental Technology, 28 (2007) 255-265.

Metcalf & Eddy (2014) Wastewater Engineering: Treatment and Resource Recovery. 5th Edition, McGraw-Hill, New York

Mulder, A.; Graaf, A.A.; Robertson, L.A.; Kuenen, J.G.; ''Anaerobic ammonium oxidation discovered in a denitrifying fluidized bed reactor'', FEMS Microbial Ecol., 16 (1995) 177–184.

Nikolaeva, Yu. A.; Kozlova, M. N.; Kevbrinaa, M. V.; Agareva, A. M.; Kallistova , A.Yu.; N. V. Pimenov .; ''Modeling of Anammox Process with the BioWin Software Suite'' Applied Biochemistry and Microbiology, 53 (2017) 78–84.

Ødegaard, H.; ‘’ Innovations in Wastewater Treatment: The Moving Bed Biofilm Process’’, Water Sci. Technol., 53 (2006) 17–33.

Ødegaard, H.; ‘’A road-map for energy-neutral wastewater treatment plants of the future based on compact technologies (including MBBR)’’, Frontiers of Environmental Science & Engineering, 10 (2016) 1007.

Petersen, B.; Gernaey, K.; Henze, M.; Vanrolleghem, P.A.; ‘’Evaluation of an ASM1 model calibration procedure on a municipal-industrial wastewater treatment plant’’, J. Hydroinfor, 4 (2002) 15-38.

Phumza Vuyokazi Tikilili.; ‘’Performance And modelling of nan-granular Anammox culture for wastewater treatment’’ PhD Thesis, University of Pretoria, Faculty of Engineering, The Built Environment and Information Technology, Department of Chemical Engineering, Pretoria, South Africa (2017).

Revilla, M.; Viguri, J.; Galán B.; ‘’Simulation and Optimization of Biofilm Activated Sludge Process for the Biological Treatment of Effluents from Cellulose and Viscose Industry’’, Computer Aided Chemical Engineering, 33 (2014) 1117-1122.

Rittmann, B.E.; Boltz, J.P.; Brockmann, D.; Daigger, G.T.; Morgenroth, E; Sørensen, K.H,; Takács, I.; van Loosdrecht, M.;Vanrolleghem, P.A. “A framework for good biofilm reactor modeling practice (GBRMP)” Water Science & Technology (2018)

Rothstein E.; Medina D.; ‘’Shortcut Nitrogen Removal-Nitrite Shunt and Deammonification’’, WEF, Alexandria, USA, (2015) 34-35.

Scalindua profunda’ illustrates the versatility of this globally important nitrogen cycle bacterium ‘’, Environmental Microbiology (2013) 1275-1289.

Sedlak, R.I.; ‘’ Phosphorus and Nitrogen Removal From Municipal Wastewater’’, Lewis

Publishers, USA (1991).

Stein, L.Y.; Koltz, M.G.; ‘’The Nitrogen Cycle’’, Current Biology, 26 (2016) 83-101.

Strous, M.; Heijnen, J.; Kuenen, J. G.; Jetten, M.S.M.; ‘’The sequencing batch reactor as a powerful tool for the study of slowly growing anaerobic ammonium-oxidizing microorganisms’’, Appl. Microbiol. Biotechnol., 50 (1998) 589–596.

Strous, M.; Jetten, M.S.M.; Katinka T. van de Pas-Schoonen.; Jos Schalk Udo.;van Dongen, G.J.M.; Astrid A. van de Graaf .; Logemann, S.; Muyzer, G.; Mark C.M. van Loosdrecht.; Kuenen, J.; ‘’The anaerobic oxidation of ammonium’’, Microbiology Reviews, 22 (1998) 421-437.

Suarez, C.; Persson, F.; Hermansson, M.; ‘’Predation of nitritation–anammox biofilms used for nitrogen removal from wastewater’’, FEMS Microbiology Ecology, 91 (2015) 124.

Szatkowska, A.B.; Paulsrud, B.; ‘’The anammox process for nitrogen removal from wastewater – achievements and future challenges’’ Aquateam COWI (2014) 186-194.

Tchobanoglous G.; Burton F.L.; Stensel H.D.; ‘’Metcalf & Eddy - Wastewater Engineering, Treatment and Reuse’’ McGraw Hill Education, New York, USA (2003).

Third, K.A.; Paxman, J.; Schmid, M.; Strous, M.; Jetten, M.S.M.; ‘’Enrichment of Anammox from activated sludge and its application in the CANON process ‘’, Microbial Ecol., 49 (2005) 236-244.

Trojanowicz, K.; Plaza, E.; Trela, J.; ‘’Model extension, calibration and validation of partial nitritation–anammox process in moving bed biofilm reactor (MBBR) for reject and mainstream wastewater’’, Environmental Technology, 9 (2017) 1-22.

Wett, B.; Omari, A.; Podmirseg, S. M.; Han, M.; Akintayo, O.; Gómez Brandón, M.; Murthy, S.; Bott, C.; Hell, M.; Takács, I.; Nyhuis, G.; O'Shaughnessy, M.; ‘’Going for mainstream

deammonification from bench to full scale for maximized resource efficiency.'' Water Sci Technol (2013) 68 (2): 283–289.

Wett, B.; Murthy, S.; Takács, I.; Hell, M.; Bowden, G.; Deur, A.; O'Shaughnessy, M.; ''Key Parameters for Control of DEMON Deammonification Process'', Water Practice, 5 (2007) 1-11.

Winkler, S.; Rieger, L.; Gillot, S.; Langergraber, G.; Ohtsuki, T.; Shaw, A.; Takacs, I.; ''Guidelines for Using Activated Sludge Models'', IWA Publishing, London, UK (2013).

Xiao, Y.; Xiao, Q.; Xiang, S.; ''Modeling of Simultaneous Partial Nitrification, Anammox and Denitrification Process In a Single Reactor'', Environmental & Analytical Toxicology, 4 (2014) 204.

Yao, Z., Lu, P., Zhang, D., Wan, X., Li, Y. and Peng, S., "Stoichiometry and kinetics of the anaerobic ammonium oxidation (anammox) with trace hydrazine addition" Bioresource Technology, (2015) 198, 70-76.

Zhu, S. and Chen, S. ''Impacts of Reynolds number on nitrification biofilm kinetics'', Aquacultural Engineering, 24 (3) (2001), 213-229.

Zekker, I.; Rikmann, E.; Tenno, T.; Lemmiksoo, V.; Menert, A.; Loorits, L.; Vabama, P.; Tomingas, P.; Tenno, T.; ''Anammox enrichment from reject water on blank biofilm carriers and carriers containing nitrifying biomass: operation of two moving bed biofilm reactors (MBBR)'', Biodegradation, 23 (2011) 547–560

CIRRICULUM VITAE

Name: Neslican Uzkurt Kaljunen

Place of Birth: Adana, Turkey

Date of Birth: January 16, 1992

Address: Environmental Engineering Department, Faculty of Engineering, Marmara University, Istanbul, Turkey

Tel: +90 542 764 7971

E-mail: neslicanuzkurt@gmail.com

Qualifications:

2010 – 2014 Environmental Engineering, Faculty of Engineering, Istanbul University, Istanbul, Turkey (BSc)

January 2014 – June 2014 Environmental Engineering, Faculty of Engineering, Jan Evangelista Purkyně University in Ústí nad Labem, Usti Nad Labem/Czech Republic (B.Sc-Exchange Programme)

2015 – present Environmental Engineering, Institute of Graduate Studies in Pure and Applied Sciences, Marmara University, Istanbul, Turkey (MSc)

Working Experiences:

2015 – 2019 Process Engineer, Va Tech Wabag GmbH, Istanbul, Turkey

Presentations in International Conferences:

1. Uzkurt Kaljunen, N., Alpaslan Kocamemi, B. Sensitivity analysis of MBBR deammonification system with model developed in BioWin software. IV. Eurasian Conference on Civil and Environmental Engineering, June 17-18, 2019, Istanbul, Turkey (Oral Presentation)
2. Uzkurt Kaljunen, N., Alpaslan Kocamemi, B. Process Performance Optimization for Mainstream MBBR Partial Nitritation-Anammox systems: The Use of Model Predictive DO Control. YWP Conference on Water for All- Water for Nature, Reliable Water Supply, Wastewater Treatment and Reuse, September 1-5, 2019, Prague, Czechia (Oral Presentation)

Annex 1- Table 1. Kinetic, stoichiometric and general bioflm parameters used for Set-up 1 and Set-up 2 in BioWin® 6.0.

	KINETIC PARAMETERS	Default
RUN	**General Parameters**	
1	Hydrolysis rate [1/d]	2,1
2	Hydrolysis half sat. [-]	0,06
3	Anoxic hydrolysis factor [-]	0,28
4	Anaerobic hydrolysis factor (AS) [-]	0,04
5	Anaerobic hydrolysis factor (AD) [-]	0,5
6	Adsorption rate of colloids [L/(mgCOD d)]	0,15
7	Ammonification rate [L/(mgCOD d)]	0,08
8	Assimilative nitrate/nitrite reduction rate [1/d]	0,5
9	Endogenous products decay rate [1/d]	0
	AOB	
10	Max. spec. growth rate [1/d]	0,9
11	Substrate (NH4) half sat. [mgN/L]	0,7
12	Byproduct NH4 logistic slope [-]	50
13	Byproduct NH4 inflection point [mgN/L]	1,4
14	AOB denite DO half sat. [mg/L]	0,1
15	AOB denite HNO2 half sat. [mgN/L]	5E-06
16	Aerobic decay rate [1/d]	0,17
17	Anoxic/anaerobic decay rate [1/d]	0,08
18	KiHNO2 [mmol/L]	0,005
	NOB	
19	Max. spec. growth rate [1/d]	0,7
20	Substrate (NO2) half sat. [mgN/L]	0,1
21	Aerobic decay rate [1/d]	0,17
22	Anoxic/anaerobic decay rate [1/d]	0,08
23	KiNH3 [mmol/L]	0,075

Annex 1- Table 1 - continue

	AAO	
24	Max. spec. growth rate [1/d]	0,2
25	Substrate (NH4) half sat. [mgN/L]	2
26	Substrate (NO2) half sat. [mgN/L]	1
27	Aerobic decay rate [1/d]	0,019
28	Anoxic/anaerobic decay rate [1/d]	9,50E-03
29	Ki Nitrite [mgN/L]	1000
30	Nitrite sensitivity constant [L / (d mgN)]	0,016
	OHO	
31	Max. spec. growth rate [1/d]	3,2
32	Substrate half sat. [mgCOD/L]	5
33	Anoxic growth factor [-]	0,5
34	Denite N2 producers (NO3 or NO2) [-]	0,5
35	Aerobic decay rate [1/d]	0,62
36	Anoxic decay rate [1/d]	0,233
37	Anaerobic decay rate [1/d]	0,131
38	Fermentation rate [1/d]	1,6
39	Fermentation half sat. [mgCOD/L]	5
40	Fermentation growth factor (AS) [-]	0,25
41	Free nitrous acid inhibition [mol/L]	1,00E-07
	METHYLOTOTROPS	
42	Max. spec. growth rate [1/d]	1,3
43	Methanol half sat. [mgCOD/L]	0,5
44	Denite N2 producers (NO3 or NO2) [-]	0,5
45	Aerobic decay rate [1/d]	0,04
46	Anoxic/anaerobic decay rate [1/d]	0,03
47	Free nitrous acid inhibition [mmol/L]	1,00E-07
	PAO	
48	Max. spec. growth rate [1/d]	0,95

Annex 1- Table 1 - continue

49	Max. spec. growth rate, P-limited [1/d]	0,42
50	Substrate half sat. [mgCOD(PHB)/mgCOD(Zbp)]	0,1
51	Substrate half sat., P-limited [mgCOD(PHB)/mgCOD(Zbp)]	0,05
52	Magnesium half sat. [mgMg/L]	0,1
53	Cation half sat. [mmol/L]	0,1
54	Calcium half sat. [mgCa/L]	0,1
55	Aerobic/anoxic decay rate [1/d]	0,01
56	Aerobic/anoxic maintenance rate [1/d]	0
57	Anaerobic decay rate [1/d]	0,04
58	Anaerobic maintenance rate [1/d]	0,01
59	Sequestration rate [1/d]	4,5
60	Anoxic growth factor [-]	0,33
	PROPIONIC ACETOGENIC	
61	Max. spec. growth rate [1/d]	0,25
62	Substrate half sat. [mgCOD/L]	10
63	Acetate inhibition [mgCOD/L]	10000
64	Anaerobic decay rate [1/d]	0,05
65	Aerobic/anoxic decay rate [1/d]	0,52
	METHANOGENIC	
66	Acetoclastic max. spec. growth rate [1/d]	0,3
67	H2-utilizing max. spec. growth rate [1/d]	1,4
68	Acetoclastic substrate half sat. [mgCOD/L]	100
69	Acetoclastic methanol half sat. [mgCOD/L]	0,5
70	H2-utilizing CO2 half sat. [mmol/L]	0,1
71	H2-utilizing substrate half sat. [mgCOD/L]	1
72	H2-utilizing methanol half sat. [mgCOD/L]	0,5
73	Acetoclastic propionic inhibition [mgCOD/L]	10000
74	Acetoclastic anaerobic decay rate [1/d]	0,13
75	Acetoclastic aerobic/anoxic decay rate [1/d]	0,6

Annex 1- Table 1 - continue

76	H2-utilizing anaerobic decay rate [1/d]	0,13
77	H2-utilizing aerobic/anoxic decay rate [1/d]	2,8
	SULFUR REDUCING	
78	Propionic max. spec. growth rate [1/d]	0,583
79	Propionic acid half sat. [mgCOD/L]	295
80	Hydrogen sulfide inhibition coefficient [mgS/L]	185
81	Sulfate (SO4=) half sat. [mgS/L]	2,47
82	Decay rate [1/d]	0,0185
83	Acetotrophic max. spec. growth rate [1/d]	0,612
84	Acetic acid half sat. [mgCOD/L]	24
85	Hydrogen sulfide inhibition coefficient [mgS/L]	164
86	Sulfate (SO4=) half sat. [mgS/L]	6,41
87	Decay rate [1/d]	0,0275
88	Hydrogenotrophic max. spec. growth rate with SO4= [1/d]	2,8
89	Hydrogenotrophic max. spec. growth rate with S [1/d]	0,1
90	Hydrogen half sat. [mgCOD/L]	0,07
91	Hydrogen sulfide inhibition coefficient [mgS/L]	550
92	Sulfate (SO4=) half sat. [mgS/L]	6,41
93	Sulfur (S) half sat. [mgS/L]	50
94	Decay rate [1/d]	0,06
	SULFUR OXIDIZING	
95	Maximum specific growth rate (sulfide) [1/d]	0,75
96	Maximum specific growth rate (sulfur) [1/d]	0,1
97	Substrate (H2S) half sat. [mgS/L]	1
98	Substrate (sulfur) half sat. [mgS/L]	1
99	Anoxic growth factor [-]	0,5
100	Decay rate [1/d]	0,04
	SWITCHES	
101	Ordinary heterotrophic DO half sat. [mgO2/L]	0,15

Annex 1- Table 1 - continue

102	Phosphorus accumulating DO half sat. [mgO2/L]	0,05
103	Anoxic/anaerobic NOx half sat. [mgN/L]	0,15
104	Ammonia oxidizing DO half sat. [mgO2/L]	0,25
105	Nitrite oxidizing DO half sat. [mgO2/L]	0,5
106	Anaerobic ammonia oxidizing DO half sat. [mgO2/L]	0,01
107	Sulfur oxidizing sulfate pathway DO half sat. [mgO2/L]	0,25
108	Sulfur oxidizing sulfur pathway DO half sat. [mgO2/L]	0,05
109	Anoxic NO3(->NO2) half sat. [mgN/L]	0,1
110	Anoxic NO3(->N2) half sat. [mgN/L]	0,05
111	Anoxic NO2(->N2) half sat. (mgN/L)	0,01
112	NH3 nutrient half sat. [mgN/L]	5,00E-03
113	PolyP half sat. [mgP/mgCOD]	0,01
114	VFA sequestration half sat. [mgCOD/L]	5
115	P uptake half sat. [mgP/L]	0,15
116	P nutrient half sat. [mgP/L]	1,00E-03
117	Autotrophic CO2 half sat. [mmol/L]	0,1
118	H2 low/high half sat. [mgCOD/L]	1
119	Propionic acetogenic H2 inhibition [mgCOD/L]	5
120	Synthesis anion/cation half sat. [meq/L]	0,01
	BIOFILM GENERAL PARAMETERS	
121	Attachment rate [g / (m2 d)]	8
122	Attachment TSS half sat. [mg/L]	100
123	Detachment rate [g/(m3 d)]	8000
124	Solids movement factor []	10
125	Diffusion neta []	0,8
126	Thin film limit [mm]	0,5
127	Thick film limit [mm]	3
128	Assumed Film thickness for tank volume correction (temp independent) [mm]	1,25

Annex 1- Table 1 - continue

129	Film surface area to media area ratio - Max.[ ]	1
130	Minimum biofilm conc. for streamer formation [gTSS/m2]	4
	STOICHIOMETRIC PARAMETERS	
	Common	
131	Biomass/Endog Ca content (gCa/gCOD)	3,91E-03
132	Biomass/Endog Mg content (gMg/gCOD)	3,91E-03
133	Biomass/Endog other cations content (mol/gCOD)	5,12E-04
134	Biomass/Endog other Anions content (mol/gCOD)	1,41E-04
135	N in endogenous residue [mgN/mgCOD]	0,07
136	P in endogenous residue [mgP/mgCOD]	0,022
137	Ca content of slowly biodegradabe (gCa/gCOD)	3,91E-03
138	Mg content of slowly biodegradabe (gMg/gCOD)	3,70E-04
139	Endogenous residue COD:VSS ratio [mgCOD/mgVSS]	1,42
140	Particulate substrate COD:VSS ratio [mgCOD/mgVSS]	1,6327
141	Particulate inert COD:VSS ratio [mgCOD/mgVSS]	1,6
142	Cellulose COD:VSS ratio [mgCOD/mgVSS]	1,4
143	External organic COD:VSS ratio [mgCOD/mgVSS]	1,6
144	Molecular weight of other anions [mg/mmol]	35,5
145	Molecular weight of other cations [mg/mmol]	39,0983
	AOB	
146	Yield [mgCOD/mgN]	0,15
147	Denite NO2 fraction as TEA [-]	0,5
148	Byproduct NH4 fraction to N2O [-]	2,50E-03
149	N in biomass [mgN/mgCOD]	0,07
150	P in biomass [mgP/mgCOD]	0,022
151	Fraction to endogenous residue [-]	0,08
152	COD:VSS ratio [mgCOD/mgVSS]	1,42
	NOB	
153	Yield [mgCOD/mgN]	0,09

Annex 1- Table 1 - continue

154	N in biomass [mgN/mgCOD]	0,07
155	P in biomass [mgP/mgCOD]	0,022
156	Fraction to endogenous residue [-]	0,08
157	COD:VSS ratio [mgCOD/mgVSS]	1,42
	AAO	
158	Yield [mgCOD/mgN]	0,114
159	Nitrate production [mgN/mgBiomassCOD]	2,28
160	N in biomass [mgN/mgCOD]	0,07
161	P in biomass [mgP/mgCOD]	0,022
162	Fraction to endogenous residue [-]	0,08
163	COD:VSS ratio [mgCOD/mgVSS]	1,42
	OHO	
164	Yield (aerobic) [-]	0,666
165	Yield (fermentation, low H2) [-]	0,1
166	Yield (fermentation, high H2) [-]	0,1
167	H2 yield (fermentation low H2) [-]	0,35
168	H2 yield (fermentation high H2) [-]	0,0001
169	Propionate yield (fermentation, low H2) [-]	0,0001
170	Propionate yield (fermentation, high H2) [-]	0,7
171	CO2 yield (fermentation, low H2) [-]	0,7
172	CO2 yield (fermentation, high H2) [-]	0
173	N in biomass [mgN/mgCOD]	0,07
174	P in biomass [mgP/mgCOD]	0,022
175	Endogenous fraction - aerobic [-]	0,08
176	Endogenous fraction - anoxic [-]	0,103
177	Endogenous fraction - anaerobic [-]	0,184
178	COD:VSS ratio [mgCOD/mgVSS]	1,42
179	Yield (anoxic) [-]	0,54
180	Yield propionic (aerobic) [-]	0,64

Annex 1- Table 1 - continue

181	Yield propionic (anoxic) [-]	0,46
182	Yield acetic (aerobic) [-]	0,6
183	Yield acetic (anoxic) [-]	0,43
184	Yield methanol (aerobic) [-]	0,5
185	Adsorp. max. [-]	1
186	Max fraction to N2O at high FNA over nitrate [-]	0,05
187	Max fraction to N2O at high FNA over nitrite [-]	0,1
	PAO	
188	Yield (aerobic) [-]	0,639
189	Yield (anoxic) [-]	0,52
190	Aerobic P/PHA uptake [mgP/mgCOD]	0,93
191	Anoxic P/PHA uptake [mgP/mgCOD]	0,35
192	Yield of PHA on sequestration [-]	0,889
193	N in biomass [mgN/mgCOD]	0,07
194	N in sol. inert [mgN/mgCOD]	0,07
195	P in biomass [mgP/mgCOD]	0,022
196	Fraction to endogenous part. [-]	0,25
197	Inert fraction of endogenous sol. [-]	0,2
198	P/Ac release ratio [mgP/mgCOD]	0,51
199	COD:VSS ratio [mgCOD/mgVSS]	1,42
200	Yield of low PP [-]	0,94
201	Mg to P mole ratio in polyphosphate [mmolMg/mmolP]	0,3
202	Cation to P mole ratio in polyphosphate [meq/mmolP]	0,15
203	Ca to P mole ratio in polyphosphate [mmolCa/mmolP]	0,05
	PROPIONIC ACETOGENIC	
204	Yield [-]	0,1
205	H2 yield [-]	0,4
206	CO2 yield [-]	1
207	N in biomass [mgN/mgCOD]	0,07

Annex 1- Table 1 - continue

208	P in biomass [mgP/mgCOD]	0,022
209	Fraction to endogenous residue [-]	0,08
210	COD:VSS ratio [mgCOD/mgVSS]	1,42
	METHANOGENIC	
211	Acetoclastic yield [-]	0,1
212	Acetoclastic yield on methanol[-]	0,1
213	H2-utilizing yield [-]	0,1
214	H2-utilizing yield on methanol [-]	0,1
215	N in acetoclastic biomass [mgN/mgCOD]	0,07
216	N in H2-utilizing biomass [mgN/mgCOD]	0,07
217	P in acetoclastic biomass [mgP/mgCOD]	0,022
218	P in H2-utilizing biomass [mgP/mgCOD]	0,022
219	Acetoclastic fraction to endog. residue [-]	0,08
220	H2-utilizing fraction to endog. residue [-]	0,08
221	Acetoclastic COD:VSS ratio [mgCOD/mgVSS]	1,42
222	H2-utilizing COD:VSS ratio [mgCOD/mgVSS]	1,42
	METHYLOTOTROPIC	
223	Yield (anoxic) [-]	0,4
224	N in biomass [mgN/mgCOD]	0,07
225	P in biomass [mgP/mgCOD]	0,022
226	Fraction to endogenous residue [-]	0,08
227	COD:VSS ratio [mgCOD/mgVSS]	1,42
228	Max fraction to N2O at high FNA over nitrate [-]	0,1
229	Max fraction to N2O at high FNA over nitrite [-]	0,15
	SULFUR OXIDIZING	
230	Yield (aerobic) [mgCOD/mgS]	0,5
231	Yield (Anoxic) [mgCOD/mgS]	0,35
232	N in biomass [mgN/mgCOD]	0,07
233	P in biomass [mgP/mgCOD]	0,022

Annex 1- Table 1 - continue

234	Fraction to endogenous residue [-]	0,08
235	COD:VSS ratio [mgCOD/mgVSS]	1,42
	SULFUR REDUCING	
236	Yield [mgCOD/mg H2 COD]	0,0712
237	Yield [mgCOD/mg Ac COD]	0,047
238	Yield [mgCOD/mg Pr COD]	0,0384
239	N in biomass [mgN/mgCOD]	0,07
240	P in biomass [mgP/mgCOD]	0,022
241	Fraction to endogenous residue [-]	0,08
242	COD:VSS ratio [mgCOD/mgVSS]	1,42

Annex 2 - Table 1. Sensitivity Analysis results for kinetic, stoichiometric and general bioflm parameters used in BioWin® 6.0.

RUN NO	R-S1T1-SS-20-DO2-5 $S_{i,j} = \| \Delta Y / Y_i \| / \| \Delta X / X_i \|$ PARAMETERS	X_i	ΔX	New	S_{ij} Values for Effluent Parameters TN				NH_4^+-N				NO_3^--N				NO_2^--N			
					Y_i	Y_e	ΔY	S_{ij}	Y_i	Y_e	ΔY	S_{ij}	Y_i	Y_e	ΔY	Sij	Y_i	Y_e	ΔY	S_{ij}
	KINETIC PARAMETERS																			
	General Parameters																			
1	Hydrolysis rate [1/d]	2.1	1.1	2.3	8.7	9.8	1.1	1.3	5.5	6.6	1.2	2.2	0.0	0.0	0.0	-	0.8	0.7	0.1	1.0
2	Hydrolysis half sat. [-]	0.1	1.1	0.1	8.7	8.5	0.2	0.3	5.5	5.2	0.2	0.4	0.0	0.0	0.0	-	0.8	0.8	0.0	0.1
3	Anoxic hydrolysis factor [-]	0.3	1.1	0.3	8.7	8.9	0.2	0.2	5.5	5.7	0.2	0.4	0.0	0.0	0.0	-	0.8	0.8	0.0	0.2
4	Anaerobic hydrolysis factor (AS) [-]	0.0	1.1	0.0	8.7	8.7	0.0	0.0	5.5	5.5	0.0	0.0	0.0	0.0	0.0	-	0.8	0.8	0.0	0.1
5	Anaerobic hydrolysis factor (AD) [-]	0.5	1.1	0.6	8.7	8.7	0.0	0.0	5.5	5.5	0.0	0.0	0.0	0.0	0.0	-	0.8	0.8	0.0	0.0
6	Adsorption rate of colloids [L/(mgCOD d)]	0.2	1.1	0.2	8.7	8.7	0.0	0.0	5.5	5.4	0.0	0.1	0.0	0.0	0.0	-	0.8	0.8	0.0	0.0
7	Ammonification rate [L/(mgCOD d)]	0.1	1.1	0.1	8.7	15.4	6.7	7.6	5.5	7.2	1.7	3.2	0.0	0.0	0.0	-	0.8	5.8	5.0	61.7
8	Assimilative nitrate/nitrite reduction rate [1/d]	0.5	1.1	0.6	8.7	8.7	0.0	0.0	5.5	5.5	0.0	0.0	0.0	0.0	0.0	-	0.8	0.8	0.0	0.0
9	Endogenous products decay rate [1/d]	0.0	1.1	0.1	8.7	10.5	1.8	0.0	5.5	7.3	1.8	0.0	0.0	0.0	0.0	-	0.8	0.7	0.1	0.0
	AOB																			
10	Max. spec. growth rate [1/d]	0.9	1.1	1.0	8.7	6.8	1.9	2.2	5.5	3.4	2.1	3.8	0.0	0.0	0.0	-	0.8	1.0	0.2	2.1
11	Substrate (NH4) half sat. [mgN/L]	0.7	1.1	0.8	8.7	9.1	0.3	0.4	5.5	5.8	0.3	0.6	0.0	0.0	0.0	-	0.8	0.8	0.0	0.2
12	Byproduct NH4 logistic slope [-]	50.0	1.1	55.0	8.7	8.7	0.0	0.0	5.5	5.5	0.0	0.0	0.0	0.0	0.0	-	0.8	0.8	0.0	0.0
13	Byproduct NH4 inflection point [mgN/L]	1.4	1.1	1.5	8.7	8.7	0.0	0.0	5.5	5.5	0.0	0.0	0.0	0.0	0.0	-	0.8	0.8	0.0	0.0
14	AOB denite DO half sat. [mg/L]	0.1	1.1	0.1	8.7	8.7	0.0	0.0	5.5	5.5	0.0	0.0	0.0	0.0	0.0	-	0.8	0.8	0.0	0.0
15	AOB denite HNO2 half sat. [mgN/L]	0.0	1.1	0.0	8.7	8.7	0.0	0.0	5.5	5.5	0.0	0.0	0.0	0.0	0.0	-	0.8	0.8	0.0	0.0
16	Aerobic decay rate [1/d]	0.2	1.1	0.2	8.7	9.4	0.7	0.8	5.5	6.2	0.7	1.3	0.0	0.0	0.0	-	0.8	0.8	0.0	0.5
17	Anoxic/anaerobic decay rate [1/d]	0.1	1.1	0.1	8.7	9.3	0.5	0.6	5.5	6.0	0.6	1.1	0.0	0.0	0.0	-	0.8	0.8	0.0	0.4
18	KiHNO2 [mmol/L]	0.0	1.1	0.0	8.7	8.7	0.0	0.0	5.5	5.4	0.0	0.0	0.0	0.0	0.0	-	0.8	0.8	0.0	0.0
	NOB																			

Annex 2 - Table 1 - continue

19	Max. spec. growth rate [1/d]	0.7	1.1	0.8	8.7	8.8	0.0	0.0	5.5	5.5	0.0	0.1	0.0	0.0	0.0	-	0.8	0.8	0.0	0.1
20	Substrate (NO2) half sat. [mgN/L]	0.1	1.1	0.1	8.7	14.8	6.1	7.0	5.5	6.9	1.5	2.7	0.0	0.0	0.0	-	0.8	5.4	4.6	57.0
21	Aerobic decay rate [1/d]	0.2	1.1	0.2	8.7	8.7	0.0	0.0	5.5	5.4	0.0	0.0	0.0	0.0	0.0	-	0.8	0.8	0.0	0.0
22	Anoxic/anaerobic decay rate [1/d]	0.1	1.1	0.1	8.7	8.7	0.0	0.0	5.5	5.4	0.0	0.0	0.0	0.0	0.0	-	0.8	0.8	0.0	0.0
23	KiNH3 [mmol/L]	0.1	1.1	0.1	8.7	8.7	0.0	0.0	5.5	5.5	0.0	0.0	0.0	0.0	0.0	-	0.8	0.8	0.0	0.0
	AAO																			
24	Max. spec. growth rate [1/d]	0.2	1.1	0.2	8.7	8.7	0.0	0.0	5.5	5.5	0.0	0.0	0.0	0.0	0.0	-	0.8	0.8	0.1	0.7
25	Substrate (NH4) half sat. [mgN/L]	2.0	1.1	2.2	8.7	8.8	0.0	0.0	5.5	5.4	0.0	0.0	0.0	0.0	0.0	-	0.8	0.8	0.0	0.1
26	Substrate (NO2) half sat. [mgN/L]	1.0	1.1	1.1	8.7	8.8	0.0	0.0	5.5	5.4	0.0	0.0	0.0	0.0	0.0	-	0.8	0.9	0.0	0.6
27	Aerobic decay rate [1/d]	0.0	1.1	0.0	8.7	8.8	0.0	0.0	5.5	5.4	0.0	0.0	0.0	0.0	0.0	-	0.8	0.8	0.0	0.4
28	Anoxic/anaerobic decay rate [1/d]	0.0	1.1	0.0	8.7	8.7	0.0	0.0	5.5	5.5	0.0	0.0	0.0	0.0	0.0	-	0.8	0.8	0.0	0.0
29	Ki Nitrite [mgN/L]	1000.0	1.1	1100.0	8.7	8.7	0.0	0.0	5.5	5.5	0.0	0.0	0.0	0.0	0.0	-	0.8	0.8	0.0	0.0
30	Nitrite sensitivity constant [L / (d mgN)]	0.0	1.1	0.0	8.7	13.3	4.6	5.3	5.5	6.4	0.9	1.7	0.0	0.0	0.0	-	0.8	4.5	3.7	45.6
	OHO																			
31	Max. spec. growth rate [1/d]	3.2	1.1	3.5	8.7	8.3	0.4	0.5	5.5	5.0	0.5	0.8	0.0	0.0	0.0	-	0.8	0.8	0.0	0.1
32	Substrate half sat. [mgCOD/L]	5.0	1.1	5.5	8.7	8.9	0.2	0.2	5.5	5.6	0.2	0.3	0.0	0.0	0.0	-	0.8	0.8	0.0	0.1
33	Anoxic growth factor [-]	0.5	1.1	0.6	8.7	8.8	0.1	0.1	5.5	5.6	0.1	0.2	0.0	0.0	0.0	-	0.8	0.8	0.0	0.2
34	Denite N2 producers (NO3 or NO2) [-]	0.5	1.1	0.6	8.7	8.8	0.1	0.1	5.5	5.6	0.1	0.2	0.0	0.0	0.0	-	0.8	0.8	0.0	0.2
35	Aerobic decay rate [1/d]	0.6	1.1	0.7	8.7	8.8	0.1	0.1	5.5	5.5	0.0	0.1	0.0	0.0	0.0	-	0.8	0.8	0.0	0.1
36	Anoxic decay rate [1/d]	0.2	1.1	0.3	8.7	14.3	5.5	6.3	5.5	6.7	1.2	2.2	0.0	0.0	0.0	-	0.8	5.1	4.3	53.2
37	Anaerobic decay rate [1/d]	0.1	1.1	0.1	8.7	8.7	0.0	0.0	5.5	5.4	0.0	0.1	0.0	0.0	0.0	-	0.8	0.8	0.0	0.0
38	Fermentation rate [1/d]	1.6	1.1	1.8	8.7	8.8	0.1	0.1	5.5	5.5	0.1	0.1	0.0	0.0	0.0	-	0.8	0.8	0.0	0.0
39	Fermentation half sat. [mgCOD/L]	5.0	1.1	5.5	8.7	8.7	0.1	0.1	5.5	5.4	0.1	0.1	0.0	0.0	0.0	-	0.8	0.8	0.0	0.0
40	Fermentation growth factor (AS) [-]	0.3	1.1	0.3	8.7	8.8	0.1	0.1	5.5	5.5	0.1	0.1	0.0	0.0	0.0	-	0.8	0.8	0.0	0.1
41	Free nitrous acid inhibition [mol/L]	0.0	1.1	0.0	8.7	8.7	0.0	0.0	5.5	5.5	0.0	0.0	0.0	0.0	0.0	-	0.8	0.8	0.0	0.0
	METHYLOTOTROPS																			
42	Max. spec. growth rate [1/d]	1.3	1.1	1.4	8.7	8.7	0.0	0.0	5.5	5.5	0.0	0.0	0.0	0.0	0.0	-	0.8	0.8	0.0	0.0
43	Methanol half sat. [mgCOD/L]	0.5	1.1	0.6	8.7	8.7	0.0	0.0	5.5	5.4	0.0	0.0	0.0	0.0	0.0	-	0.8	0.8	0.0	0.0
44	Denite N2 producers (NO3 or NO2) [-]	0.5	1.1	0.6	8.7	8.7	0.0	0.0	5.5	5.4	0.0	0.0	0.0	0.0	0.0	-	0.8	0.8	0.0	0.0
45	Aerobic decay rate [1/d]	0.0	1.1	0.0	8.7	8.7	0.0	0.0	5.5	5.4	0.0	0.0	0.0	0.0	0.0	-	0.8	0.8	0.0	0.0
46	Anoxic/anaerobic decay rate [1/d]	0.0	1.1	0.0	8.7	8.7	0.0	0.0	5.5	5.4	0.0	0.0	0.0	0.0	0.0	-	0.8	0.8	0.0	0.0

Annex 2 - Table 1 - continue

47	Free nitrous acid inhibition [mmol/L]	0.0	1.1	0.0	8.7	8.7	0.0	0.0	5.5	5.4	0.0	0.0	0.0	0.0	0.0	-	0.8	0.8	0.0	0.0
	PAO																			
48	Max. spec. growth rate [1/d]	1.0	1.1	1.0	8.7	7.6	1.2	1.3	5.5	4.1	1.4	2.6	0.0	0.0	0.0	-	0.8	1.0	0.2	2.8
49	Max. spec. growth rate, P-limited [1/d]	0.4	1.1	0.5	8.7	8.7	0.0	0.0	5.5	5.5	0.0	0.0	0.0	0.0	0.0	-	0.8	0.8	0.0	0.0
50	Substrate half sat. [mgCOD(PHB)/mgCOD(Zbp)]	0.1	1.1	0.1	8.7	8.7	0.0	0.0	5.5	5.5	0.0	0.0	0.0	0.0	0.0	-	0.8	0.8	0.0	0.0
51	Substrate half sat., P-limited [mgCOD(PHB)/mgCOD(Zbp)]	0.1	1.1	0.1	8.7	8.7	0.0	0.0	5.5	5.5	0.0	0.0	0.0	0.0	0.0	-	0.8	0.8	0.0	0.0
52	Magnesium half sat. [mgMg/L]	0.1	1.1	0.1	8.7	8.7	0.0	0.0	5.5	5.5	0.0	0.0	0.0	0.0	0.0	-	0.8	0.8	0.0	0.0
53	Cation half sat. [mmol/L]	0.1	1.1	0.1	8.7	8.7	0.0	0.0	5.5	5.5	0.0	0.0	0.0	0.0	0.0	-	0.8	0.8	0.0	0.0
54	Calcium half sat. [mgCa/L]	0.1	1.1	0.1	8.7	8.7	0.0	0.0	5.5	5.5	0.0	0.0	0.0	0.0	0.0	-	0.8	0.8	0.0	0.0
55	Aerobic/anoxic decay rate [1/d]	0.0	1.1	0.0	8.7	8.7	0.0	0.0	5.5	5.5	0.0	0.0	0.0	0.0	0.0	-	0.8	0.8	0.0	0.0
56	Aerobic/anoxic maintenance rate [1/d]	0.0	1.1	0.1	8.7	8.7	0.0	0.0	5.5	5.5	0.0	0.0	0.0	0.0	0.0	-	0.8	0.8	0.0	0.0
57	Anaerobic decay rate [1/d]	0.0	1.1	0.0	8.7	8.7	0.0	0.0	5.5	5.5	0.0	0.0	0.0	0.0	0.0	-	0.8	0.8	0.0	0.0
58	Anaerobic maintenance rate [1/d]	0.0	1.1	0.1	8.7	8.7	0.0	0.0	5.5	5.5	0.0	0.0	0.0	0.0	0.0	-	0.8	0.8	0.0	0.0
59	Sequestration rate [1/d]	4.5	1.1	5.0	8.7	8.7	0.0	0.0	5.5	5.5	0.0	0.0	0.0	0.0	0.0	-	0.8	0.8	0.0	0.0
60	Anoxic growth factor [-]	0.3	1.1	0.4	8.7	8.7	0.0	0.0	5.5	5.5	0.0	0.0	0.0	0.0	0.0	-	0.8	0.8	0.0	0.0
	PROPIONIC ACETOGENIC																			
61	Max. spec. growth rate [1/d]	0.3	1.1	0.3	8.7	8.7	0.0	0.0	5.5	5.5	0.0	0.0	0.0	0.0	0.0	-	0.8	0.8	0.0	0.0
62	Substrate half sat. [mgCOD/L]	10.0	1.1	11.0	8.7	8.7	0.0	0.0	5.5	5.5	0.0	0.0	0.0	0.0	0.0	-	0.8	0.8	0.0	0.0
63	Acetate inhibition [mgCOD/L]	10000	1.1	11000.0	8.7	8.7	0.0	0.0	5.5	5.5	0.0	0.0	0.0	0.0	0.0	-	0.8	0.8	0.0	0.0
64	Anaerobic decay rate [1/d]	0.1	1.1	0.1	8.7	8.7	0.0	0.0	5.5	5.5	0.0	0.0	0.0	0.0	0.0	-	0.8	0.8	0.0	0.0
65	Aerobic/anoxic decay rate [1/d]	0.5	1.1	0.6	8.7	8.7	0.0	0.0	5.5	5.5	0.0	0.0	0.0	0.0	0.0	-	0.8	0.8	0.0	0.0
	METHANOGENIC																			
66	Acetoclastic max. spec. growth rate [1/d]	0.3	1.1	0.3	8.7	8.7	0.0	0.0	5.5	5.5	0.0	0.0	0.0	0.0	0.0	-	0.8	0.8	0.0	0.0
67	H2-utilizing max. spec. growth rate [1/d]	1.4	1.1	1.5	8.7	8.7	0.0	0.0	5.5	5.5	0.0	0.0	0.0	0.0	0.0	-	0.8	0.8	0.0	0.0
68	Acetoclastic substrate half sat. [mgCOD/L]	100.0	1.1	110.0	8.7	8.7	0.0	0.0	5.5	5.5	0.0	0.0	0.0	0.0	0.0	-	0.8	0.8	0.0	0.0
69	Acetoclastic methanol half sat. [mgCOD/L]	0.5	1.1	0.6	8.7	8.7	0.0	0.0	5.5	5.5	0.0	0.0	0.0	0.0	0.0	-	0.8	0.8	0.0	0.0

Annex 2 - Table 1 - continue

70	H2-utilizing CO2 half sat. [mmol/L]	0.1	1.1	0.1	8.7	8.7	0.0	0.0	5.5	5.5	0.0	0.0	0.0	0.0	0.0	-	0.8	0.8	0.0	0.0
71	H2-utilizing substrate half sat. [mgCOD/L]	1.0	1.1	1.1	8.7	8.7	0.0	0.0	5.5	5.5	0.0	0.0	0.0	0.0	0.0	-	0.8	0.8	0.0	0.0
72	H2-utilizing methanol half sat. [mgCOD/L]	0.5	1.1	0.6	8.7	8.7	0.0	0.0	5.5	5.5	0.0	0.0	0.0	0.0	0.0	-	0.8	0.8	0.0	0.0
73	Acetoclastic propionic inhibition [mgCOD/L]	10000	1.1	11000.0	8.7	8.7	0.0	0.0	5.5	5.5	0.0	0.0	0.0	0.0	0.0	-	0.8	0.8	0.0	0.0
74	Acetoclastic anaerobic decay rate [1/d]	0.1	1.1	0.1	8.7	8.7	0.0	0.0	5.5	5.5	0.0	0.0	0.0	0.0	0.0	-	0.8	0.8	0.0	0.0
75	Acetoclastic aerobic/anoxic decay rate [1/d]	0.6	1.1	0.7	8.7	8.7	0.0	0.0	5.5	5.5	0.0	0.0	0.0	0.0	0.0	-	0.8	0.8	0.0	0.0
76	H2-utilizing anaerobic decay rate [1/d]	0.1	1.1	0.1	8.7	8.7	0.0	0.0	5.5	5.5	0.0	0.0	0.0	0.0	0.0	-	0.8	0.8	0.0	0.0
77	H2-utilizing aerobic/anoxic decay rate [1/d]	2.8	1.1	3.1	8.7	8.7	0.0	0.0	5.5	5.5	0.0	0.0	0.0	0.0	0.0	-	0.8	0.8	0.0	0.0
	SULFUR REDUCING														0.0					
78	Propionic max. spec. growth rate [1/d]	0.6	1.1	0.6	8.7	8.7	0.0	0.0	5.5	5.5	0.0	0.0	0.0	0.0	0.0	-	0.8	0.8	0.0	0.0
79	Propionic acid half sat. [mgCOD/L]	295.0	1.1	324.5	8.7	8.7	0.0	0.0	5.5	5.5	0.0	0.0	0.0	0.0	0.0	-	0.8	0.8	0.0	0.0
80	Hydrogen sulfide inhibition coefficient [mgS/L]	185.0	1.1	203.5	8.7	8.7	0.0	0.0	5.5	5.5	0.0	0.0	0.0	0.0	0.0	-	0.8	0.8	0.0	0.0
81	Sulfate (SO4=) half sat. [mgS/L]	2.5	1.1	2.7	8.7	8.7	0.0	0.0	5.5	5.5	0.0	0.0	0.0	0.0	0.0	-	0.8	0.8	0.0	0.0
82	Decay rate [1/d]	0.0	1.1	0.0	8.7	8.7	0.0	0.0	5.5	5.5	0.0	0.0	0.0	0.0	0.0	-	0.8	0.8	0.0	0.0
83	Acetotrophic max. spec. growth rate [1/d]	0.6	1.1	0.7	8.7	8.7	0.0	0.0	5.5	5.5	0.0	0.0	0.0	0.0	0.0	-	0.8	0.8	0.0	0.0
84	Acetic acid half sat. [mgCOD/L]	24.0	1.1	26.4	8.7	8.7	0.0	0.0	5.5	5.5	0.0	0.0	0.0	0.0	0.0	-	0.8	0.8	0.0	0.0
85	Hydrogen sulfide inhibition coefficient [mgS/L]	164.0	1.1	180.4	8.7	8.7	0.0	0.0	5.5	5.5	0.0	0.0	0.0	0.0	0.0	-	0.8	0.8	0.0	0.0
86	Sulfate (SO4=) half sat. [mgS/L]	6.4	1.1	7.1	8.7	8.7	0.0	0.0	5.5	5.5	0.0	0.0	0.0	0.0	0.0	-	0.8	0.8	0.0	0.0
87	Decay rate [1/d]	0.0	1.1	0.0	8.7	8.7	0.0	0.0	5.5	5.5	0.0	0.0	0.0	0.0	0.0	-	0.8	0.8	0.0	0.0
88	Hydrogenotrophic max. spec. growth rate with SO4= [1/d]	2.8	1.1	3.1	8.7	8.7	0.0	0.0	5.5	5.5	0.0	0.0	0.0	0.0	0.0	-	0.8	0.8	0.0	0.0
89	Hydrogenotrophic max. spec. growth rate with S [1/d]	0.1	1.1	0.1	8.7	8.7	0.0	0.0	5.5	5.5	0.0	0.0	0.0	0.0	0.0	-	0.8	0.8	0.0	0.0

Annex 2 - Table 1 - continue

90	Hydrogen half sat. [mgCOD/L]	0.1	1.1	0.1	8.7	8.7	0.0	0.0	5.5	5.5	0.0	0.0	0.0	0.0	0.0	-	0.8	0.8	0.0	0.0
91	Hydrogen sulfide inhibition coefficient [mgS/L]	550.0	1.1	605.0	8.7	8.7	0.0	0.0	5.5	5.5	0.0	0.0	0.0	0.0	0.0	-	0.8	0.8	0.0	0.0
92	Sulfate (SO4=) half sat. [mgS/L]	6.4	1.1	7.1	8.7	8.7	0.0	0.0	5.5	5.5	0.0	0.0	0.0	0.0	0.0	-	0.8	0.8	0.0	0.0
93	Sulfur (S) half sat. [mgS/L]	50.0	1.1	55.0	8.7	8.7	0.0	0.0	5.5	5.5	0.0	0.0	0.0	0.0	0.0	-	0.8	0.8	0.0	0.0
94	Decay rate [1/d]	0.1	1.1	0.1	8.7	8.7	0.0	0.0	5.5	5.5	0.0	0.0	0.0	0.0	0.0	-	0.8	0.8	0.0	0.0
	SULFUR OXIDIZING																			
95	Maximum specific growth rate (sulfide) [1/d]	0.8	1.1	0.8	8.7	8.7	0.0	0.0	5.5	5.5	0.0	0.0	0.0	0.0	0.0	-	0.8	0.8	0.0	0.0
96	Maximum specific growth rate (sulfur) [1/d]	0.1	1.1	0.1	8.7	8.7	0.0	0.0	5.5	5.5	0.0	0.0	0.0	0.0	0.0	-	0.8	0.8	0.0	0.0
97	Substrate (H2S) half sat. [mgS/L]	1.0	1.1	1.1	8.7	8.7	0.0	0.0	5.5	5.5	0.0	0.0	0.0	0.0	0.0	-	0.8	0.8	0.0	0.0
98	Substrate (sulfur) half sat. [mgS/L]	1.0	1.1	1.1	8.7	8.7	0.0	0.0	5.5	5.5	0.0	0.0	0.0	0.0	0.0	-	0.8	0.8	0.0	0.0
99	Anoxic growth factor [-]	0.5	1.1	0.6	8.7	8.7	0.0	0.0	5.5	5.5	0.0	0.0	0.0	0.0	0.0	-	0.8	0.8	0.0	0.0
100	Decay rate [1/d]	0.0	1.1	0.0	8.7	8.7	0.0	0.0	5.5	5.5	0.0	0.0	0.0	0.0	0.0	-	0.8	0.8	0.0	0.0
	SWITCHES																			
101	Ordinary heterotrophic DO half sat. [mgO2/L]	0.2	1.1	0.2	8.7	8.5	0.2	0.2	5.5	5.2	0.2	0.4	0.0	0.0	0.0	-	0.8	0.8	0.0	0.0
102	Phosphorus accumulating DO half sat. [mgO2/L]	0.1	1.1	0.1	8.7	8.7	0.0	0.0	5.5	5.5	0.0	0.0	0.0	0.0	0.0	-	0.8	0.8	0.0	0.0
103	Anoxic/anaerobic NOx half sat. [mgN/L]	0.2	1.1	0.2	8.7	8.8	0.0	0.0	5.5	5.5	0.0	0.1	0.0	0.0	0.0	-	0.8	0.8	0.0	0.1
104	Ammonia oxidizing DO half sat. [mgO2/L]	0.3	1.1	0.3	8.7	10.4	1.7	1.9	5.5	7.2	1.7	3.2	0.0	0.0	0.0	-	0.8	0.7	0.1	0.9
105	Nitrite oxidizing DO half sat. [mgO2/L]	0.5	1.1	0.6	8.7	8.7	0.0	0.0	5.5	5.4	0.0	0.0	0.0	0.0	0.0	-	0.8	0.8	0.0	0.0
106	Anaerobic ammonia oxidizing DO half sat. [mgO2/L]	0.0	1.1	0.0	8.7	8.7	0.0	0.0	5.5	5.5	0.0	0.0	0.0	0.0	0.0	-	0.8	0.8	0.0	0.1
107	Sulfur oxidizing sulfate pathway DO half sat. [mgO2/L]	0.3	1.1	0.3	8.7	8.7	0.1	0.1	5.5	5.4	0.1	0.1	0.0	0.0	0.0	-	0.8	0.8	0.0	0.0
108	Sulfur oxidizing sulfur pathway DO half sat. [mgO2/L]	0.1	1.1	0.1	8.7	8.7	0.1	0.1	5.5	5.4	0.1	0.1	0.0	0.0	0.0	-	0.8	0.8	0.0	0.0
109	Anoxic NO3(->NO2) half sat. [mgN/L]	0.1	1.1	0.1	8.7	8.7	0.0	0.0	5.5	5.4	0.0	0.0	0.0	0.0	0.0	-	0.8	0.8	0.0	0.0
110	Anoxic NO3(->N2) half sat. [mgN/L]	0.1	1.1	0.1	8.7	15.4	6.7	7.6	5.5	7.2	1.7	3.1	0.0	0.0	0.0	-	0.8	5.8	5.0	61.5

Annex 2 - Table 1 - continue

111	Anoxic NO2(->N2) half sat. (mgN/L)	0.0	1.1	0.0	8.7	8.7	0.0	0.0	5.5	5.4	0.0	0.0	0.0	0.0	0.0	-	0.8	0.8	0.0	0.0
112	NH3 nutrient half sat. [mgN/L]	0.0	1.1	0.0	8.7	8.7	0.0	0.0	5.5	5.5	0.0	0.0	0.0	0.0	0.0	-	0.8	0.8	0.0	0.0
113	PolyP half sat. [mgP/mgCOD]	0.0	1.1	0.0	8.7	8.7	0.0	0.0	5.5	5.5	0.0	0.0	0.0	0.0	0.0	-	0.8	0.8	0.0	0.0
114	VFA sequestration half sat. [mgCOD/L]	5.0	1.1	5.5	8.7	8.7	0.0	0.0	5.5	5.5	0.0	0.0	0.0	0.0	0.0	-	0.8	0.8	0.0	0.0
115	P uptake half sat. [mgP/L]	0.2	1.1	0.2	8.7	8.7	0.0	0.0	5.5	5.5	0.0	0.0	0.0	0.0	0.0	-	0.8	0.8	0.0	0.0
116	P nutrient half sat. [mgP/L]	0.0	1.1	0.0	8.7	8.7	0.0	0.0	5.5	5.5	0.0	0.0	0.0	0.0	0.0	-	0.8	0.8	0.0	0.0
117	Autotrophic CO2 half sat. [mmol/L]	0.1	1.1	0.1	8.7	8.7	0.0	0.0	5.5	5.5	0.0	0.0	0.0	0.0	0.0	-	0.8	0.8	0.0	0.0
118	H2 low/high half sat. [mgCOD/L]	1.0	1.1	1.1	8.7	8.7	0.0	0.0	5.5	5.5	0.0	0.0	0.0	0.0	0.0	-	0.8	0.8	0.0	0.0
119	Propionic acetogenic H2 inhibition [mgCOD/L]	5.0	1.1	5.5	8.7	8.7	0.0	0.0	5.5	5.5	0.0	0.0	0.0	0.0	0.0	-	0.8	0.8	0.0	0.0
120	Synthesis anion/cation half sat. [meq/L]	0.0	1.1	0.0	8.7	8.8	0.0	0.0	5.5	5.5	0.0	0.0	0.0	0.0	0.0		0.8	0.8	0.0	0.0
	BIOFILM GENERAL PARAMETERS																			
121	Attachment rate [g / (m2 d)]	8.0	1.1	8.8	8.7	8.4	0.4	0.4	5.5	5.1	0.4	0.7	0.0	0.0	0.0	-	0.8	0.8	0.0	0.1
122	Attachment TSS half sat. [mg/L]	100.0	1.1	110.0	8.7	8.9	0.1	0.1	5.5	5.6	0.1	0.2	0.0	0.0	0.0	-	0.8	0.8	0.0	0.0
123	Detachment rate [g/(m3 d)]	8000.0	1.1	8800.0	8.7	9.1	0.4	0.4	5.5	5.8	0.4	0.7	0.0	0.0	0.0	-	0.8	0.8	0.0	0.1
124	Solids movement factor []	10.0	1.1	11.0	8.7	15.4	6.7	7.7	5.5	7.2	1.7	3.1	0.0	0.0	0.0	-	0.8	5.8	5.0	61.6
125	Diffusion neta []	0.8	1.1	0.9	8.7	6.9	1.9	2.2	5.5	3.4	2.1	3.9	0.0	0.0	0.0	-	0.8	1.0	0.2	2.7
126	Thin film limit [mm]	0.5	1.1	0.6	8.7	7.5	1.3	1.5	5.5	4.0	1.5	2.8	0.0	0.0	0.0	-	0.8	1.0	0.2	2.7
127	Thick film limit [mm]	3.0	1.1	3.3	8.7	8.7	0.0	0.0	5.5	5.5	0.0	0.0	0.0	0.0	0.0	-	0.8	0.8	0.0	0.0
128	Assumed Film thickness for tank volume correction (temp independent) [mm]	1.3	1.1	1.4	8.7	9.0	0.2	0.3	5.5	5.7	0.3	0.5	0.0	0.0	0.0	-	0.8	0.8	0.0	0.2
129	Film surface area to media area ratio - Max.[ ]	1.0	1.1	1.1	8.7	8.3	0.5	0.6	5.5	3.1	2.4	4.3	0.0	0.0	0.0	-	0.8	2.7	1.9	23.2
130	Minimum biofilm conc. for streamer formation [gTSS/m2]	4.0	1.1	4.4	8.7	8.7	0.0	0.0	5.5	5.5	0.0	0.0	0.0	0.0	0.0	-	0.8	0.8	0.0	0.0
	STOICHIOMETRIC PARAMETERS																			
	Common																			
131	Biomass/Endog Ca content (gCa/gCOD)	0.0	1.1	0.0	8.7	8.7	0.0	0.0	5.5	5.5	0.0	0.0	0.0	0.0	0.0	-	0.8	0.8	0.0	0.0

Annex 2 - Table 1 - continue

132	Biomass/Endog Mg content (gMg/gCOD)	0.0	1.1	0.0	8.7	8.7	0.0	0.0	5.5	5.5	0.0	0.0	0.0	0.0	0.0	-	0.8	0.8	0.0	0.0
133	Biomass/Endog other cations content (mol/gCOD)	0.0	1.1	0.0	8.7	8.7	0.0	0.0	5.5	5.5	0.0	0.0	0.0	0.0	0.0	-	0.8	0.8	0.0	0.0
134	Biomass/Endog other Anions content (mol/gCOD)	0.0	1.1	0.0	8.7	8.7	0.0	0.0	5.5	5.5	0.0	0.0	0.0	0.0	0.0	-	0.8	0.8	0.0	0.0
135	N in endogenous residue [mgN/mgCOD]	0.1	1.1	0.1	8.7	8.7	0.0	0.0	5.5	5.5	0.0	0.0	0.0	0.0	0.0	-	0.8	0.8	0.0	0.0
136	P in endogenous residue [mgP/mgCOD]	0.0	1.1	0.0	8.7	8.7	0.0	0.0	5.5	5.5	0.0	0.0	0.0	0.0	0.0	-	0.8	0.8	0.0	0.0
137	Ca content of slowly biodegradabe (gCa/gCOD)	0.0	1.1	0.0	8.7	8.7	0.0	0.0	5.5	5.5	0.0	0.0	0.0	0.0	0.0	-	0.8	0.8	0.0	0.0
138	Mg content of slowly biodegradabe (gMg/gCOD)	0.0	1.1	0.0	8.7	8.7	0.0	0.0	5.5	5.5	0.0	0.0	0.0	0.0	0.0	-	0.8	0.8	0.0	0.0
139	Endogenous residue COD:VSS ratio [mgCOD/mgVSS]	1.4	1.1	1.6	8.7	8.7	0.0	0.0	5.5	5.5	0.0	0.0	0.0	0.0	0.0	-	0.8	0.8	0.0	0.0
140	Particulate substrate COD:VSS ratio [mgCOD/mgVSS]	1.6	1.1	1.8	8.7	8.7	0.0	0.0	5.5	5.5	0.0	0.0	0.0	0.0	0.0	-	0.8	0.8	0.0	0.0
141	Particulate inert COD:VSS ratio [mgCOD/mgVSS]	1.6	1.1	1.8	8.7	8.7	0.0	0.0	5.5	5.5	0.0	0.0	0.0	0.0	0.0	-	0.8	0.8	0.0	0.0
142	Cellulose COD:VSS ratio [mgCOD/mgVSS]	1.4	1.1	1.5	8.7	8.7	0.0	0.0	5.5	5.5	0.0	0.0	0.0	0.0	0.0	-	0.8	0.8	0.0	0.0
143	External organic COD:VSS ratio [mgCOD/mgVSS]	1.6	1.1	1.8	8.7	8.7	0.0	0.0	5.5	5.5	0.0	0.0	0.0	0.0	0.0	-	0.8	0.8	0.0	0.0
144	Molecular weight of other anions [mg/mmol]	35.5	1.1	39.1	8.7	8.7	0.0	0.0	5.5	5.5	0.0	0.0	0.0	0.0	0.0	-	0.8	0.8	0.0	0.0
145	Molecular weight of other cations [mg/mmol]	39.1	1.1	43.0	8.7	8.7	0.0	0.0	5.5	5.5	0.0	0.0	0.0	0.0	0.0	-	0.8	0.8	0.0	0.0
	AOB																			
146	Yield [mgCOD/mgN]	0.2	1.1	0.2	8.7	8.7	0.1	0.1	5.5	5.4	0.1	0.1	0.0	0.0	0.0	-	0.8	0.8	0.0	0.0
147	Denite NO2 fraction as TEA [-]	0.5	1.1	0.6	8.7	8.7	0.0	0.0	5.5	5.5	0.0	0.0	0.0	0.0	0.0	-	0.8	0.8	0.0	0.0
148	Byproduct NH4 fraction to N2O [-]	0.0	1.1	0.0	8.7	8.7	0.0	0.0	5.5	5.5	0.0	0.0	0.0	0.0	0.0	-	0.8	0.8	0.0	0.0
149	N in biomass [mgN/mgCOD]	0.1	1.1	0.1	8.7	8.7	0.0	0.0	5.5	5.5	0.0	0.0	0.0	0.0	0.0	-	0.8	0.8	0.0	0.0
150	P in biomass [mgP/mgCOD]	0.0	1.1	0.0	8.7	8.7	0.0	0.0	5.5	5.5	0.0	0.0	0.0	0.0	0.0	-	0.8	0.8	0.0	0.0
151	Fraction to endogenous residue [-]	0.1	1.1	0.1	8.7	8.7	0.0	0.0	5.5	5.5	0.0	0.0	0.0	0.0	0.0	-	0.8	0.8	0.0	0.0

Annex 2 - Table 1 - continue

152	COD:VSS ratio [mgCOD/mgVSS]	1.4	1.1	1.6	8.7	8.7	0.0	0.0	5.5	5.5	0.0	0.0	0.0	0.0	0.0	-	0.8	0.8	0.0	0.0
	NOB																			
153	Yield [mgCOD/mgN]	0.1	1.1	0.1	8.7	15.5	6.8	7.8	5.5	7.2	1.7	3.2	0.0	0.0	0.0	-	0.8	5.9	5.1	62.5
154	N in biomass [mgN/mgCOD]	0.1	1.1	0.1	8.7	8.7	0.0	0.0	5.5	5.5	0.0	0.0	0.0	0.0	0.0	-	0.8	0.8	0.0	0.0
155	P in biomass [mgP/mgCOD]	0.0	1.1	0.0	8.7	8.7	0.0	0.0	5.5	5.5	0.0	0.0	0.0	0.0	0.0	-	0.8	0.8	0.0	0.0
156	Fraction to endogenous residue [-]	0.1	1.1	0.1	8.7	8.7	0.0	0.0	5.5	5.5	0.0	0.0	0.0	0.0	0.0	-	0.8	0.8	0.0	0.0
157	COD:VSS ratio [mgCOD/mgVSS]	1.4	1.1	1.6	8.7	8.7	0.0	0.0	5.5	5.5	0.0	0.0	0.0	0.0	0.0	-	0.8	0.8	0.0	0.0
	AAO																			
158	Yield [mgCOD/mgN]	0.1	1.1	0.1	8.7	15.5	6.8	7.8	5.5	7.2	1.7	3.2	0.0	0.0	0.0	-	0.8	5.9	5.0	62.2
159	Nitrate production [mgN/mgBiomassCOD]	2.3	1.1	2.5	8.7	8.8	0.0	0.0	5.5	5.5	0.0	0.0	0.0	0.0	0.0	-	0.8	0.8	0.0	0.0
160	N in biomass [mgN/mgCOD]	0.1	1.1	0.1	8.7	8.7	0.0	0.0	5.5	5.5	0.0	0.0	0.0	0.0	0.0	-	0.8	0.8	0.0	0.0
161	P in biomass [mgP/mgCOD]	0.0	1.1	0.0	8.7	8.7	0.0	0.0	5.5	5.5	0.0	0.0	0.0	0.0	0.0	-	0.8	0.8	0.0	0.0
162	Fraction to endogenous residue [-]	0.1	1.1	0.1	8.7	8.7	0.0	0.0	5.5	5.5	0.0	0.0	0.0	0.0	0.0	-	0.8	0.8	0.0	0.0
163	COD:VSS ratio [mgCOD/mgVSS]	1.4	1.1	1.6	8.7	8.7	0.0	0.0	5.5	5.5	0.0	0.0	0.0	0.0	0.0	-	0.8	0.8	0.0	0.0
	OHO																			
164	Yield (aerobic) [-]	0.7	1.1	0.7	8.7	14.0	5.3	6.0	5.5	4.4	1.1	2.0	0.0	0.0	0.0	-	0.8	7.2	6.4	78.6
165	Yield (fermentation, low H2) [-]	0.1	1.1	0.1	8.7	8.7	0.0	0.0	5.5	5.5	0.0	0.0	0.0	0.0	0.0	-	0.8	0.8	0.0	0.0
166	Yield (fermentation, high H2) [-]	0.1	1.1	0.1	8.7	8.7	0.0	0.0	5.5	5.5	0.0	0.0	0.0	0.0	0.0	-	0.8	0.8	0.0	0.0
167	H2 yield (fermentation low H2) [-]	0.4	1.1	0.4	8.7	8.7	0.0	0.0	5.5	5.5	0.0	0.0	0.0	0.0	0.0	-	0.8	0.8	0.0	0.0
168	H2 yield (fermentation high H2) [-]	0.0	1.1	0.0	8.7	8.8	0.1	0.1	5.5	5.5	0.1	0.1	0.0	0.0	0.0	-	0.8	0.8	0.0	0.1
169	Propionate yield (fermentation, low H2) [-]	0.0	1.1	0.0	8.7	8.7	0.0	0.0	5.5	5.5	0.0	0.0	0.0	0.0	0.0	-	0.8	0.8	0.0	0.0
170	Propionate yield (fermentation, high H2) [-]	0.7	1.1	0.8	8.7	8.7	0.0	0.0	5.5	5.5	0.0	0.0	0.0	0.0	0.0	-	0.8	0.8	0.0	0.0
171	CO2 yield (fermentation, low H2) [-]	0.7	1.1	0.8	8.7	8.7	0.0	0.0	5.5	5.5	0.0	0.0	0.0	0.0	0.0	-	0.8	0.8	0.0	0.0
172	CO2 yield (fermentation, high H2) [-]	0.0	1.1	0.0	8.7	8.7	0.0	0.0	5.5	5.5	0.0	0.0	0.0	0.0	0.0	-	0.8	0.8	0.0	0.0
173	N in biomass [mgN/mgCOD]	0.1	1.1	0.1	8.7	8.7	0.0	0.0	5.5	5.5	0.0	0.0	0.0	0.0	0.0	-	0.8	0.8	0.0	0.0
174	P in biomass [mgP/mgCOD]	0.0	1.1	0.0	8.7	8.7	0.0	0.0	5.5	5.4	0.0	0.0	0.0	0.0	0.0	-	0.8	0.8	0.0	0.1
175	Endogenous fraction - aerobic [-]	0.1	1.1	0.1	8.7	8.7	0.1	0.1	5.5	5.4	0.1	0.1	0.0	0.0	0.0	-	0.8	0.8	0.0	0.0
176	Endogenous fraction - anoxic [-]	0.1	1.1	0.1	8.7	8.6	0.1	0.1	5.5	5.3	0.1	0.2	0.0	0.0	0.0	-	0.8	0.8	0.0	0.0
177	Endogenous fraction - anaerobic [-]	0.2	1.1	0.2	8.7	15.5	6.7	7.7	5.5	7.2	1.7	3.1	0.0	0.0	0.0	-	0.8	5.8	5.0	61.9

Annex 2 - Table 1 - continue

178	COD:VSS ratio [mgCOD/mgVSS]	1.4	1.1	1.6	8.7	8.8	0.0	0.1	5.5	5.5	0.0	0.1	0.0	0.0	0.0	-	0.8	0.8	0.0	0.0
179	Yield (anoxic) [-]	0.5	1.1	0.6	8.7	12.6	3.8	4.4	5.5	5.5	0.0	0.0	0.0	0.0	0.0	-	0.8	4.7	3.8	47.4
180	Yield propionic (aerobic) [-]	0.6	1.1	0.7	8.7	15.4	6.7	7.7	5.5	7.2	1.7	3.1	0.0	0.0	0.0	-	0.8	5.8	5.0	61.6
181	Yield propionic (anoxic) [-]	0.5	1.1	0.5	8.7	8.7	0.0	0.0	5.5	5.4	0.0	0.0	0.0	0.0	0.0	-	0.8	0.8	0.0	0.0
182	Yield acetic (aerobic) [-]	0.6	1.1	0.7	8.7	8.5	0.2	0.2	5.5	5.2	0.2	0.4	0.0	0.0	0.0	-	0.8	0.8	0.0	0.0
183	Yield acetic (anoxic) [-]	0.4	1.1	0.5	8.7	8.6	0.1	0.1	5.5	5.3	0.1	0.2	0.0	0.0	0.0	-	0.8	0.8	0.0	0.0
184	Yield methanol (aerobic) [-]	0.5	1.1	0.6	8.7	8.7	0.0	0.0	5.5	5.5	0.0	0.0	0.0	0.0	0.0	-	0.8	0.8	0.0	0.0
185	Adsorp. max. [-]	1.0	1.1	1.1	8.7	8.7	0.0	0.0	5.5	5.4	0.0	0.0	0.0	0.0	0.0	-	0.8	0.8	0.0	0.0
186	Max fraction to N2O at high FNA over nitrate [-]	0.1	1.1	0.1	8.7	8.7	0.0	0.0	5.5	5.5	0.0	0.0	0.0	0.0	0.0	-	0.8	0.8	0.0	0.0
187	Max fraction to N2O at high FNA over nitrite [-]	0.1	1.1	0.1	8.7	8.7	0.0	0.0	5.5	5.5	0.0	0.0	0.0	0.0	0.0	-	0.8	0.8	0.0	0.0
	PAO																			
188	Yield (aerobic) [-]	0.6	1.1	0.7	8.7	8.7	0.0	0.0	5.5	5.5	0.0	0.0	0.0	0.0	0.0	-	0.8	0.8	0.0	0.0
189	Yield (anoxic) [-]	0.5	1.1	0.6	8.7	8.7	0.0	0.0	5.5	5.5	0.0	0.0	0.0	0.0	0.0	-	0.8	0.8	0.0	0.0
190	Aerobic P/PHA uptake [mgP/mgCOD]	0.9	1.1	1.0	8.7	8.7	0.0	0.0	5.5	5.5	0.0	0.0	0.0	0.0	0.0	-	0.8	0.8	0.0	0.0
191	Anoxic P/PHA uptake [mgP/mgCOD]	0.4	1.1	0.4	8.7	8.7	0.0	0.0	5.5	5.5	0.0	0.0	0.0	0.0	0.0	-	0.8	0.8	0.0	0.0
192	Yield of PHA on sequestration [-]	0.9	1.1	1.0	8.7	8.7	0.0	0.0	5.5	5.5	0.0	0.0	0.0	0.0	0.0	-	0.8	0.8	0.0	0.0
193	N in biomass [mgN/mgCOD]	0.1	1.1	0.1	8.7	8.7	0.0	0.0	5.5	5.5	0.0	0.0	0.0	0.0	0.0	-	0.8	0.8	0.0	0.0
194	N in sol. inert [mgN/mgCOD]	0.1	1.1	0.1	8.7	8.7	0.0	0.0	5.5	5.5	0.0	0.0	0.0	0.0	0.0	-	0.8	0.8	0.0	0.0
195	P in biomass [mgP/mgCOD]	0.0	1.1	0.0	8.7	8.7	0.0	0.0	5.5	5.5	0.0	0.0	0.0	0.0	0.0	-	0.8	0.8	0.0	0.0
196	Fraction to endogenous part. [-]	0.3	1.1	0.3	8.7	8.7	0.0	0.0	5.5	5.5	0.0	0.0	0.0	0.0	0.0	-	0.8	0.8	0.0	0.0
197	Inert fraction of endogenous sol. [-]	0.2	1.1	0.2	8.7	8.7	0.0	0.0	5.5	5.5	0.0	0.0	0.0	0.0	0.0	-	0.8	0.8	0.0	0.0
198	P/Ac release ratio [mgP/mgCOD]	0.5	1.1	0.6	8.7	8.7	0.0	0.0	5.5	5.5	0.0	0.0	0.0	0.0	0.0	-	0.8	0.8	0.0	0.0
199	COD:VSS ratio [mgCOD/mgVSS]	1.4	1.1	1.6	8.7	8.7	0.0	0.0	5.5	5.5	0.0	0.0	0.0	0.0	0.0	-	0.8	0.8	0.0	0.0
200	Yield of low PP [-]	0.9	1.1	1.0	8.7	8.7	0.0	0.0	5.5	5.5	0.0	0.0	0.0	0.0	0.0	-	0.8	0.8	0.0	0.0
201	Mg to P mole ratio in polyphosphate [mmolMg/mmolP]	0.3	1.1	0.3	8.7	8.7	0.0	0.0	5.5	5.5	0.0	0.0	0.0	0.0	0.0	-	0.8	0.8	0.0	0.0
202	Cation to P mole ratio in polyphosphate [meq/mmolP]	0.2	1.1	0.2	8.7	8.7	0.0	0.0	5.5	5.5	0.0	0.0	0.0	0.0	0.0	-	0.8	0.8	0.0	0.0
203	Ca to P mole ratio in polyphosphate [mmolCa/mmolP]	0.1	1.1	0.1	8.7	8.7	0.0	0.0	5.5	5.5	0.0	0.0	0.0	0.0	0.0	-	0.8	0.8	0.0	0.0
	PROPIONIC ACETOGENIC																			

Annex 2 - Table 1 - continue

204	Yield [-]	0.1	1.1	0.1	8.7	8.7	0.0	0.0	5.5	5.5	0.0	0.0	0.0	0.0	0.0	-	0.8	0.8	0.0	0.0
205	H2 yield [-]	0.4	1.1	0.4	8.7	8.7	0.0	0.0	5.5	5.5	0.0	0.0	0.0	0.0	0.0	-	0.8	0.8	0.0	0.0
206	CO2 yield [-]	1.0	1.1	1.1	8.7	8.7	0.0	0.0	5.5	5.5	0.0	0.0	0.0	0.0	0.0	-	0.8	0.8	0.0	0.0
207	N in biomass [mgN/mgCOD]	0.1	1.1	0.1	8.7	8.7	0.0	0.0	5.5	5.5	0.0	0.0	0.0	0.0	0.0	-	0.8	0.8	0.0	0.0
208	P in biomass [mgP/mgCOD]	0.0	1.1	0.0	8.7	8.7	0.0	0.0	5.5	5.5	0.0	0.0	0.0	0.0	0.0	-	0.8	0.8	0.0	0.0
209	Fraction to endogenous residue [-]	0.1	1.1	0.1	8.7	8.7	0.0	0.0	5.5	5.5	0.0	0.0	0.0	0.0	0.0	-	0.8	0.8	0.0	0.0
210	COD:VSS ratio [mgCOD/mgVSS]	1.4	1.1	1.6	8.7	8.7	0.0	0.0	5.5	5.5	0.0	0.0	0.0	0.0	0.0	-	0.8	0.8	0.0	0.0
	METHANOGENIC																			
211	Acetoclastic yield [-]	0.1	1.1	0.1	8.7	8.7	0.0	0.0	5.5	5.5	0.0	0.0	0.0	0.0	0.0	-	0.8	0.8	0.0	0.0
212	Acetoclastic yield on methanol[-]	0.1	1.1	0.1	8.7	8.7	0.0	0.0	5.5	5.5	0.0	0.0	0.0	0.0	0.0	-	0.8	0.8	0.0	0.0
213	H2-utilizing yield [-]	0.1	1.1	0.1	8.7	8.7	0.0	0.0	5.5	5.5	0.0	0.0	0.0	0.0	0.0	-	0.8	0.8	0.0	0.0
214	H2-utilizing yield on methanol [-]	0.1	1.1	0.1	8.7	8.7	0.0	0.0	5.5	5.5	0.0	0.0	0.0	0.0	0.0	-	0.8	0.8	0.0	0.0
215	N in acetoclastic biomass [mgN/mgCOD]	0.1	1.1	0.1	8.7	8.7	0.0	0.0	5.5	5.5	0.0	0.0	0.0	0.0	0.0	-	0.8	0.8	0.0	0.0
216	N in H2-utilizing biomass [mgN/mgCOD]	0.1	1.1	0.1	8.7	8.7	0.0	0.0	5.5	5.5	0.0	0.0	0.0	0.0	0.0	-	0.8	0.8	0.0	0.0
217	P in acetoclastic biomass [mgP/mgCOD]	0.0	1.1	0.0	8.7	8.7	0.0	0.0	5.5	5.5	0.0	0.0	0.0	0.0	0.0	-	0.8	0.8	0.0	0.0
218	P in H2-utilizing biomass [mgP/mgCOD]	0.0	1.1	0.0	8.7	8.7	0.0	0.0	5.5	5.5	0.0	0.0	0.0	0.0	0.0	-	0.8	0.8	0.0	0.0
219	Acetoclastic fraction to endog. residue [-]	0.1	1.1	0.1	8.7	8.7	0.0	0.0	5.5	5.5	0.0	0.0	0.0	0.0	0.0	-	0.8	0.8	0.0	0.0
220	H2-utilizing fraction to endog. residue [-]	0.1	1.1	0.1	8.7	8.7	0.0	0.0	5.5	5.5	0.0	0.0	0.0	0.0	0.0	-	0.8	0.8	0.0	0.0
221	Acetoclastic COD:VSS ratio [mgCOD/mgVSS]	1.4	1.1	1.6	8.7	8.7	0.0	0.0	5.5	5.5	0.0	0.0	0.0	0.0	0.0	-	0.8	0.8	0.0	0.0
222	H2-utilizing COD:VSS ratio [mgCOD/mgVSS]	1.4	1.1	1.6	8.7	8.7	0.0	0.0	5.5	5.5	0.0	0.0	0.0	0.0	0.0	-	0.8	0.8	0.0	0.0
	METHYLOTOTROPIC																			
223	Yield (anoxic) [-]	0.4	1.1	0.4	8.7	8.7	0.0	0.0	5.5	5.5	0.0	0.0	0.0	0.0	0.0	-	0.8	0.8	0.0	0.0
224	N in biomass [mgN/mgCOD]	0.1	1.1	0.1	8.7	8.7	0.0	0.0	5.5	5.5	0.0	0.0	0.0	0.0	0.0	-	0.8	0.8	0.0	0.0
225	P in biomass [mgP/mgCOD]	0.0	1.1	0.0	8.7	8.7	0.0	0.0	5.5	5.5	0.0	0.0	0.0	0.0	0.0	-	0.8	0.8	0.0	0.0
226	Fraction to endogenous residue [-]	0.1	1.1	0.1	8.7	8.7	0.0	0.0	5.5	5.5	0.0	0.0	0.0	0.0	0.0	-	0.8	0.8	0.0	0.0
227	COD:VSS ratio [mgCOD/mgVSS]	1.4	1.1	1.6	8.7	8.7	0.0	0.0	5.5	5.5	0.0	0.0	0.0	0.0	0.0	-	0.8	0.8	0.0	0.0
228	Max fraction to N2O at high FNA over nitrate [-]	0.1	1.1	0.1	8.7	8.7	0.0	0.0	5.5	5.5	0.0	0.0	0.0	0.0	0.0	-	0.8	0.8	0.0	0.0

Annex 2 - Table 1 - continue

229	Max fraction to N2O at high FNA over nitrite [-]	0.2	1.1	0.2	8.7	8.7	0.0	0.0	5.5	5.5	0.0	0.0	0.0	0.0	0.0	-	0.8	0.8	0.0	0.0
	SULFUR OXIDIZING																			
230	Yield (aerobic) [mgCOD/mgS]	0.5	1.1	0.6	8.7	8.7	0.0	0.0	5.5	5.5	0.0	0.0	0.0	0.0	0.0	-	0.8	0.8	0.0	0.0
231	Yield (Anoxic) [mgCOD/mgS]	0.4	1.1	0.4	8.7	8.7	0.0	0.0	5.5	5.5	0.0	0.0	0.0	0.0	0.0	-	0.8	0.8	0.0	0.0
232	N in biomass [mgN/mgCOD]	0.1	1.1	0.1	8.7	8.7	0.0	0.0	5.5	5.5	0.0	0.0	0.0	0.0	0.0	-	0.8	0.8	0.0	0.0
233	P in biomass [mgP/mgCOD]	0.0	1.1	0.0	8.7	8.7	0.0	0.0	5.5	5.5	0.0	0.0	0.0	0.0	0.0	-	0.8	0.8	0.0	0.0
234	Fraction to endogenous residue [-]	0.1	1.1	0.1	8.7	8.7	0.0	0.0	5.5	5.5	0.0	0.0	0.0	0.0	0.0	-	0.8	0.8	0.0	0.0
235	COD:VSS ratio [mgCOD/mgVSS]	1.4	1.1	1.6	8.7	8.7	0.0	0.0	5.5	5.5	0.0	0.0	0.0	0.0	0.0	-	0.8	0.8	0.0	0.0
	SULFUR REDUCING																			
236	Yield [mgCOD/mg H2 COD]	0.1	1.1	0.1	8.7	8.7	0.0	0.0	5.5	5.5	0.0	0.0	0.0	0.0	0.0	-	0.8	0.8	0.0	0.0
237	Yield [mgCOD/mg Ac COD]	0.0	1.1	0.1	8.7	8.7	0.0	0.0	5.5	5.5	0.0	0.0	0.0	0.0	0.0	-	0.8	0.8	0.0	0.0
238	Yield [mgCOD/mg Pr COD]	0.0	1.1	0.0	8.7	8.7	0.0	0.0	5.5	5.5	0.0	0.0	0.0	0.0	0.0	-	0.8	0.8	0.0	0.0
239	N in biomass [mgN/mgCOD]	0.1	1.1	0.1	8.7	8.7	0.0	0.0	5.5	5.5	0.0	0.0	0.0	0.0	0.0	-	0.8	0.8	0.0	0.0
240	P in biomass [mgP/mgCOD]	0.0	1.1	0.0	8.7	8.7	0.0	0.0	5.5	5.5	0.0	0.0	0.0	0.0	0.0	-	0.8	0.8	0.0	0.0
241	Fraction to endogenous residue [-]	0.1	1.1	0.1	8.7	8.7	0.0	0.0	5.5	5.5	0.0	0.0	0.0	0.0	0.0	-	0.8	0.8	0.0	0.0
242	COD:VSS ratio [mgCOD/mgVSS]	1.4	1.1	1.6	8.7	8.7	0.0	0.0	5.5	5.5	0.0	0.0	0.0	0.0	0.0	-	0.8	0.8	0.0	0.0